ACTA PROTOZOOLOGICA

NENCKI INSTITUTE OF EXPERIMENTAL BIOLOGY
WARSAW, POLAND
1999
VOLUME 38 NUMBER 4
ISSN 0065-1583

Polish Academy of Sciences
Nencki Institute of Experimental Biology
and
Polish Society of Cell Biology

ACTA PROTOZOOLOGICA

International Journal on Protistology

ACTA PROTOZOOLOGICA appears quarterly.

The price (including Air Mail postage) of subscription to ACTA PROTOZOOLOGICA at 1999 is: US $ 180.- by institutions and US $ 120.- by individual subscribers. Limited numbers of back volumes at reduced rate are available. TERMS OF PAYMENT: check, money oder or payment to be made to the Nencki Institute of Experimental Biology account: 11101053-3522-2700-1-34 at Państwowy Bank Kredytowy XIII Oddz. Warszawa, Poland. For matters regarding ACTA PROTOZOOLOGICA, contact Editor, Nencki Institute of Experimental Biology, ul. Pasteura 3, 02-093 Warszawa, Poland; Fax: (4822) 822 53 42; E-mail: jurek@ameba.nencki.gov.pl For more information see Web page **http://www.nencki.gov.pl/public.htm**).

Front cover: *Trichomonas aotus* sp. n. In: F. F. Pindak and M. Mora de Pindak (1998) Diagnostic characteristics of owl monkey *(Aotus trivignatus)* intestinal trichomonads. *Acta Protozool.* **37:** 159-172

This publication is supported by the State Committee for Scientific Research

Desktop processing: Justyna Osmulska, Data Processing Laboratory of the Nencki Institute
Printed at the MARBIS, ul. Kombatantów 60, 05-070 Sulejówek, Poland

Acta Protozool. (1999) 38: 263 - 271

ACTA
PROTOZOOLOGICA

Components of Perinuclear and Intranuclear Cytoskeleton in the Intact Cells and in the Isolated Nuclei of *Amoeba proteus*

Lucyna GRĘBECKA, Paweł POMORSKI, Andrzej GRĘBECKI and Anna ŁOPATOWSKA

Department of Cell Biology, Nencki Institute of Experimental Biology, Warszawa, Poland

Summary. Filamentous actin was detected close to or in contact with the cytoplasmic side of nuclear envelope, by transmission electron microscopy and by fluorescent phalloidin staining of normal migrating cells of *Amoeba proteus*, after fixation. Thick myosin-like filaments were also found around the nucleus. The nuclei micrurgically isolated from amoebae and washed, preserved these cytoskeletal shells on their surface. Actin, myosin and spectrin were identified around such isolated nuclei, by indirect immunofluorescence. Biomechanical functions of the perinuclear cytoskeleton of amoebae are discussed. Inside the nucleus, thin actin filaments were also detected, often in connection with lamins of the honeycomb layer and with RNA containing helical structures. Undefined filaments intermediate in size lay free in the peripheral karyoplasm or are connected with the honeycomb layer. Thick filaments of the polymerized myosin size were not found inside the nuclei.

Key words: actin, *Amoeba proteus,* cell nucleus, cytoskeleton, honeycomb layer, intranuclear helices, myosin, nuclear envelope.

INTRODUCTION

The nuclear envelope forms, together with lamins and other associated proteins, an active boundary between the cytoplasm and the nuclear genetic machinery involved in control of nucleus shape, nucleo-cytoplasmic communication, regulation of DNA expression and replication and, may be, even in regulation of protein synthesis and processing (for review see Georgatos 1994). However, we know more about the structure and function of nuclear envelope itself than about cytoskeletal proteins present on its both sides.

There are few reports about the cytoskeleton components inside and around the nuclei of free living amoebae. An actin isoform has been extracted from nuclei of *Acanthamoeba castellanii* by Kumar *et al.* (1984). In *Amoeba proteus,* Lesson and Bhatnagar (1975 a, b) presented electron microscope pictures of bundles of thin filaments, probably actin, at nuclear periphery along the inner side of honeycomb lamin layer; undefined thicker filaments were shown in the mitotic nuclei by Gromov (1985); actin and myosin filaments were described at

Address for correspondence: Lucyna Grębecka, Department of Cell Biology, Nencki Institute of Experimental Biology, ul. Pasteura 3, 02-093 Warszawa, Poland; Fax: (48 22) 822 53 42; E-mail: grebecki@nencki.gov.pl

nucleus-cytoplasm boundary in an ultrastructural study of glycerinated models of *A. proteus* by Sonobe and Kuroda (1986). Stockem *et al.* (1984) published an immunofluorescence picture of the cytoskeleton of *A. proteus*, in which the perinuclear actin shell is very clearly seen, but not commented at all. Moreover, a spectrin isoform was detected with a specific monoclonal antibody at cytoplasmic face of the nuclear envelope of *A. proteus* by Choi and Jeon (1989).

It has long been known that actin is present in the nuclear matrix of at least some tissue cells. An actin-like protein was first extracted from thymus cell nuclei by Ohnishi *et al.* (1963). Intranuclear actin microfilaments were later described, *i. a.*, in oocytes of *Xenopus* (Clark and Rosenbaum 1979), in bovine lymphocytes and mouse leukemia cells (Nakayasu and Ueda 1984, 1985), carcinoma cells (Fukuda *et al.* 1987), silk moth ovarian follicles and *Drosophila* salivary gland cells (Sauman and Berry 1994), and in frog oocytes (Parfenov *et al.* 1995). Some authors have, however, demonstrated that intranuclear actin is an isoform which isoelectric point is different from the cytoplasmic actin (Bremer *et al.* 1981, Kumar *et al.* 1984). It was shown later that in interphasal nuclei of neurons the filamentous actin might be colocalised with myosin (Milankov and DeBoni 1993). Some possible actomyosin functions in the nuclear matrix are suggested by observations that nuclear actin disruption affects DNA fragmentation (Kolber *et al.* 1990), gene expression (Zambetti *et al.* 1991) and rate of DNA synthesis (Karim *et al.* 1992).

Other functions, mostly biomechanical ones, could be attributed to actin microfilaments abundant on the cytoplasmic side of nuclear envelope. Perinuclear actin microfilaments as well as thick myosin filaments and microtubules were discovered during the fifties and sixties in a large variety of Protista and of animal and plant cells (for a review see Franke 1971). Recently the perinuclear actin was studied in giant polyploid silk gland epithelium (Henderson and Locke 1992), in dividing insect epidermal cells (Jeun and Locke 1993) and also in vertebrate cells in culture (Clubb and Locke 1996). Perinuclear actin filaments may be involved in control of nucleus shape, volume and intranuclear hydrostatic pressure, movements of nuclei through the cytoplasm and/or a stabilization of their position, as well as in mechanical stress transmission from the cell periphery to the nucleus.

We have earlier examined the F-actin perinuclear layer in *Amoeba proteus* by staining it with FITC-phalloidin and have demonstrated its involvement in the nuclear division, transient anchoring of nucleus to the cell cortex and its movements inside the cell (Pomorski and Grębecka 1993, 1995). In the present study we use, besides phalloidin staining, the indirect immunofluorescence for detection of actin, myosin and spectrin, and electron microscopy. Besides intact amoebae, we examine the surface of nuclei micrurgically removed from cells, which is pertinent to our parallel study of contractility of the isolated nuclei of *A. proteus* (in preparation).

MATERIALS AND METHODS

Amoeba proteus, a clone belonging to the strain C and characterized by transparent cytoplasm poor in crystal inclusions (Nikolajeva *et al.* 1980), was cultured at room temperature in the standard Pringsheim medium ($Ca(NO_3)_2 \cdot 4H_2O$ - 200 mg/ml, $MgSO_4 \cdot 7H_2O$ - 20 mg/ml, $Na_2HPO_4 \cdot 2H_2O$ - 20 mg/ml, KCl - 26 mg/ml, $FeSO_4 \cdot 7H_2O$ - 2 mg/ml). Amoebae were fed on *Tetrahymena pyriformis*. Intact interphase cells as well as isolated nuclei were examined. Nuclei were micrurgically separated by disrupting amoebae with glass needles held in a de Fonbrune micromanipulator and subsequent rinsing with incubation buffer (25 mM imidazole, 25 mM KCl, 4 mM $MgCl_2$, 1 mM EGTA). Nuclei are the only organelles that strongly stick to the glass and stay on slide, when other cell remnants are washed out.

For normal light and fluorescence microscopy the slides with intact migrating amoebae, or with adhering isolated nuclei, were bordered with two longitudinal parafilm strips which served as spacers suspending a cover slip about 100 μm over the slide. This enabled an easy exchange of the medium. The cells and the separated nuclei were fixed, following the method of Korohoda and Stockem (1975), in 3% paraformaldehyde with 0.5% acrolein added to facilitate the reagents penetration. Actin microfilaments were stained with 1% (w/v) FITC-conjugated phalloidin. Total actin, myosin and spectrin distributions were examined by indirect immunochemistry. Polyclonal antibodies against muscle actin (Sigma A-2668), against smooth and skeletal muscle myosin (Sigma M-7648) and against spectrin (Sigma S-1390), were applied, diluted 1:40. These primary markers were subsequently visualised by FITC-conjugated antibody against IgG (Sigma F-0382). Its application without primary antibodies gave always negative results.

A Nikon Diaphot inverted microscope was used, with Nomarski differential interference contrast (with Plan 10 DIC 0.25, Plan 20 DIC 0.4 and Plan 40 DIC LWD 0.55 lenses) and an epifluorescence device (with Nikon B2A and G2A filter blocks). To minimalize photo bleaching, glucose-oxydase-catalase system was applied (1 mg/ml glucose oxydase, 0,2 mg/ml catalase, 30 mg/ml glucose). The microscope was equipped with a CCD camera Panasonic WV-BL 600/g, a Hamamatsu Argus 10 image processor for contrast enhancement, noise reduction and digital enlargement, and a Panasonic NV-FS88 S-VHS video recorder. Selected pictures were collected using a frame grabber and stored in computer memory, and printed on a Mitsubishi CP700DE digital colour printer.

For the electron microscopy amoebae were fixed either in paraformaldehyde with acrolein, as described above or, for a rapid fixation, in aliquots of 6% glutaraldehyde, 2% osmium tetroxide and 0.05M cacody-

late buffer, and after fixation thoroughly washed in cacodylate buffer. After dehydration in 30%, 50%, 70%, 90%, 95% and twice in 100% ethanol, the cells were embedded in White acrylic resin with 1% benzoil (both from Sigma) and cut in an LKB microtome. The sections were transferred to formvar coated grids and contrasted during 30-60 min. in 1:1 mixture of saturated uranyl acetate and 100% ethanol, then dried, incubated 5 min in 0.2% lead citrate in 1N NaOH, and washed in the deionized water. They were examined and photographed in a JEEM 1200EX transmission electron microscope.

RESULTS

Staining and identification of perinuclear cytoskeletal proteins

The polymerized actin was demonstrated in abundance around the nuclei of *A. proteus* intact cells after fixation

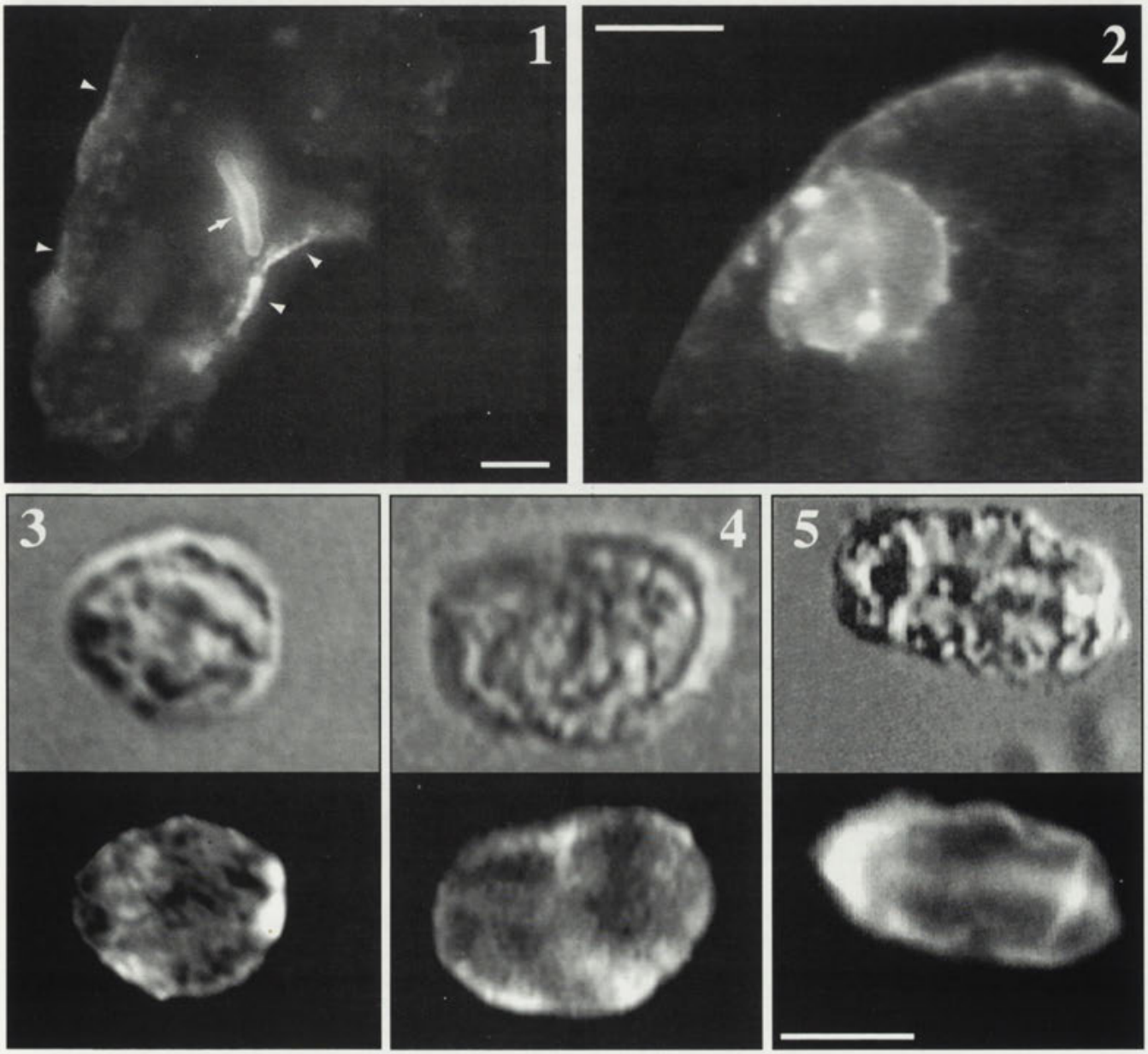

Fig. 1. FITC-phalloidin staining of the cortical submembraneous F-actin (arrowheads) and the perinuclear F-actin cytoskeleton (arrow). The nucleus is vertically oriented. Scale bar - 25 μm. Fig. 2. A higher magnification of another nucleus, in the horizontal position. Note the continuous F-actin layer around it with several discrete agglomerations. Scale bar - 25 μm. Figs. 3-5. Demonstration of actin (Fig. 3), myosin (Fig. 4) and spectrin (Fig. 5) by indirect antibody staining of the perinuclear cytoskeleton of nuclei isolated from amoebae. The nuclei are shown in the Nomarski differential interference contrast (top) and in fluorescence microscope (bottom). Scale bar - 10 μm

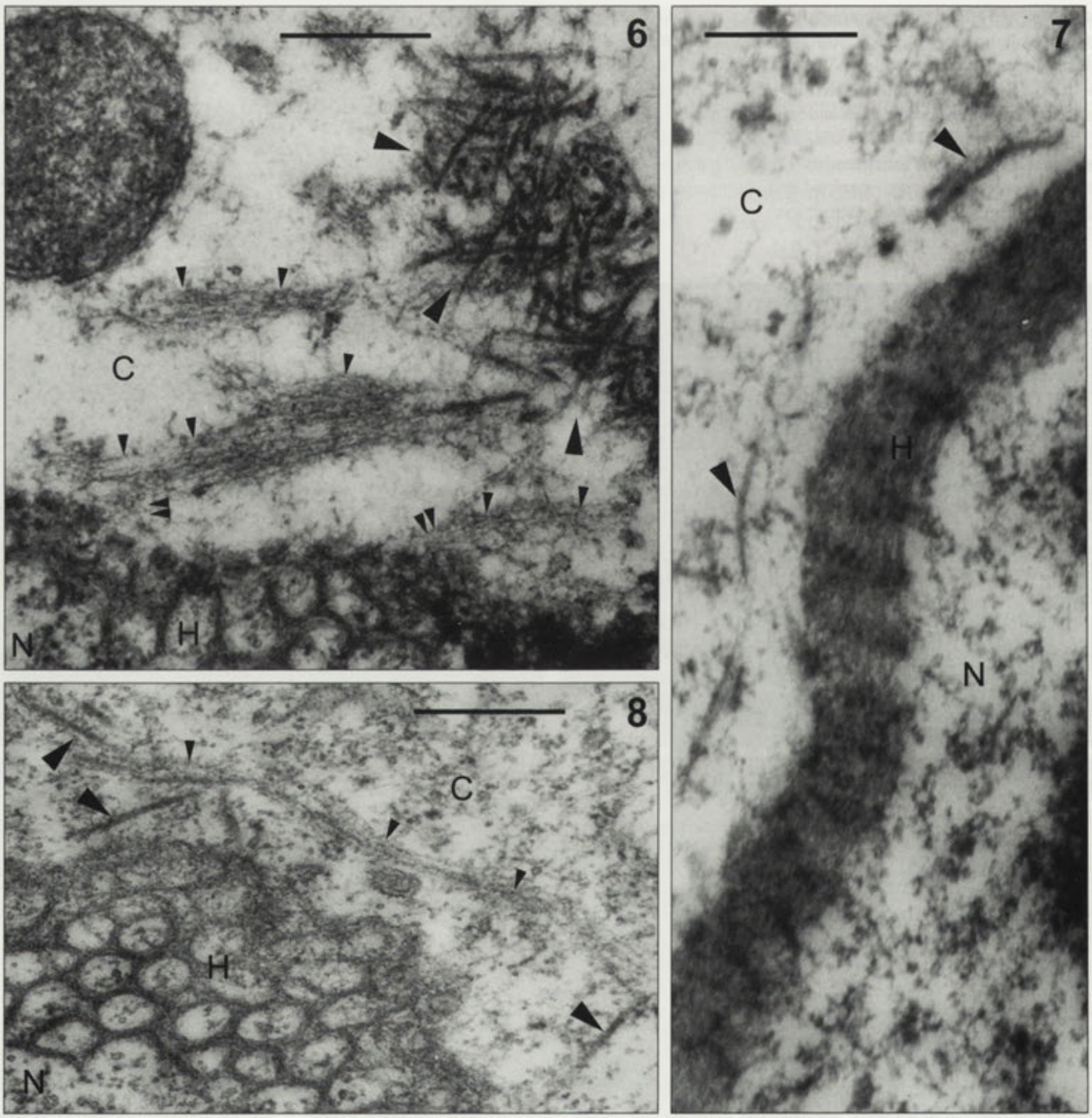

Fig. 6. Bundles of actin microfilaments in the perinuclear cytoplasm, their contacts with outer side of the nuclear envelope, and a cluster of thick myosin filaments. Scale bars - 0.5 μm. C - cytoplasm, H - honeycomb layer, N - karyoplasm, small arrowheads - thin filament bundles, large arrowheads - thick filaments, double arrowheads - contacts between filaments and the nucleus-cytoplasm boundary. The same symbols and scale bars are used in Figs. 7-11. Fig. 7. Single thick myosin filaments aligned in the perinuclear cytoplasm along the nuclear boundary. Fig. 8. A bundle of actin microfilaments parallel to the nuclear envelope and accompanied by thick myosin filaments

in paraformaldehyde with acrolein and staining with FITC-conjugated phalloidin. The nuclei of amoebae were easily recognized by their morphology in the Nomarski contrast and, moreover, they were several times identified also by a parallel DNA marking with DAPI. Phalloidin specifically binds only to F-actin which is in functional state, *i.e.*, it is organized in microfilament bundles or networks, whereas the diffuse G-actin cannot produce

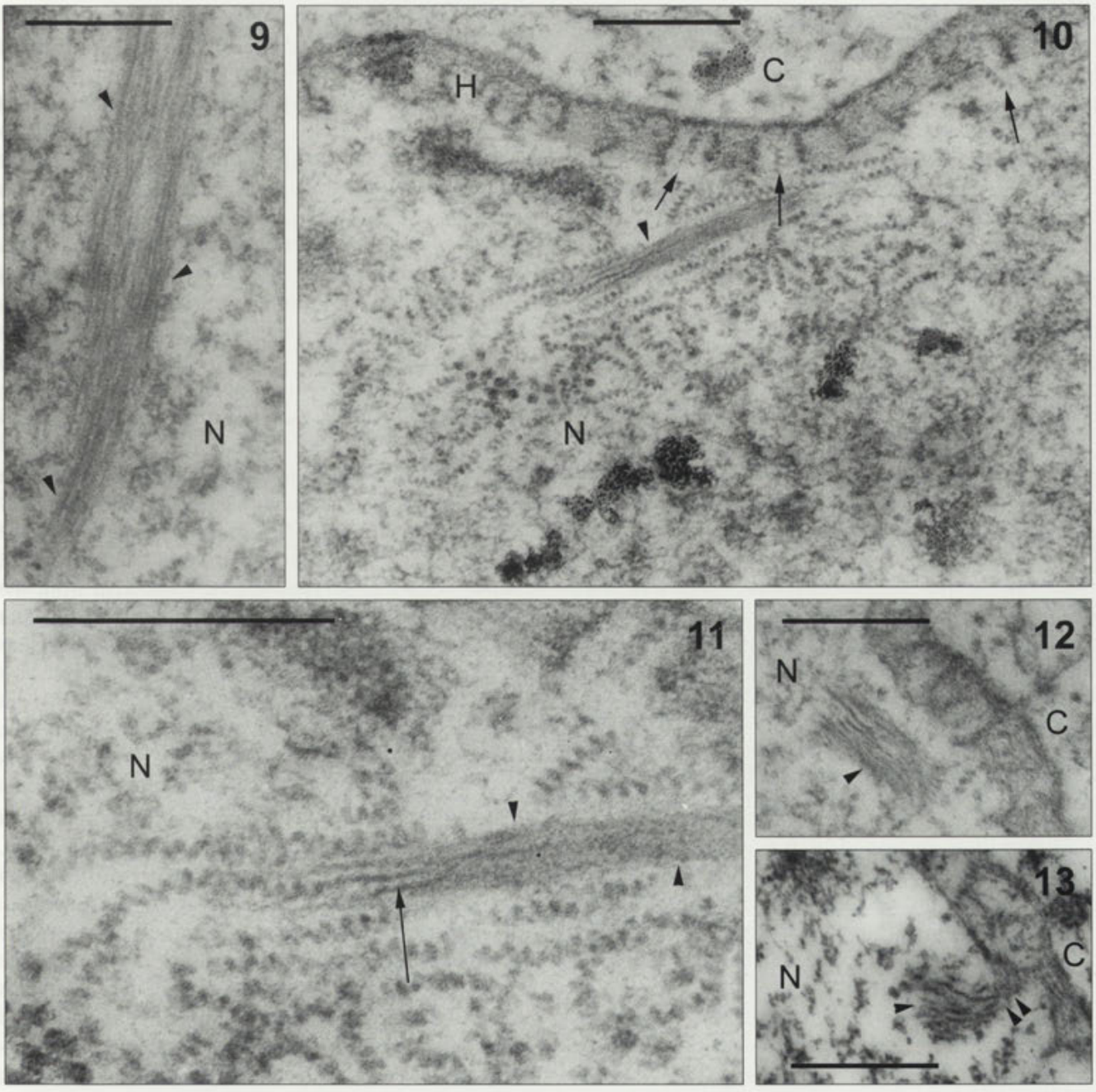

Fig. 9. A large bundle of thin filaments in the nuclear matrix, about 1.5 μm from the nuclear boundary (not seen). Fig. 10. A bundle of thin filaments surrounded by intranuclear helical structures, and penetration of some helices through the honeycomb layer (arrows). Fig. 11. Continuity of thin filaments and intranuclear helices (arrow); higher magnification of a fragment of the section shown in Fig. 10. Figs. 12, 13. Bundles of undefined intermediate (?) filaments close to the nuclear boundary (arrowheads in Fig. 12), and in junction with the honeycomb layer (double arrowheads in Fig. 13)

any background noise. In the normally migrating amoebae (Fig. 1) FITC-phalloidin fluorescence is always seen beneath the plasma membrane, where the contractile F-actin cortex is present, as well as around the cell nucleus. At a higher magnification the perinuclear F-actin appears as a continuous layer, sometimes with discrete dot-like agglomerations (Fig. 2).

Some cytoskeletal proteins were identified at the nucleus-cytoplasm boundary by indirect immunocytochemical method. In this case the nuclei were, before staining,

micrurgically isolated from amoebae to avoid the problem of insufficient antibody penetration through the cell-medium barrier. On the other side, it complemented our parallel tests of contractility of the isolated nuclei of *A. proteus* (in preparation).

Nuclei were isolated, rinsed and incubated in the imidazole buffer. Polyclonal antibodies against total actin, myosin and spectrin, were used as primary markers. The positive results of staining confirm the presence of actin (Fig. 3, bottom), and demonstrate the presence of myosin (Fig. 4, bottom) and spectrin (Fig. 5, bottom) in the perinuclear region of *A. proteus*. Some brighter spaces located apparently inside these nuclei are optical artefacts: they reflect merely the surface relief (seen in the Nomarski contrast in Figs. 3-5, top) with sloping edges which in projection produce stronger signals than the flat horizontal areas. Staining of actin, myosin and spectrin by the antibodies without permeabilization of the nuclear envelope, which should not be penetrated by immunoglobulins, indicates that these cytoskeletal proteins are bound to the outer side of the nuclear envelope. Therefore, their attachment should be strong enough to resist the procedure of extracting the nuclei from the cells and washing them in the buffer. However, it does not exclude the presence of some cytoskeletal proteins also in the nuclear matrix.

Thin and thick filaments at the perinuclear boundary of intact amoebae

The question of actin and myosin localisation, either at the outer or at the inner side of the nuclear boundary, was further examined by electron microscopy of the nucleus periphery and of the surrounding cytoplasm after fixation of intact cells. Earlier data on the filaments present in this zone of *A. proteus* were rather scarce (see Introduction).

Figure 6 shows an area in the cytoplasm surrounding a nucleus, after fixation in paraformaldehyde with acrolein. The perinuclear cytoplasm is intersected by bundles of thin filaments, typical of actin (arrowheads). Some of them are connected in the plane of the picture (as indicated by double arrowheads) to the outer side of membranes, which form the nuclear envelope. An aggregation of thick filaments is also seen (Fig. 6, large arrowheads). However, such dense and large aggregations of thick filaments appear only after fixation of amoebae in paraformaldehyde. Therefore, they may be products of centripetal contractions provoked by this slowly working fixative. In contrast, after rapid fixation in the glutaraldehyde with osmium tetroxide, numerous individual thick filaments become seen surrounding the nucleus close to the nuclear envelope, either alone (Fig. 7) or in association with thin filaments (Fig. 8), instead of accumulating far off in the cytoplasm.

Large bundles of thin filaments can be found as well inside the nucleus, in the nuclear matrix (Fig. 9). Intranuclear thin filaments are mostly found close to the honeycomb layer, a structure characteristic of *A. proteus* and some other amoebae, which major constituents are lamins bound to the inner side of the nuclear envelope. Thin filaments in many cases accompany the intranuclear helical structures; these structures, which are randomly arranged elsewhere, in the vicinity of thin filaments are ordered parallel to them (Fig. 10). Sometimes a helice looks like a coiled extension of a microfilament (Fig. 11, arrow). Some helices are seen penetrating into the honeycomb layer of the nuclear envelope (Fig. 10, arrows).

Short bundles of other filaments, larger in diameter, are also distributed predominantly at the nucleus periphery (Fig. 12, arrowheads), often in direct contact with the internal face of the honeycomb layer of lamins (Fig. 13, double arrowheads). They are very different from the thick filaments seen on the cytoplasmic side of the nuclear envelope (compare Figs. 7-8). We never saw any myosin-like thick filaments inside the nucleus.

DISCUSSION

In early studies of the cytoskeleton fine structure in A. *proteus* (for example, Rinaldi and Hrebenda 1975, Grębecka and Hrebenda 1979, Stockem *et al.* 1982) thin filaments around the cell nucleus were not described. They are seen in our present micrographs close to the nuclear envelope on its cytoplasmic side and they have the same dimensions and shapes as actin microfilaments demonstrated by us and other authors in the contractile cell cortex of *A. proteus*. The perinuclear microfilaments were earlier detected in glycerinated models of this amoeba, but they appeared straighter and slightly thicker, which might be an artefact of glycerinating (Sonobe and Kuroda 1986). The present study has confirmed their F-actin nature by phalloidin staining of intact cells and anti-actin antibody treatment of the isolated naked nuclei.

The thick filaments found by us around interphase nuclei appear similar in structure to the cytoplasmic thick filaments of glycerinated *A. discoides* (Holberton and Preston 1970) and they have the same dimensions as the thick filaments of glycerinated *A. proteus,* according to Sonobe and Kuroda (1986). The conclusion that they represent the polymerized myosin is supported by staining

the surface of the isolated nuclei of *A. proteus* by a polyclonal antibody against myosin.

The existence of links between the actin microfilaments and the cytoplasmic face of the nuclear envelope, which is suggested by our micrographs, is well corroborated by binding of a polyclonal antibody against spectrin to the isolated nuclei. This is not a new information. Earlier, Choi and Jeon (1989) have produced monoclonal antibodies against different spectrin epitopes of *A. proteus*, and demonstrated a specific spectrin isoform connected to the nuclear envelope, different from that which is associated with the plasma membrane of this cell. Presence of the spectrin beside F-actin and myosin indicates that the perinuclear shell of *A. proteus*, in connection with the nuclear membrane, forms a unit capable of performing mechanical functions.

We have also confirmed the old but never reproduced finding of Lesson and Bhatnagar (1975 a, b) that in *A. proteus* bundles of microfilaments are present as well in the nuclear matrix and that they can be bound to the inner side of the honeycomb layer of lamins. Some uncertainty remains about their motor functions, since we were unable to detect any myosin-like thick filaments inside the nucleus. However, myosin II in the dimeric or oligomeric form, and/or myosins I may be present in the karyoplasm. There is no information available yet about other actin binding proteins organizing the microfilament bundles and/or linking them to other structures inside the nucleus.

On the other hand however, we have demonstrated that the intranuclear filaments can be arranged in bundles close to the intranuclear helices. Both structures either are intimately interconnected or one of them may be an extension of another. The intranuclear helices were discovered in *A. proteus* by Pappas (1956), described in four different species of *Amoeba* by Flickinger (1974), and in *Chaos glabrum* by Smirnov and Goodkov (1997). They are known to consist of RNA and protein complex (Wise *et al.* 1972), disappear during mitosis but abound in interphasal nuclei (Roth *et al.* 1960, Minassian and Bell 1976), and move through the nuclear envelope from the nucleus to the cytoplasm (Ord 1979). Intranuclear helices in amoebae are homologous as to their composition, dynamics and function to the ribonucleoprotein (RNP) particles or fibrils in Metazoan cells (see review by Berezney *et al.* 1995). Therefore, our observation of the continuity of some intranuclear thin filaments with the helicoidal structures in amoebae might contribute to understanding of the postulated involvement of intranuclear cytoskeleton in protein synthesis and transport from the nucleus to the cytoplasm (see Introduction).

The short bundles of thicker filaments, that we found close or attached to the inner side of the honeycomb layer of interphasal nuclei, are similar in size and arrangement of filaments, to the undefined filament bundles described in the dividing nuclei of *A. proteus* by Gromov (1985). Continuity of some of these bundles with the honeycomb layer may suggest that they belong, like the laminar material, to the family of intermediate filaments, although the nuclear lamins of amoebae and of metazoan cells are not exactly homologous (Schmidt *et al.* 1995).

As to the perinuclear cytoskeleton of amoebae, its biomechanical functions seem to be evident and differentiated. First, it is involved in the nuclear division. In a large variety of Protista the nucleus is not disassembled at prophase as in the higher animal and plant cells, but in contrast a closed mitosis occurs: the nuclear envelope persists and is divided by cleavage (Heath 1980, Cavalier-Smith 1988). The mitosis of *A. proteus* is defined as "semi-open" (Gromov 1985). We have shown that in this amoeba the perinuclear actin aggregates to form a constriction ring at the equator of the telophase nucleus and separates the daughter nuclei (Pomorski and Grębecka 1993).

Secondly, the perinuclear actin cytoskeleton in *A. proteus* has transient connections with submembraneous actin cell cortex, which were demonstrated by rotation of three-dimensional reconstruction produced in a confocal microscope (Pomorski and Grębecka 1995). As a result, the quick transport of the nucleus by endoplasmic streaming toward the cell front is periodically interrupted by a temporary anchoring it to the cell periphery. This maintains the nucleus at a nearly central position in amoeba. A role of actin cytoskeleton in establishing links between the nucleus and the cell periphery is also expressed in epithelial cells, in the form of parallel cell and nucleus shape changes (Pienta and Coffey 1992, Sims *et al.* 1992). Contacts between perinuclear and cortical actin layers are not only involved in stabilizing the position of nuclei, but they can on the contrary provoke dynamic interactions, resulting in rotations of nuclei, as demonstrated in fibroblasts (Paddock and Albrecht-Buehler 1986 a, b), hepatocytes (Barni and Scherini 1991) and *A. proteus* (Pomorski and Grębecka 1995). Finally, the continuity of the actin cytoskeleton from the cell periphery to the nuclear boundary may be important for mechanical signal transduction according to the tensegrity model proposed by Ingber (1993) or the percolation model of

Forgacs (1995). In the case of *A. proteus* the presence of perinuclear actin is essential for these hypotheses, because other cytoskeletal components play a minor, if any, role in the interphase cells cytoplasm of this protist (Christiani *et al.* 1986, Stockem and Kłopocka 1988). It makes perinuclear actin the only candidate for a tension transducer, whereas in other cell types microtubules and intermediate filaments may also perform this function (Paddy *et al.* 1990, Staiger and Cande 1990, Pienta and Coffey 1992).

Another possible function of the perinuclear actomyosin cytoskeleton is to control, by contraction, the shape and volume of the nucleus; that is obviously related with a control of intranuclear hydrostatic pressure and water movements through the nuclear envelope. The changes in volume of isolated *A. proteus* nuclei were produced with different experimental procedures by Korohoda *et al.* (1968) and Opas *et al.* (1978). The present evidence of the preservation of actin, myosin and spectrin on the surface of micrurgically isolated nuclei of amoebae allowed us to reinvestigate the behaviour of this model under conditions commonly used in studies of the actomyosin system *in vitro* (in preparation).

Acknowledgement. We thank Dr. Krystyna Golińska for her very important contribution to the electron microscope part of this study.

REFERENCES

Barni S., Scherini E. (1991) Possible patterns of nuclear rotation in binucleate hepatocytes in vivo: static examination with fluorescence and electron microscopy. *In Vivo* **5:** 167-170

Berezney R., Mortillaro M. J., Hong Ma, Xiangyun Wei, Samarabandu J. (1995) The nuclear matrix: a structural milieu for genomic function. *Int. Rev. Cytol.* **162A:** 1-65

Bremer J. W., Busch H., Yeoman L. C. (1981) Evidence for a species of nuclear actin distinct from cytoplasmic and muscles actins. *Biochemistry* **20:** 2013-2017

Cavalier-Smith T. (1988) Origin of the cell nucleus. *Bio Essays* **9:** 72-78

Choi E. Y., Jeon K. W. (1989) A spectrin-like protein present on membranes of *Amoeba proteus* as studied with monoclonal antibodies. *Exp. Cell Res.* **185:** 154-165

Christiani A., Hügelmeyer P., Stockem W. (1986) Morphological evidence for the existence of a more complex cytoskeleton in *Amoeba proteus*. *Cell Tissue Res.* **246:** 163-168

Clark T. G., Rosenbaum J. L. (1979) An actin filament matrix in hand-isolated nuclei of *X. laevis* oocytes. *Cell* **18:** 1101-1108

Clubb B. H., Locke M. (1996) F-actin forms transient perinuclear shells at the mitosis-interphase transition. *Cell Motil. Cytoskeleton* **33:** 151-162

Flickinger C. J. (1974) The fine structure of four species of *Amoeba*. *J. Protozool.* **21:** 59-68

Forgacs G. (1995) On the possible role of cytoskeletal filamentous networks in intracellular signaling: an approach based on percolation. *J. Cell Sci.* **108:** 2131-2143

Franke W. W. (1971) Relationship of nuclear membranes with filaments and microtubules. *Protoplasma* **73:** 263-292

Fukuda Y., Uchiyama S., Masuda Y., Masugi Y. (1987) Intranuclear rod-shaped actin filament bundles in poorly differentiated axillary adenosquamous cell carcinoma. *Cancer* **60:** 2972-2984

Georgatos S. D. (1994) Towards an understanding of nuclear morphogenesis. *J. Cell Biochem.* **55:** 69-76

Grębecka L., Hrebenda B. (1979) Topography of cortical layer in *Amoeba proteus* as related to the dynamic morphology of moving cell. *Acta Protozool.* **18:** 481-490

Gromov D. B. (1985) Ultrastructure of mitosis in *Amoeba proteus*. *Protoplasma* **130:** 130-139

Heath I. B. (1980) Variant mitosis in lower eukaryotes: indicators of the evolution of mitosis? *Int. Rev. Cytol.* **64:** 1-80

Henderson S. C., Locke M. (1992) A shell of F-actin surrounds the branched nuclei of silk gland cells. *Cell Motil. Cytoskeleton* **23:** 169-187

Holberton D. V., Preston T. M. (1970) Arrays of thick filaments in ATP-activated *Amoeba* model cells. *Exp. Cell Res.* **62:** 473-477

Ingber D. E. (1993) Cellular tensegrity: defining new rules of biological design that govern the cytoskeleton. *J. Cell Sci.* **104:** 613-627

Jeun G., Locke M. (1993) The timing of division in twin cell doublets. *Tissue Cell* **25:** 295-304

Karim O. M., Seki N., Pienta K. J., Mostwin J. L. (1992) The effect of age on the response of the detrusor to intracellular mechanical stimulus: DNA replication and the cell actin matrix. *J. Cell Biochem.* **48:** 373-384

Kolber M. A., Broschat K. O., Landa-Gonzalez B. (1990) Cytochalasin B induces cellular DNA fragmentation. *FASEB J.* **4:** 3021-3027

Korohoda W., Stockem W. (1975) On the nature of hyaline zones in the cytoplasm of *Amoeba proteus*. *Microsc. Acta* **77:** 129-141

Korohoda W., Forrester J. A., Moreman K. G., Ambrose E. J. (1968) Size changes in isolated nuclei of *Amoeba proteus* on treatment with polyionic substances. *Nature* **217:** 615-617

Kumar A., Riaziuddin S., Finlay T. H., Thomas J.O., Szer W. (1984) Isolation of a minor species of actin from the nuclei of *Acanthamoeba castellanii*. *Biochemistry* **23:** 6753-6757

Lesson T.S., Bhatnagar R. (1975 a) Microfibrillar structures in the nucleus and cytoplasm of *Amoeba proteus*. *J. Exp. Zool.* **192:** 265-270

Lesson T.S., Bhatnagar R. (1975 b) *Amoeba proteus*: The nuclear periphery. *Diff.* **4:** 79-86

Milankov K., DeBoni U. (1993) Cytochemical localization of actin and myosin aggregates in interphase nuclei in situ. *Exp. Cell Res.* **209:** 189-199

Minassian I., Bell L. G. B. (1976) Studies on changes in the nuclear helices of *Amoeba proteus* during the cell cycle. *J. Cell Sci.* **20:** 273-287

Nakayasu H., Ueda K. (1984) Small nuclear RNA-protein complex anchors on the actin filaments in bovine lymphocyte nuclear matrix. *Cell Struct. Funct.* **9:** 317-325

Nakayasu H., Ueda K. (1985) Ultrastructural localization of actin in nuclear matrices from mouse leukemia L5178Y cells. *Cell Struct. Funct.* **10:** 305-309

Nikolajeva G. V., Kalinina L. V., Sikora J. (1980) Transparent *Amoeba proteus* originated from the strain C. *Acta Protozool.* **14:** 327-334

Ohnishi T., Kawamura H., Yamamoto T. (1963) Extraktion eines dem Aktin ähnlichen Proteins aus dem Zellkern des Kalbsthymus. *J. Biochem.* **54:** 298-300

Opas M., Hrebenda B., Tołłoczko B. (1978) Contractility of glycerol-extracted nuclei of *Amoeba proteus*. *Acta Protozool.* **17:** 369-374

Ord M. J. (1979) The effect of chemicals and radiations within the cell: An ultrastructural and micrurgical study using *Amoeba proteus* as a single-cell model. *Int. Rev. Cytol.* **61:** 229-281

Paddock S. W., Albrecht-Buehler G. (1986 a) Distribution of microfilament bundles during rotation of the nucleus in 3T3 cells treated with monensin. *Exp. Cell Res.* **163:** 525-538

Paddock S. W., Albrecht-Buehler, G. (1986 b) The degree of coupling of nuclear rotation in binucleate 3T3 cells. *Exp. Cell Res.* **166:** 113-126

Paddy M. R., Belmont A. S., Saumweber H., Agard D. A., Sedat J. W. (1990) Interphase nuclear envelope lamins form a discontinuous network that interacts with only a fraction of the chromatin in the nuclear periphery. *Cell* **62:** 89-106

Pappas G. D. (1956) Helical structures in the nucleus of *Amoeba proteus*. *J. Biophys. Biochem. Cytol.* **2:** 221-222.

Parfenov V. N., Davis D. S., Pochukalina G. N., Sample C. E., Bugaeva E. A., Murti K. G. (1995) Nuclear actin filaments and their topological changes in frog oocytes. *Exp. Cell Res.* **217:** 385-394

Pienta K.J., Coffey D.S. (1992) Nuclear-cytoskeletal interactions: evidence for physical connections between the nucleus and cell periphery and their alteration by transformation. *J. Cell Biochem.* **49:** 357-365

Pomorski P., Grębecka L. (1993) Is actin involved in the nuclear division in *Amoeba proteus? Cell Biol. Int.* **17:** 521-524

Pomorski P., Grębecka L. (1995) Nuclear movements and nuclear actin in bilobed nuclei of *Amoeba proteus*. *Europ. J. Protistol.* **31:** 260-267

Rinaldi R. A., Hrebenda B. (1975) Oriented thick and thin filaments in *Amoeba proteus*. *J. Cell Biol.* **66:** 193-198

Roth L. E., Obetz S. W., Daniels E. W. (1960) Electron microscopic studies of mitosis in amebae. I. *Amoeba proteus*. *J. Biophys. Biochem. Cytol.* **8:** 207-220

Sauman I., Berry S. J. (1994) An actin infrastructure is associated with eukaryotic chromosomes: structural and functional significance. *Eur. J. Cell Biol.* **64:** 348-356

Schmidt M., Grossmann U., Krohne G. (1995) The nuclear membrane-associated honeycomb structure of the unicellular organism *Amoeba proteus:* On the search for homologies with the nuclear lamina of metazoa. *Eur. J. Cell Biol.* **67:** 199-208

Sims J. R., Karp S., Ingber D. E. (1992) Altering the cellular mechanical force balance results in integrated changes in cell, cytoskeletal and nuclear shape. *J. Cell Sci.* **103:** 1215-1222

Smirnov A. V., Goodkov A. V. (1997) Description of the large multinucleate lobose amoeba *Chaos glabrum* sp. n. (Lobosea, Amoebidae), with notes on the diagnosis of the genus *Chaos*. *Acta Protozool.* **36:** 227-233

Sonobe S., Kuroda K. (1986) Ultrastructural aspects of a glycerinated model of *Amoeba proteus*. *Protoplasma* **130:** 41-50

Staiger C. J., Cande W. Z. (1990) Microtubule distribution in *dv*, a maize meiotic mutant defective in the prophase to metaphase transition. *Dev Biol* **138:** 231-242

Stockem W., Kłopocka W. (1988) Ameboid movement and related phenomena. *Int. Rev. Cytol.* **112:** 137-183

Stockem W., Hoffmann H-U., Gawlitta W. (1982) Spatial organization and fine structure of the cortical filament layer in normal locomoting Amoeba *proteus*. *Cell Tiss. Res.* **221:** 505-519

Stockem W., Naib-Majani W., Wohlfarth-Bottermann K.E. (1984) Preservation and phallotoxin-staining of the microfilament system in *Amoeba proteus*. *Cell Biol. Int. Rep.* **8:** 207-213

Wise G. E., Stevens A. R., Prescott D. M. (1972) Evidence of RNA in the helices of *Amoeba proteus*. *Exp. Cell Res.* **75:** 347-352.

Zambetti G., Ramsey-Ewing A., Bortell R., Stein G., Stein J. (1991) Disruption of the cytoskeleton with cytochalasin D induces c-fos gene expression. *Exp. Cell Res.* **192:** 93-101

Received on 27th April, 1999; accepted on 1st July, 1999

Acta Protozool. (1999) 38: 273 - 290

ACTA
PROTOZOOLOGICA

Ontogenesis in a Trachelocercid Ciliate (Ciliophora: Karyorelictea), *Sultanophrys arabica*, with an Account of Evolution at the Base of the Ciliate Tree

Wilhelm FOISSNER[1] and Khaled A. S. AL-RASHEID[2]

[1]Universität Salzburg, Institut für Zoologie, Salzburg, Austria; [2]King Saud University, Zoology Department, Riyadh, Saudi Arabia

Summary. Ontogenesis in *Sultanophrys arabica* Foissner & AL-Rasheid, 1999, a trachelocercid karyorelictid ciliate, was investigated using live observation, silver impregnation, and scanning electron microscopy. Division is homothetogenic and occurs in freely motile (non-encysted) condition. The parental oral apparatus does not reorganise and cell shape is maintained. Stomatogenesis is parakinetal, that is, the anlage for the opisthe oral apparatus is derived directly from the first ordinary somatic ciliary row right of the glabrous stripe and has no connection with parental mouth structures. The oral primordium appears slightly subequatorially and consists of an anarchic field of basal bodies, from which many dikinetidal kinetofragments differentiate. The kinetofragments migrate centrifugally and assemble to a circumoral kinety and three minute brosse kineties. The somatic kineties, the bristle kinety, and the lateral kinety divide without anlagen formation, that is, are disrupted by cytokinesis. Thus, morphogenesis of trachelocercid karyorelictids is distinctly different from that of loxodid karyorelictids, which generate the oral primordium buccokinetally. This shows that different stomatogenic modes developed early in ciliate evolution, which is emphasised by the heterotrichs, whose parakinetal stomatogenesis is rather different from that of the trachelocercids. Nevertheless, our data give some support for the subphyletic division suggested by Lynn (1996), but do not corroborate any of the hypotheses on evolution of ciliate cytoarchitecture. Both, loxodid and trachelocercid karyorelictids have conspicuous ontogenetic similarities (scutica-like structure, "director meridian") with oligohymenophoreans. This is sustained by the trachelocercid brosse kineties, which resemble oligohymenophorean and prostomatid adoral membranelles. Whether these traits evolved convergently or have a deeper meaning needs further investigations.

Key words: interstitial ciliates, morphogenesis, Postciliodesmatophora, stomatogenesis.

INTRODUCTION

SSrRNA gene sequences indicate a common ancestor for karyorelictids, such as *Loxodes* and *Trachelocerca*, which have non-dividing macronuclei, and heterotrichs, such as *Climacostomum* and *Eufolliculina*, which have dividing macronuclei (for reviews, see Lynn and Small 1997, Hirt *et al.* 1998). A close relationship between karyorelictids and heterotrichs is also suggested by the unique somatic cortical fine structure, that is, the postciliary microtubular ribbons overlap to form conspicuous postciliodesmata right of the ciliary rows (Raikov *et al.* 1975, Gerassimova and Seravin 1976). Accordingly, Lynn (1996) united karyorelictids and heterotrichs in the subphylum Postciliodesmatophora Gerassimova & Seravin,

Address for correspondence: Wilhelm Foissner, Universität Salzburg, Institut für Zoologie, Hellbrunnerstrasse 34, A-5020 Salzburg, Austria; Fax: +43 (0) 662 8044-5698

1976 and established the subphylum Intramacronucleata to contain all other ciliates. Lynn's proposal, which requires that macronuclear division has arisen independently twice during ciliate evolution, is supported to some extent by ontogenetic data, which show that at least heterotrichs have a specific (parakinetal) stomatogenic mode, where the new mouth originates, without any participation of parental oral structures, from an anarchic field of basal bodies produced postorally by a few stomatogenic ciliary rows (for reviews, see Foissner 1996b, Aescht and Foissner 1998). A parakinetal stomatogenesis was also proposed for *Loxodes* (Tuffrau 1961), but recently disproved by Bardele and Klindworth (1996), who showed that *Loxodes* generates the opisthe's oral apparatus buccokinetally, that is, with participation of parental oral structures.

Karyorelictids continuously played an important role in understanding ciliate nuclear dimorphism and phylogeny because their diploid macronuclei are incapable to divide and originate from micronuclei during and after cell fission (Raikov 1958, 1982; Corliss 1974; Orias 1976, 1991; Small 1984; Lynn and Small 1997). Unfortunately, most karyorelictids are, for unknown reasons, fragile and difficult to impregnate with silver compounds. Thus, detailed observations on the ontogenesis of their ciliary pattern were published only recently (Bardele and Klindworth 1996), and ontogenetic data from the largest group of karyorelictids, the trachelocercids, are entirely lacking (Foissner 1996b), although their nuclear division was thoroughly studied already in the sixties (for review, see Raikov 1982). It was only recently that Foissner and Dragesco (1996a, b) invented an appropriate technique, which we used to investigate the ontogenesis of the ciliary pattern in *Sultanophrys arabica*, a trachelocercid karyorelictid discovered recently in a brackish pond at the Saudi Arabian Gulf coast (Foissner and AL-Rasheid 1999). *Sultanophrys* has a parakinetal stomatogenesis, similar to heterotrichs, and thus supports Lynn's subphyletic division.

MATERIAL AND METHODS

Sultanophrys arabica Foissner & AL-Rasheid, 1999 was isolated from a brackish pond at the Saudi Arabian Gulf coast and cultivated as described in AL-Rasheid and Foissner (1999). Specimens divided readily and thus ample material was available.

Dividing specimens were studied *in vivo* and with the scanning electron microscope, as advised in Foissner (1991), using the fixative described by Foissner and Dragesco (1996a). The infraciliature and the nuclear apparatus were revealed with a combination of Wilbert's protargol and Fernandez-Galiano's silver carbonate technique, as described in Foissner and AL-Rasheid (1999). Preparations of extraordinary clarity were obtained with this method, which is, unfortunately, not yet fully reproducible. We were advised by one of the reviewers to emphasise that the micrographs were not touched with ink for the sake of clarity but result from the superb quality of the preparations.

Drawings were made with a camera lucida and are slightly schematised. Note that all cells are strongly contracted and inflated due to the preparation procedures. Terminology is according to Corliss (1979), Foissner (1996b) and Foissner and Dragesco (1996a).

RESULTS

Interphase morphology

See Foissner and AL-Rasheid (1999) for a detailed description of *S. arabica*. Here, we mention only details, which are important for understanding the ontogenetic processes. *In vivo*, the organism is about 800 µm long, 70 µm wide, distinctly flattened, and can contract up to half the body length (Fig. 1). On the right side are about 34 longitudinal ciliary rows, while the left is barren except for the bristle kinety, which borders the barren area, the so-called glabrous stripe (Figs. 2, 3). At the right side of the glabrous stripe are several shortened kineties, which abut to the bristle kinety forming the anterior and posterior secant system (Figs. 3, 10). Furthermore, there is a special (lateral) kinety between the left branch of the bristle kinety and the first ordinary ciliary row (Fig. 4). The lateral kinety shows various specialisations, most notably subcortical fibres forming long bundles in the posterior region of the cell (Fig. 50). The cylindroidal apical end (head) contains distinct oral structures consisting of a circumoral ciliary row and, in midline of left side, a brosse composed of three minute, oblique kineties (Fig. 2).

Ontogenesis

All divisional stages shown were observed in at least three specimens. For descriptive purposes, the process was divided into 6 stages according to characteristic events. Division occurs in freely motile (non-encysted) condition and is homothetogenic. The parental daughter (proter) does not reorganise, that is, cell shape, oral apparatus and somatic infraciliature are maintained.

Stage 1 (Figs. 3-5, 8, 9, 14). Division commences with the formation of an oral primordium for the posterior daughter (opisthe) and a flat indentation in the prospective cleavage region. Thus, stomatogenesis and cytokinesis proceed concomitantly. The oral primordium develops near the cell surface slightly subequatorially in the first

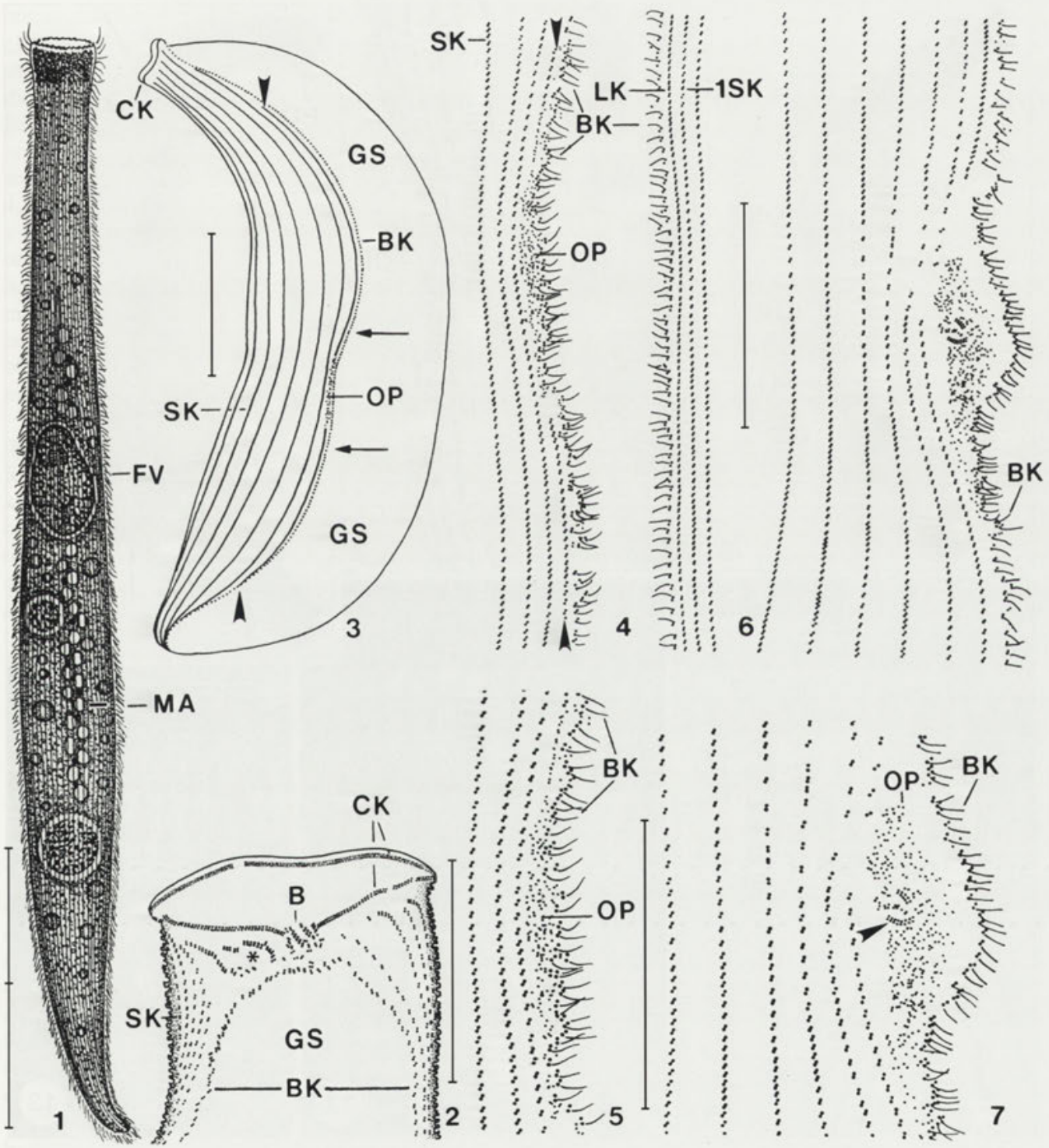

Figs. 1-7. *Sultanophrys arabica*, morphostatic (1, 2) and dividing cells (3-7) from life (1) and after silver impregnation (2-7). 1 - right side view of a fully extended specimen; 2 - left side view of anterior end. Asterisk marks kinetofragments, possibly remnants from oral primordium formation; 3-5 - very early divider, overview (3; for clarity only every second kinety is illustrated) and details of oral primordium (4, 5). Figure 4 shows the infraciliature at the right and left margin of the glabrous stripe. Arrows in Figure 3 border region shown at higher magnification in Figures 4 and 5. Arrowheads in Figure 3 mark anterior and posterior end of the stomatogenic kinety. Arrowheads in Figure 4 mark stomatogenic kinety. The oral primordium (OP) consists of an anarchic field of mainly single basal bodies. 6,7 - a slightly advanced stage showing that the bristle kinety is not involved in oral primordium formation. Dikinetidal fragments (arrowhead) commence to form in the oral primordium. B - brosse, BK - bristle kinety, CK - circumoral kinety, FV - food vacuole, GS - glabrous stripe, LK - lateral kinety, MA - macronuclear nodules, OP - oral primordium, SK - ordinary somatic kinety, 1SK - first ordinary left side somatic kinety. Bar division: 100 µm (Figs. 1, 3) and 30 µm (Figs. 2, 4-7)

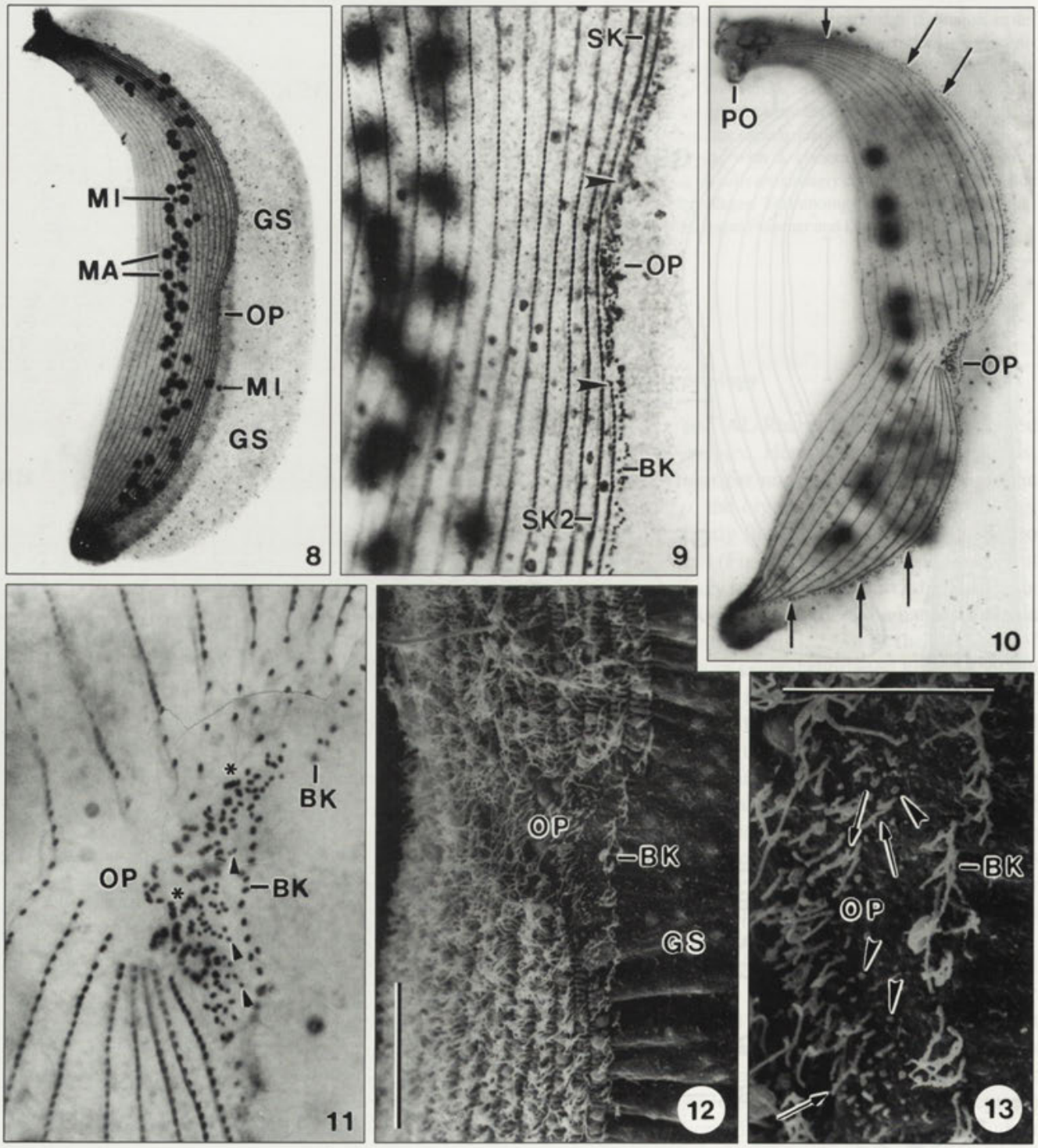

Figs. 8-13. *Sultanophrys arabica*, early dividers after silver impregnation (8 - 11) and in the scanning electron microscope (12, 13). 8, 9 - very early divider, overview and detail of oral primordium (bordered by arrowheads), which develops near mid-body in the first somatic kinety right of the glabrous stripe; 10, 11 - early divider, overview and detail showing that the bristle kinety is not involved in oral primordium formation (cp. Fig. 13). Arrows mark the anterior and posterior secant system, which is, uniquely, at the right side of the glabrous stripe in *S. arabica*. Arrowheads mark single basal bodies within the oral primordium. Asterisks denote developing dikinetidal fragments. Note that the somatic kineties divide without proliferation of basal bodies in the fission area; 12, 13 - oral primordium of an early divider, similar to that shown in Figures 10 and 11. Arrowheads mark stubs of growing cilia, arrows denote almost fully grown cilia. The bristle kinety is not involved in oral primordium formation (cp. Fig. 11). BK - bristle kinety, GS - glabrous stripe, MA - macronuclear nodules, MI - micronuclei, OP - oral primordium, PO - parental oral apparatus, SK2 - somatic kinety 2. Scale bars: 20 µm (Fig. 12) and 10 µm (Fig. 13)

ordinary somatic ciliary row at the right side of the glabrous stripe. This (stomatogenic) kinety is distinctly shortened anteriorly and posteriorly because it belongs to the secant system (Figs. 3, 10). The oral primordium is generated within an about 30 µm long area, where the ordered arrangement of the dikinetids disappears and an anarchic field of unciliated monokinetids develops (Figs. 4, 5, 9). The newly formed kinetids stain lighter and have a smaller diameter than ordinary somatic and bristle basal bodies. Within the bristle kinety, which is not involved in oral primordium formation (see next stage), rather many minute, unciliated granules appear, very likely forming basal bodies (Figs. 4, 5). The infraciliature at the left side of the glabrous stripe and the nuclear apparatus are still morphostatic (Figs. 4, 8, 14).

Stage 2 (Figs. 6, 7, 10-13, 15-17). This stage shows that the bristle kinety is not involved in oral primordium formation because a barren area develops between the kinety and the primordium. The oral primordium increases in breadth, but not in length, by further proliferation of basal bodies. The elliptical accumulation of disordered kinetids produced is clearly separate from the somatic kineties and the bristle kinety, which commences to bulge leftwards (Figs. 6, 7, 15, 16). Within the oral primordium, ciliary outgrowth commences and the kinetids become dikinetidal and some arrange to minute kinetofragments (Figs. 7, 11-13, 17). The somatic kineties right of the oral primordium become disrupted, as evident from the increased distances between the dikinetids in the prospective cleavage area (Figs. 6, 7, 10, 11). Possibly, some kinetids are also resorbed, as indicated by the rather large size of the barren area (Figs. 11, 19, 20).

Stage 3 (Figs. 18-24). This stage is characterised by curved kinetofragments in the oral primordium and the onset of micronuclear division. Compared to stage 2, the number of kinetids increases slightly in the oral primordium, which now consists mainly of dikinetids. The dikinetids commence to form short and long, curved kinetofragments which have cilia of usual length and migrate centrifugally to leave blank the prospective buccal cavity (Figs. 19, 22, 23). The somatic kineties become disrupted by stretching of the cleavage area, as indicated by the increased distances between the dikinetids and their meridional orientation (Figs. 18-21, 23), as well as by the subkinetal fibres, which project into the bare area (Fig. 20). Interestingly, kinety separation commences at both sides of the glabrous stripe and proceeds to midline of cell. Furthermore, disruption commences earlier in the kineties at the right side than at the left side of the glabrous stripe and is, at the left side, weakly correlated with stomatogenesis because it may commence in early or middle dividers. Anterior and posterior to the oral primordium, the bristle kinetids are more narrowly spaced than in morphostatic specimens, indicating that new bristles were produced, which is emphasised by rather many unciliated granules, some of which are very likely developing bristle kinetids (Fig. 23). The lateral kinety divides like the bristle kinety, that is, without anlagen formation (Fig. 23).

Usually, the nuclear apparatus commences to divide when the kinetofragments arrange around the prospective oral cavity. However, nuclear division may commence also earlier or later, indicating that it is only roughly correlated with stomatogenesis. The nuclear strand separates more or less distinctly in the cleavage area and the micronuclei get a more distinct membrane, increase in size, and stain lighter (Fig. 21). Sausage-shaped structures, possibly chromosomes, are recognisable within the micronuclei. The macronuclei do not divide.

Stage 4 (Figs. 25-33, 40, 44). Middle dividers assemble the opisthe's circumoral kinety and have metaphasic micronuclei. The kinetofragments produced in the oral primordium migrate centrifugally and assemble to a circular circumoral kinety, which surrounds a slightly elevated area, the prospective oral bulge (Figs. 25, 27-32, 40, 44). Between the newly formed circumoral kinety and the bristle kinety, which is distinctly bulged by the forming oral apparatus, remain scattered dikinetids and some short kinetofragments (Figs. 27, 29, 30, 40, 44). Most of the scattered dikinetids remain in the brosse area, while the kinetofragments become brosse kineties or migrate to the right of the brosse, where they remain (Fig. 2). Possibly, these fragments are reserved to replace lost parts of the circumoral kinety. Somatic division progresses to midline of right side. The division furrow is now distinct and slightly underneath mid-body (Figs. 28, 33). Thus, the proter is slightly larger than the opisthe.

The micronuclei increase in size approaching that of macronuclei and show metaphasic chromosomes and distinct spindle microtubules (Figs. 25, 26). Unfortunately, chromosome number could not be estimated because they were too tightly spaced.

Stage 5 (Figs. 34-39, 41-43, 47-49). Late dividers are characterised by a conspicuous division furrow (Figs. 41, 47), the disruption of the bristle kinety (Figs. 34 - 39), and the formation of the secant system (Figs. 35-39, 48, 49). The nuclear apparatus and the new (opisthe) oral apparatus are similar to those in middle dividers (cp. Figs. 29, 40, 44, 48). However, the opisthe oral apparatus accumulates highly refractive granules, like those found in the parental

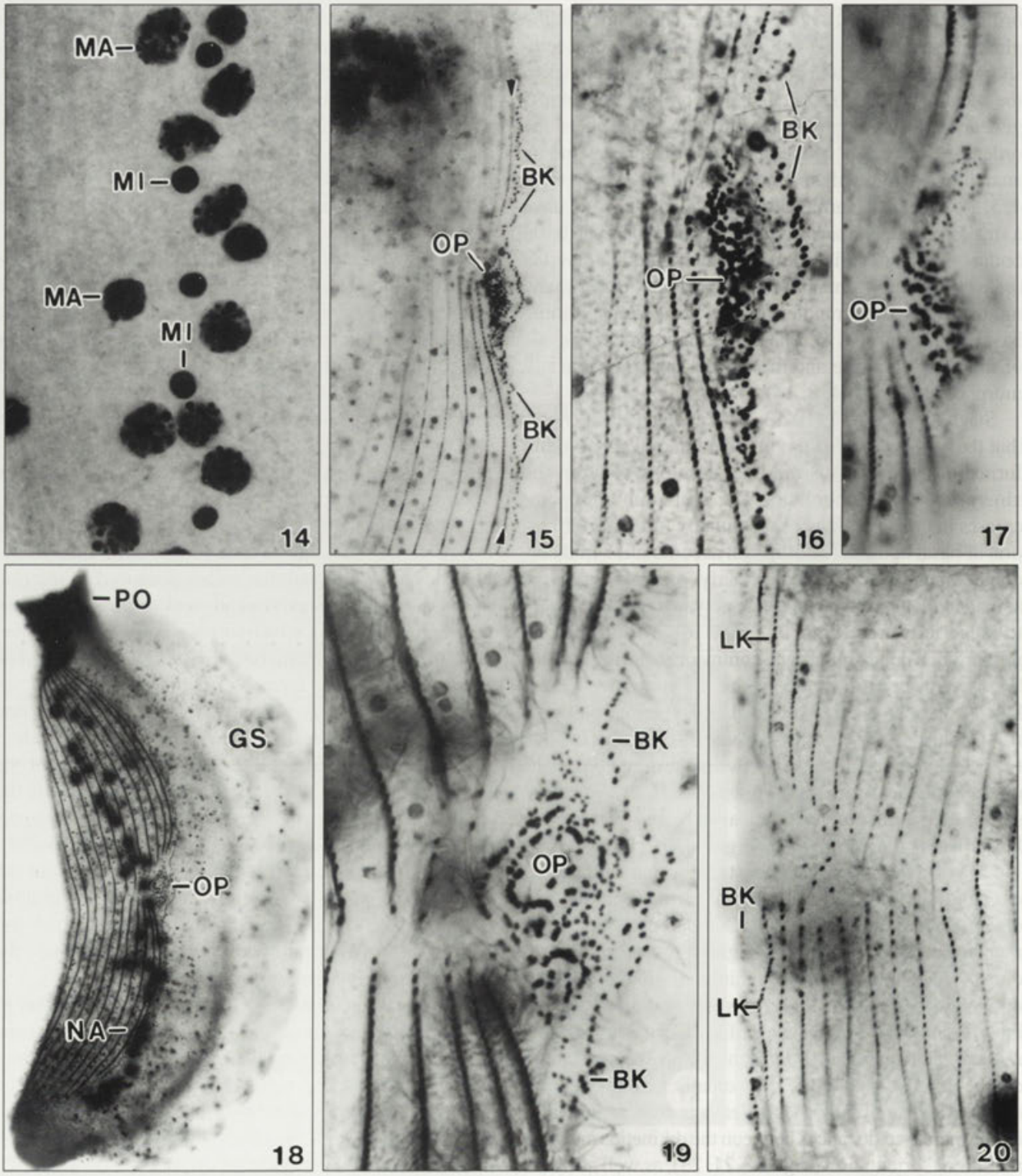

Figs. 14-20. *Sultanophrys arabica*, infraciliature and nuclear apparatus (14) of early dividers after silver impregnation. 14-17 - details from early dividers showing that the bristle kinety is not involved in oral primordium formation (15, 16) and kinetofragments are generated in the anarchic field (17). Arrowheads mark the stomatogenic kinety anterior and posterior of the oral primordium; 18-20 - overview and details of an early-middle divider; figures 19 and 20 show corresponding region at right and left margin of glabrous stripe. The kinetofragments commence to migrate around the prospective oral cavity and the somatic kineties disrupt in the fission area. BK - bristle kinety, GS - glabrous stripe, LK - lateral kinety, MA - macronuclei, MI - micronuclei, NA - nuclear apparatus, OP - oral primordium, PO - proter oral apparatus

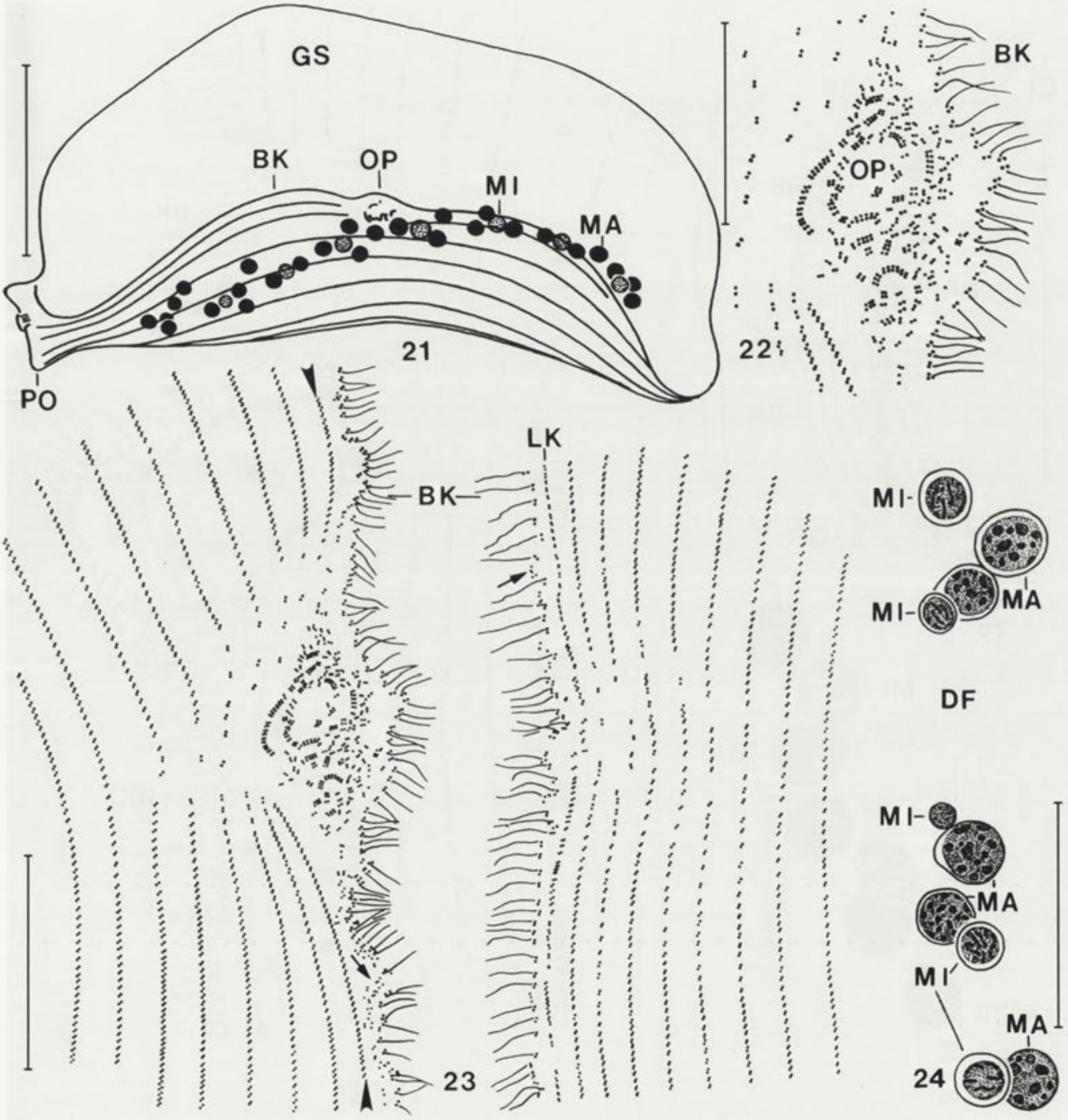

Figs. 21-24. *Sultanophrys arabica*, infraciliature of early dividers after silver impregnation. 21-23 - overview (21; for clarity only every second kinety is illustrated) and details from same specimen, showing the ciliary pattern of the division area at the right and left margin of the glabrous stripe (23). The oral primordium consists mainly of dikinetids, which arrange to curved kinetofragments around the prospective oral bulge. The somatic kineties become disrupted in the fission area; those right of the oral primordium will form proter's posterior secant system (cp. Figs. 34-39). Arrowheads mark somatic kinety 1, which generated the oral primordium (cp. Fig. 4). The bristle kinety and the lateral kinety are not involved in oral primordium formation and divide without anlagen, that is, are disrupted and new kinetids, some of which are still unciliated (arrows), are generated intrakinetally; 24 - middle region of nuclear apparatus of a similar specimen as shown in Figure 21. The nuclear strand is separating in the fission area and the micronuclei increase in size and become lighter stained (Fig. 21). The macronuclei do not divide. BK - bristle kinety, DF - division furrow, GS - glabrous stripe, MA - macronuclear nodules, MI - micronuclei, OP - oral primordium, PO - parental (proter) oral apparatus. Scale bars: 100 µm (Fig. 21), 30 µm (Figs. 23, 24), and 20 µm (Fig. 22)

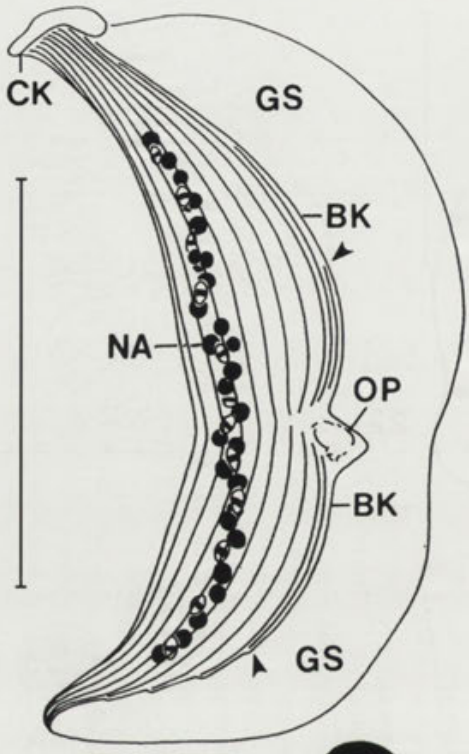

25

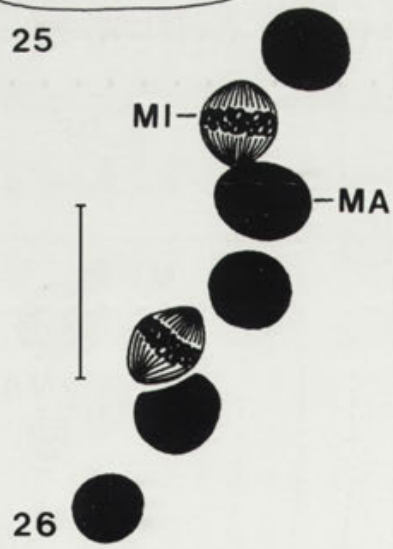

26

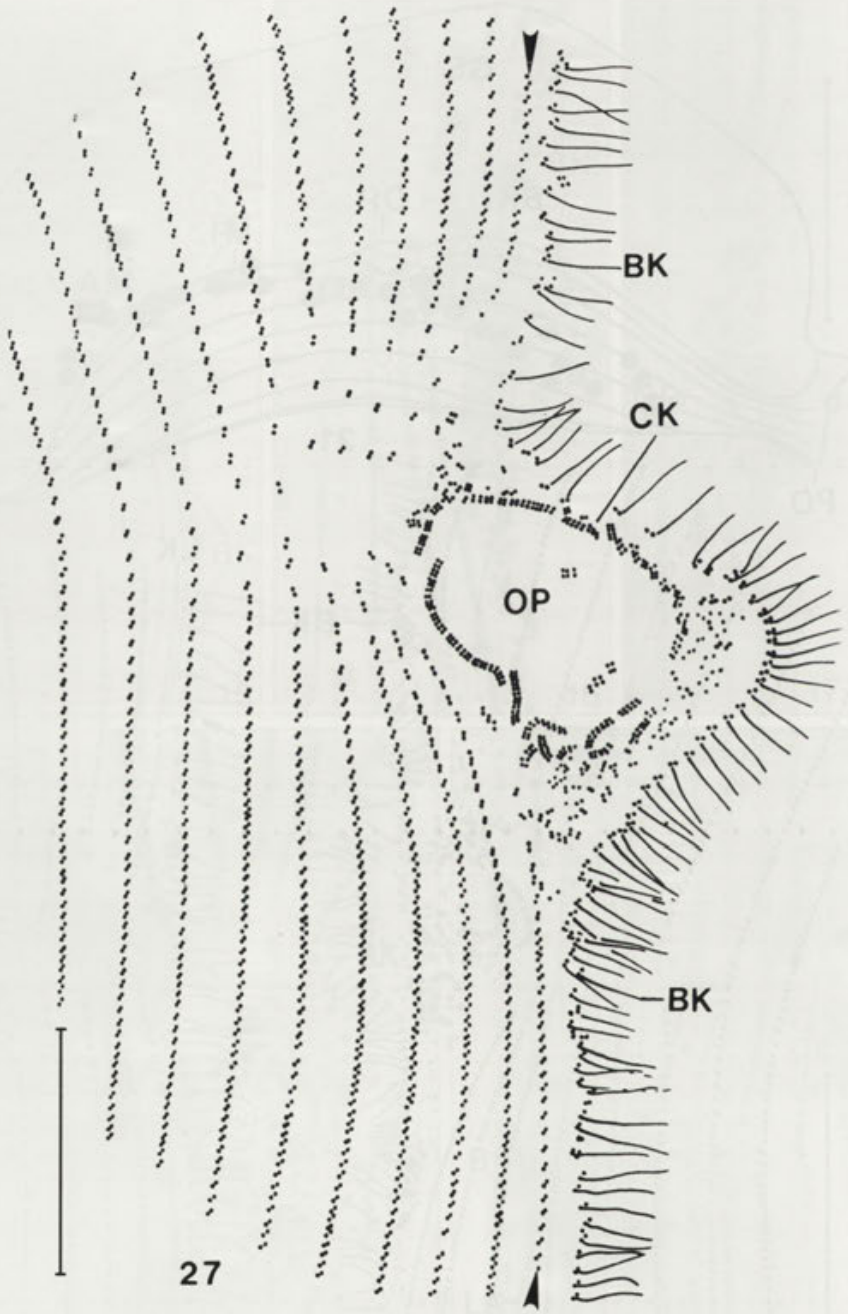

27

Figs. 25-27. *Sultanophrys arabica*, infraciliature and nuclear apparatus of a middle divider after silver impregnation (cp. Figs. 28, 33, 40, 44). Note that only half of the ciliary rows are illustrated in the overview, Figure 25. 25, 27 - middle dividers are furrowed slightly underneath mid-body and have assembled the newly formed oral kinetofragments to a distinct circumoral kinety, which surrounds the prospective oral bulge and strongly bulges the bristle kinety. Note that kinetids in the bristle kinety are more narrowly spaced than in morphostatic specimens, indicating that new kinetids were produced intrakinetally. In late dividers, the bristle kinety breaks at the summit of the bulge and orientates transversely to the cell's main axis to meet the bristle kinety at the left side of the glabrous stripe (Figs. 37-39). At the posterior margin of the circumoral kinety there are many scattered dikinetids and some small kinetofragments, some of which will become brosse kineties. Somatic division progresses to midline of right side. Arrowheads mark stomatogenic kinety anterior and posterior of the oral primordium; 26 - part of the nuclear apparatus of the specimen shown in Figure 25. The micronuclei multiply by mitosis and show distinct spindle microtubules and metaphasic chromosomes. The macronuclei do not divide. BK - bristle kinety, CK - circumoral kinety, GS - glabrous stripe, MA - macronuclear nodule, MI - micronucleus, NA - nuclear apparatus, OP - oral primordium. Scale bars: 200 µm (Fig. 25) and 20 µm (Figs. 26, 27)

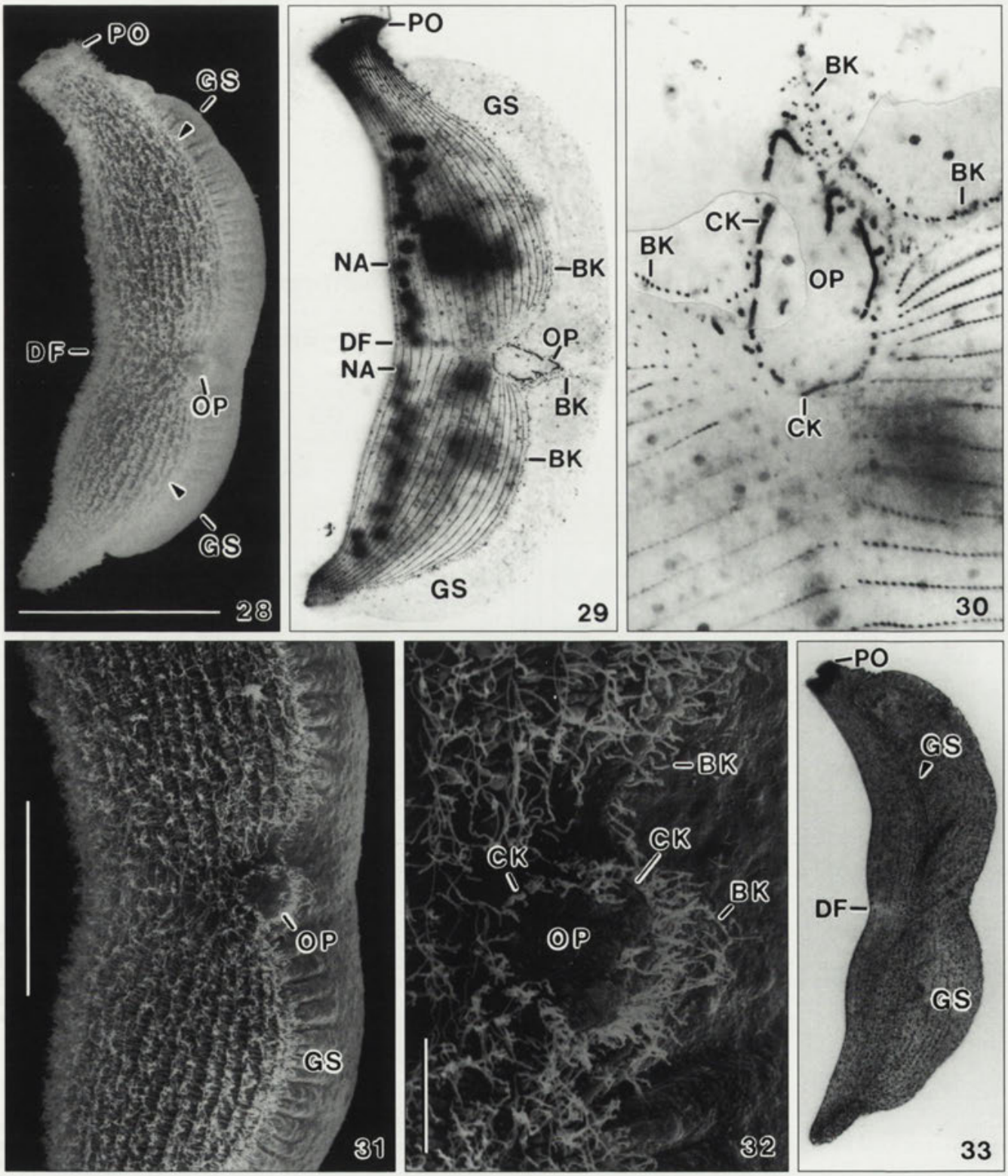

Figs. 28-33. *Sultanophrys arabica*, middle dividers in the scanning electron microscope (28, 31, 32; same specimen, overview and details of opisthe oral apparatus), after silver impregnation (29, 30; same specimen, overview and detail of opisthe oral apparatus), and from life (33). Middle dividers are furrowed slightly underneath mid-body and have assembled the newly formed oral kinetofragments to a distinct circumoral kinety, which surrounds the prospective, slightly elevated oral area. Somatic division proceeds to midline of right side. BK - bristle kinety, CK - circumoral kinety, DF - division furrow, GS - glabrous stripe, NA - nuclear apparatus, OP - oral primordium, PO - parental (proter) oral apparatus. Scale bars: 100 μm (Fig. 28), 50 μm (Fig. 31), and 10 μm (Fig. 32)

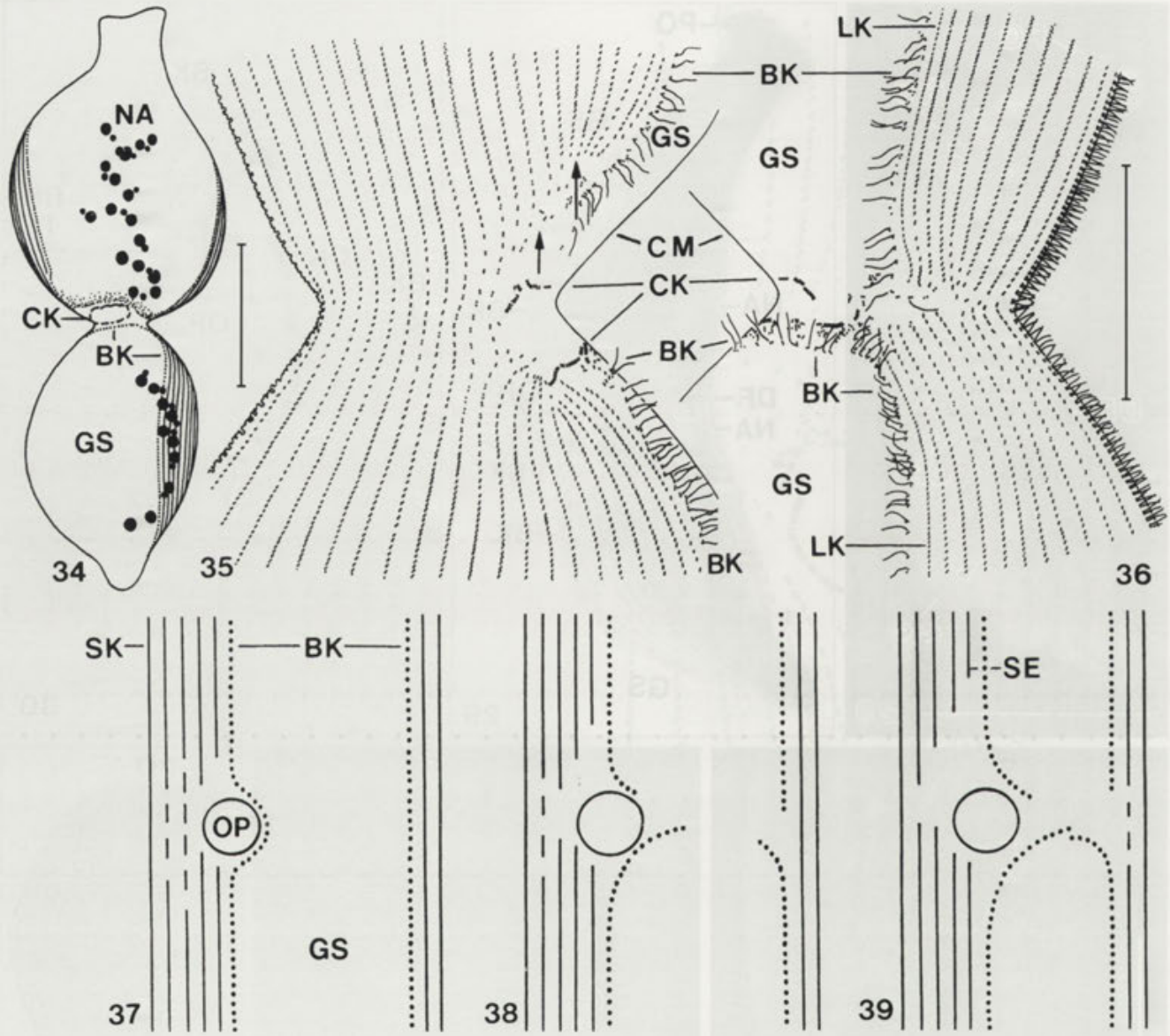

Figs. 34-39. *Sultanophrys arabica*, infraciliature of late dividers after silver impregnation. 34 - left side view showing location of opisthe's oral apparatus right of cell's midline; 35, 36 - a slightly distorted specimen, showing the cleavage area at both sides of the glabrous stripe. The bristle kinety disrupted and united with the bristle kinety extending along the left side of the glabrous stripe. Arrows mark shortened kineties, which will form proter's posterior secant system; 37-39 - scheme showing the disruption and patterning of the bristle kinety and the secant kineties. The ends of the bristle kinety unite due to the furrowing of the cell (indicated by decreased breadth of the cell in Fig. 39). BK - bristle kinety, CK - opisthe circumoral kinety, CM - cell's margin, GS - glabrous stripe, LK - lateral kinety, NA - nuclear apparatus, OP - oral primordium, SE - secant kineties, SK - ordinary somatic kinety. Scale bars: 100 μm (Fig. 34) and 50 μm (Figs. 35, 36)

Figs. 40-49. *Sultanophrys arabica*, middle (40, 44) and late (41-43, 47-49) dividers and postdividers (45, 46) from life (41-43, 45) and after silver impregnation (40, 44, 46-49). 40, 44 - opisthe oral area of middle dividers. Arrow marks kinetofragments and scattered dikinetids. For details, see explanations to Figures 27-33; 41-43 - in late dividers the new oral apparatus has accumulated highly refractive granules, which appear as black spot in the micrographs (arrow, OP); 45, 46 - postdividers have a highly characteristic, triangular shape; 47-49 - overview and details of a late divider. Figures 48 and 49 show the cleavage area right and left of the glabrous stripe. The organism is distinctly furrowed and the bristle kinety has been disrupted by cytokinesis: the posterior ends of the proter kinety will unite in postdividers, while the new (opisthe) anterior end curves left to unite with the bristle kinety at the left margin of the glabrous stripe (for a scheme, see Figs. 37-39). Arrowhead marks kinetofragments and scattered dikinetids, some of which will become brosse kineties. The shortened kineties (arrows) will form the posterior secant system, which is inconspicuous at the left margin of the glabrous stripe. BK - bristle kinety, CK - circumoral kinety, DF - division furrow, GS - glabrous stripe, NA - nuclear apparatus, OP - oral primordium (opisthe oral apparatus), PO - parental (proter) oral apparatus

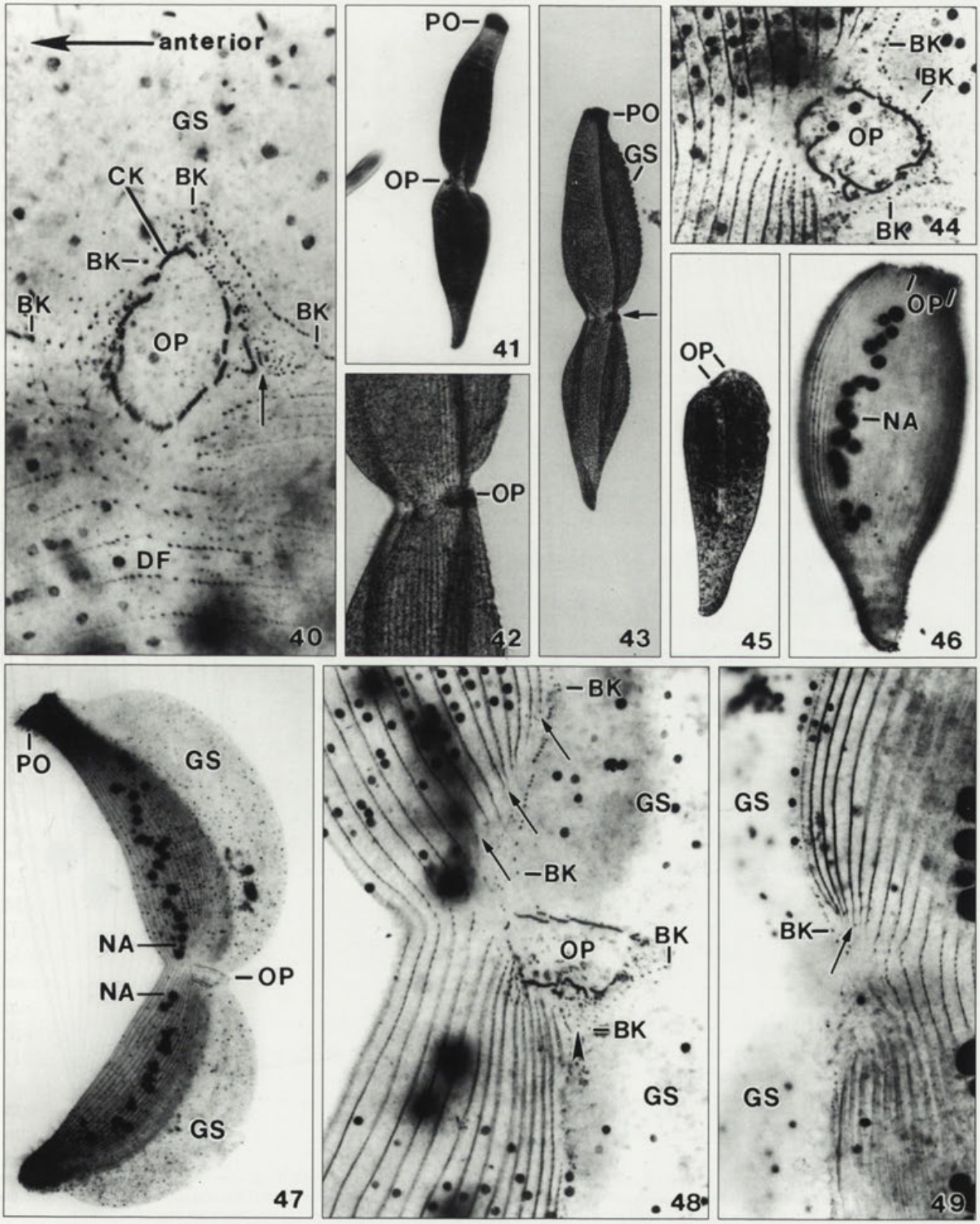

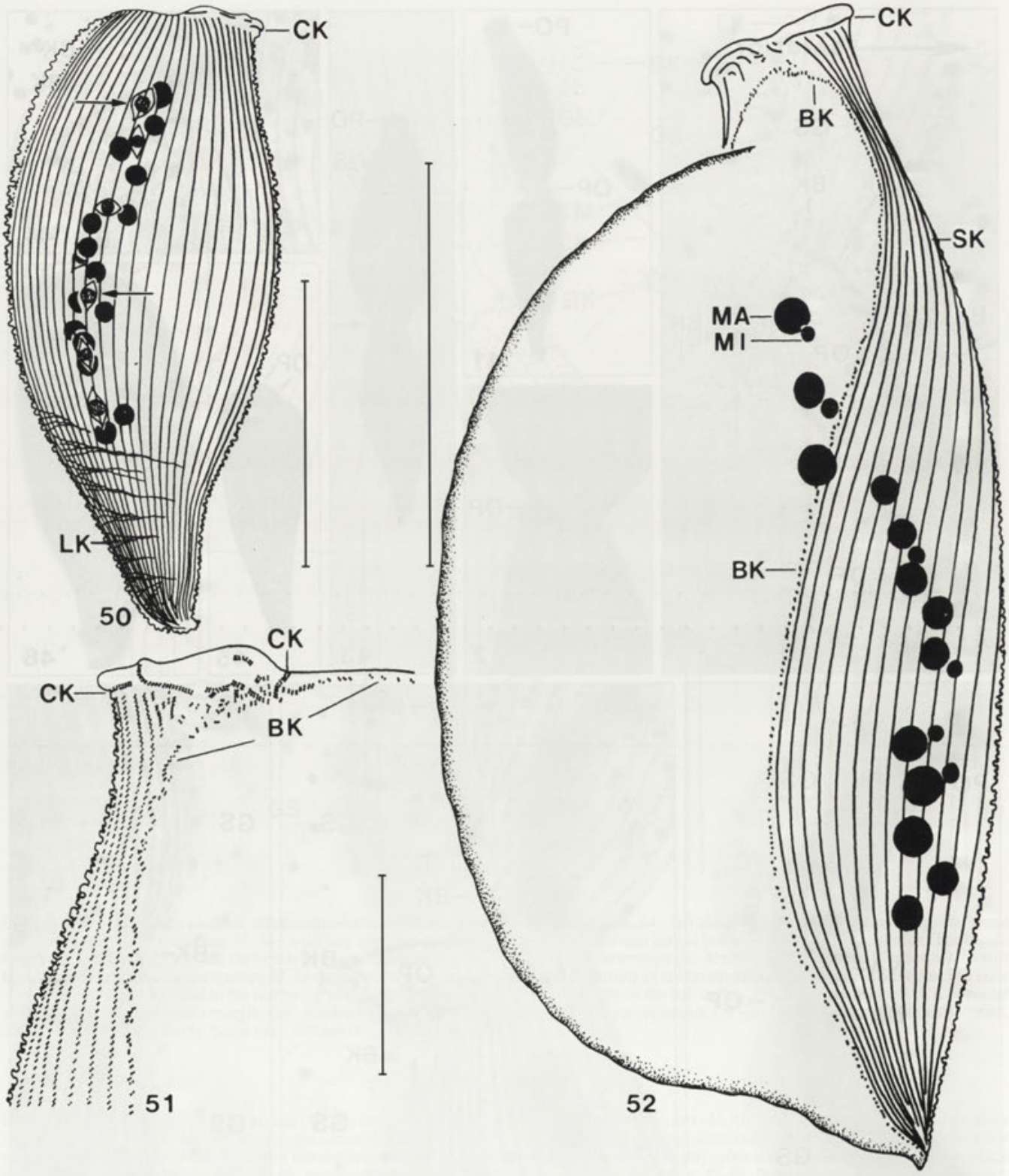

Figs. 50-52. *Sultanophrys arabica*, opisthe postdividers after silver impregnation. 50, 51 - right and left side view of an early postdivider. Arrows mark dividing micronuclei. Young opisthe postdividers have a characteristic triangular shape (cp. Fig. 45, 46), the oral apparatus left of midline, and the oral structures not yet fully assembled; 52 - late postdivider with growing neck and head. The oral structures are assembled and micronuclei division is complete. BK - bristle kinety, CK - circumoral kinety, LK - lateral kinety with conspicuous fibres, MA - macronuclear nodule, MI - micronucleus, SK - ordinary somatic kineties. Scale bars: 100 µm (Figs. 50, 52) and 30 µm (Fig. 51)

head, and thus appears as black spot, which is easily recognisable even at low magnification (x 40; Figs. 41-43). The opisthe, which is slightly smaller than the proter due to the subequatorial division furrow, obtains a very characteristic triangular shape, which is maintained in young postdividers (Figs. 41, 45). The bristle kinety breaks at the summit of the bulge formed by the oral primordium and unites, due to the decreasing diameter of the cell at the cleavage furrow, with the broken and rightwards curved end of the bristle kinety extending along the left margin of the glabrous stripe (Figs. 34-39). Details of this process are difficult to observe because the cleavage area of late dividers is usually rather distorted in the preparations. Indeed, late dividers are easily disrupted mechanically and then some oral kinetofragments of the opisthe remain at the posterior end of the proter.

Somatic division is not yet finished, that is, the kineties in the midline of the cell are still intact. The disrupted kineties along the right side of the oral primordium do not proliferate basal bodies posteriorly. Thus, the kineties, which abut to the opisthe's oral apparatus become shortened and form, when the daughters grow, the anterior and posterior secant system (Figs. 29, 30, 37-39, 47-49). The bare area is greater at the anterior than at the posterior margin of the oral primordium. Accordingly, the posterior secant system is more distinct than the anterior one. No or only an indistinct bare area occurs in the kineties at the left side of the glabrous stripe. Thus, *S. arabica* lacks a left side secant system (Foissner and AL-Rasheid 1999).

Stage 6 (Figs. 45, 46, 50-52). This stage comprises cell shaping of postdividers, which are about half the size of morphostatic specimens. Accordingly, there is distinct postdivisional growth in both cell size and kinetid number, although some are produced during division, as indicated by the decreased distances between the individual kinetids. Micronuclear division usually finishes in late dividers (Fig. 34) or young postdividers (Fig. 50). We never observed dividing micronuclei in morphostatic specimens, indicating that regulation of macronuclear and micronuclear number occurs in late dividers and postdividers by multiple division of micronuclei, as described by Raikov (1982).

Young postdivisional proters are flask-shaped, that is, much stouter than morphostatic specimens (Fig. 41); otherwise, however, they are similar to interphase cells because no changes occur in the proter during division. The posterior ends of the disrupted bristle kinety come close together during tail outgrowing. The fibres in the posterior portion of the lateral kinety increase in length and unite to the conspicuous bundles typical of interphase specimens (Fig. 50; Foissner and AL-Rasheid 1999).

Young postdivisional opisthes have a characteristic triangular shape because the parental tail is maintained and the neck and head are not yet developed (Fig. 45, 46, 50). The newly produced oral apparatus is still at the left margin of the cell and usually rather distorted, that is, the kinetofragments composing the circumoral kinety are disordered and the brosse has not yet fully assembled (Figs. 46, 50, 51). All oral structures obtain their final pattern and location only during postdivisional growth (Fig. 52).

DISCUSSION

Comparative stomatogenesis

Our investigations show that trachelocercids have a true oral apparatus consisting of a dikinetidal circumoral ciliary row and some minute, dikinetidal (brosse) kineties highly resembling prostomatid and oligohymenophorean adoral membranelles (Bardele 1989, Hiller 1992). These structures are involved in feeding (AL-Rasheid and Foissner 1999) and originate parakinetally, that is, the primordia are derived directly from a parental postoral somatic kinety and appear subequatorially at a location far removed from the parental mouth parts (Corliss 1979, Foissner 1996b). The bristle kinety and the lateral kinety are not involved in stomatogenesis and are thus specialised parts of the somatic ciliature.

A parakinetal stomatogenesis is typical of all heterotrichs *sensu stricto*[1], such as *Blepharisma* and *Eufolliculina*, and of tetrahymenine oligohymenophoreans (for review, see Foissner 1996 b). However, a more detailed analysis reveals that these parakinetal stomatogeneses are rather different, indicating convergent or long lasting separate evolution (Figs. 53-55). In heterotrichs *s. str.*, the oral primordium originates in one or several postoral kineties and then splits longitudinally: the smaller right portion becomes the paroral membrane, while the larger left part generates adoral membranelles from the centre towards the ends of the anarchic field (Fig. 54; for a detailed

[1] Note that ontogenesis in *Metopus* and relatives, considered as typical heterotrichs for more than 100 years, is very different from that of *Blepharisma* and relatives (Foissner and Agatha 1999). Thus, metopids do not belong to the heterotrichs, as also indicated by gene sequences (Lynn and Small 1997, Hirt *et al.* 1998).

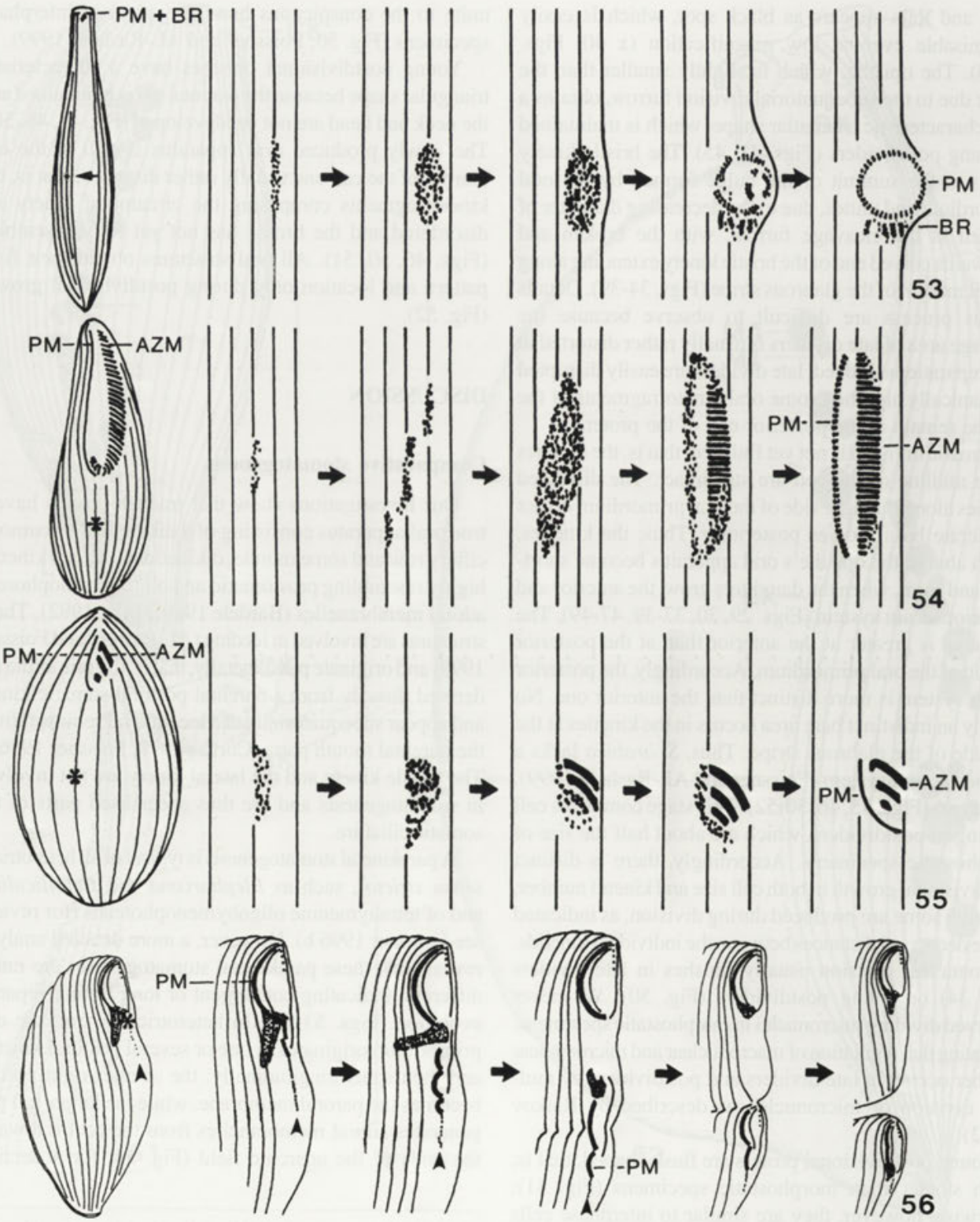

Figs. 53-56. Diagrams of parakinetal (53-55) and bucocinetal (56) stomatogenesis, 53 - a trachelocercid karyorelictean (*Sultanophrys*), 54 - a heterotrich *s. str.* (*Blepharisma*; after Aescht and Foissner 1998), 55 - a hymenostome oligohymenophorean (*Tetrahymena*, after Foissner 1996b), and 56 - buccokinetal stomatogenesis in the karyorelictean *Loxodes* (from Bardele and Klindworth 1996). Figures in the left column show the somatic and oral ciliary pattern, and the site, where the oral primordium originates, is marked by an asterisk (plus arrow in *Sultanophrys*). The somatic ciliary rows are shown as simple, straight lines. Arrowheads in *Loxodes* mark a scutica-like kinetofragment. AZM - adoral zone of membranelles, BR - brosse (possibly homologous to AZM), PM - paroral membrane (circumoral kinety). See text for detailed explanation

analysis, see Aescht and Foissner 1998). There are no migrating kinetofragments, as in *Sultanophrys*, which, on the other hand, does not split the anarchic field in a right and a left portion. In this respect and by the minute brosse kineties, *Sultanophrys* resembles hymenostome oligohymenophoreans, some of which even have minute, migrating kinetofragments, which assemble to adoral membranelles, for instance *Ichthyophthirius multifiliis* (Foissner 1996b). Furthermore, the oral primordium of *Sultanophrys* develops, like in tetrahymenine oligohymenophoreans (Foissner 1996b), within a "director meridian", that is, a specialised (shortened) postoral kinety. This kinety is generated by the special location of the forming oral apparatus within the right lateral ciliary rows. Here, the oral primordium intersects some somatic ciliary rows, which thus become postoral, at least during ontogenesis (Figs. 11, 19, 29, 37-39), and form the secant system in morphostatic cells (Fig. 10; Foissner and AL-Rasheid 1999). Thus, considered from a descriptive view, stomatogenesis of *Sultanophrys* is more similar to that of hymenostome oligohymenophoreans than to that of heterotrichs. However, the somatic ultrastructures of hymenostomes and karyorelictids are very different (for review, see Lynn 1981), indicating that the stomatogenic similarities evolved convergently.

The migrating kinetofragments of *Sultanophrys* are a conspicuous character, as they are in prostomatid ciliates, where they form, as in *Sultanophrys*, the circumoral kinety and the brosse, which, in prostomatids, is very likely homologous to the hymenostome adoral membranelles (Bardele 1989, Hiller 1992). However, these similarities are likely superficial and convergent because the prostomatid kinetofragments do not originate from an anarchic field, as in *Sultanophrys* (Fig. 19), but at the broken ends of several ventral kineties (Bardele 1989, Hiller 1992, Foissner 1996b). The same applies to the gymnostomes (litostomes), which produce kinetofragments holotelokinetally, that is, at the anterior end of *all* somatic kineties. By a slight rotation, the fragments unite to a circumoral kinety (for review, see Foissner 1996b).

Finally, we have to discuss stomatogenesis of *Loxodes*, the only other karyorelictid investigated so far. *Loxodes* has a buccokinetal stomatogenesis, where dikinetidal kinetofragments are generated at or from the posterior end of the parental paroral (Bardele and Klindworth 1996). Several such fragments are produced, migrate posteriorly, and assemble to the opisthe's paroral in mid-body. The left side oral ciliature is not generated from a special anlage but by proliferation of kinetids within the parental structures (Fig. 56). Furthermore, *Loxodes* has a ventral kinetofragment, which, in terms of location and divisional behaviour, highly resembles the scutica of oligohymenophorean scuticociliates (Bardele and Klindworth 1996, Foissner 1996b). Both a scutica-like structure and a contribution of parental mouth structures to the opisthe oral apparatus are lacking in *Sultanophrys*. Accordingly, ontogenesis looks very different in loxodid and trachelocercid karyorelictids. On the other hand, we must not overlook that the paroral ciliature is produced in both taxa by *migrating* kinetofragments, whose origin is, however, different. Of particular interest is the left side oral ciliature of *Loxodes*, which is, like ordinary somatic kineties, produced by intrakinetal proliferation of kinetids. This could indicate that these kineties are not yet fully oralised somatic ciliature (Bardele and Klindworth 1996, Foissner 1996b) and, in turn, that the oral ciliature evolved from somatic ciliature, as proposed by Small (1984) and Foissner (1995b). See last chapter for a more detailed discussion of this matter.

Evolution of stomatogenic modes

Karyorelictids and heterotrichs are sister groups and at the base of the ciliate tree, according to the somatic cortical ultrastructure and gene sequences (for reviews, see Lynn and Small 1997, Hirt *et al.* 1998). Each of these groups has a distinct stomatogenesis, and even two modes are found in the karyorelictids. Accordingly, three stomatogenic modes occur at the base of the ciliate tree, indicating an explosive radiation of this trait. Furthermore, we are confronted with the fact that the ontogenetic pattern of both loxodids and trachelocercids shows remarkable similarities with that of oligohymenophorean ciliates: the ventral kinetofragment of loxodids resembles the scutica of oligohymenophorean scuticociliates (Bardele and Klindworth 1996, Foissner 1996a), while the parakinetal stomatogenesis of trachelocercids resembles hymenostome oligohymenophoreans (for reviews, see Foissner 1995a, 1996b). Although we tend to interpret these similarities as convergently evolved, we can not exclude a deeper meaning at the present state of knowledge.

The data available do not provide unambiguous evidence, which of the three stomatogenic modes found in the Postciliodesmatophora is ancestral. There are, however, two indicators which favour the parakinetal mode: (1) it occurs in both heterotrichs and the largest group of karyorelictids, and (2) somatic division is more similar in heterotrichs and trachelocercids than in loxodids and trachelocercids (see next chapter). Bardele and Klindworth (1996), on the contrary, suggest that the parakinetal mode

evolved from the buccokinetal mode. They hypothesise that detailed analyses would probably show a scutica-like structure, similar to that found in *Loxodes*, also in typical heterotrichs, such as *Blepharisma* and *Stentor*. However, such structures were not found in a detailed reinvestigation of the stomatogenesis of *Blepharisma*, although the reorganisation anlage for the parental oral apparatus shows some similarities with a scutica (Aescht and Foissner 1998).

Comparative somatic ontogenesis

The somatic ontogenesis of *Sultanophrys* shows four peculiarities: (1) the division furrow is recognisable very early, that is, when stomatogenesis commences (Figs. 8, 10); (2) there is a distinct cleavage gradient proceeding from the margins to the centre of the ciliary field (Figs. 19, 20, 23); (3) there is not, as is usual, proliferation but rarefaction of kinetids in the cleavage area; (4) there is pronounced postdivisional patterning, which is very likely associated with the slender shape and high contractility of the trachelocercids. The rarefaction of kinetids in the cleavage area is possibly the most important feature because it is also found in *Blepharisma* (Aescht and Foissner 1998), while in *Loxodes* "the first sign of cell division is the proliferation of kinetosomes in the somatic kineties in the middle of the cell at a site of the future cleavage furrow" (Bardele and Klindworth 1996).

Loxodid and trachelocercid karyorelictids have a special (bristle) kinety, which frames a more or less broad, non-ciliated (glabrous) stripe (Foissner and Dragesco 1996b). Both the bristle kinety and the glabrous stripe are lacking in the geleiids (Dragesco and Dragesco-Kernéis 1986, own unpublished observation), the third and most enigmatic group of karyorelictids (Foissner 1998). The bristle kinety has a specialised infraciliature and very peculiar ciliation, first described by Foissner and Dragesco (1996a, b): "The bristle kinety commences subapically at the right margin of the glabrous stripe, extends posteriorly, then anteriorly at the left, to end up at the right margin again. The dikinetids of the right posterior portion of the bristle kinety have the *posterior* basal body ciliated, whereas the *anterior* basal bodies are ciliated in its left and right anterior portion". Thus, the ciliation of the dikinetids is opposed by 180° where the ends of the kinety meet. These features suggested that the bristle kinety could play a special role in ontogenesis (Foissner and Dragesco 1996b), which is, however, disproved by the present results: it simply disrupts during cytokinesis. Unfortunately, we could not observe how the peculiar ciliation at the anterior end of the bristle kinety is brought about because all very late dividers were too strongly distorted or the cilia had not impregnated clearly enough. It is, however, clear that the process occurs only in very late dividers (because the morphostatic pattern is still recognisable in late dividers, Fig. 27) and the circumoral ciliature is not involved, as speculated by Foissner and Dragesco (1996b).

In any case, the bristle kinety, although being "silent" ontogenetically, is a highly interesting specialisation, clearly defining loxodids and trachelocercids as sister groups. It is a pity that neither ontogenesis nor comparative morphology gives any information about its origin and history. We do not know of any other ciliates with a similar kinety. Thus, it is possibly a young, special trait, which could provide us with important information about the history of the karyorelictids, when we would be lucky to discover a ciliate with the plesiomorphic state.

Evolution of ciliate cytoarchitecture

This matter is thoroughly discussed in recent reviews by Bardele and Klindworth (1996) and Schlegel and Eisler (1996), to which the reader is referred for detailed information. Here, we shall discuss only some aspects which are related to the karyorelictids and the present results.

Karyorelictids have been postulated as a model for ancestral ciliates because they have non-dividing macronuclei and one of the genera, *Kentrophoros*, is even mouthless (Corliss 1974, Orias 1976, Small 1984). *Kentrophoros* has a symbiotic kitchen garden of sulphur bacteria on the glabrous stripe. The bacteria are ingested through the stripe, which stimulated Small (1984), among others, to suppose that trachelocercids also feed through the glabrous stripe. This has been disproved meanwhile (AL-Rasheid and Foissner 1999). Likewise, detailed investigations showed that *Kentrophoros* has vestiges of an oral apparatus at and near the anterior end, indicating that it is secondarily mouthless (Foissner 1995c), as also proposed by Bardele and Klindworth (1996). Accordingly, the hypotheses of Orias (1976) and Small (1984) lost a basic assumption.

Orias' (1976) and Small's (1984) hypotheses require that the oral ciliature evolved from somatic ciliature, while Eisler (1992; for an update, see Schlegel and Eisler 1996) assumes just the reverse. Based on detailed ultrastructural and ontogenetical investigations of ventrostomial ciliates, Eisler (1992) suggests that a paroral kinety (undulating membrane) gave rise, due to lateral multiplication, to

somatic ciliary rows, which, in turn, produced adoral membranelles. Accordingly, Eisler (1992) assumes that ancestral ciliates had a buccokinetal stomatogenesis. This is supported by recent data on *Loxodes* (Bardele and Klindworth 1996); however, Bardele and Klindworth (1996) conclude "none of the extant karyorelictean makes a good model for the ancestral karyorelictean species". We agree because extant karyorelictids have a highly specialised somatic ciliary pattern and trachelocercids and heterotrichs have a somatic (parakinetal) stomatogenesis, indicating that *Loxodes* is derived. Furthermore, our studies on several loxodids indicate that their oral ciliature evolved from somatic ciliature (Foissner 1995a, b).

Lynn's (1996) subphyletic division of ciliates

The present data and those from *Metopus* (Foissner and Agatha 1999) provide little insights into the subphyletic division suggested by Lynn (1996) and Lynn and Small (1997). However, at least the main stomatogenic mode is the same in heterotrichs *s. str.* and trachelocercid karyorelictids, that is, in two groups classified by Lynn and Small (1997) in the subphylum Postciliodesmatophora. If the parakinetal stomatogenesis of certain oligohymenophoreans is considered as convergently evolved or as at all different from that of heterotrichs and karyorelictids, as suggested by Foissner (1996b), then the parakinetal stomatogenic mode is unique to the Postciliodesmatophora. Loxodids then must be considered as derived, and the Geleiidae await further investigations.

Due to the experience with metopids and trachelocercids, we agree with Lynn (personal communication) that stomatogenic modes can hardly be used to unravel the main paths of ciliate evolution, as long as we do not know the underlying mechanisms to differentiate between analogies and homologies. Our present terms (parakinetal, buccokinetal....) are purely descriptive for *where* the replication and patterning of the oral apparatus occur.

Acknowledgements. The senior author thanks the King Saud University at Riyadh for invitation and financial support. The technical assistance of B. Moser, Dr. E. Herzog, and Mag. E. Strobl is greatly appreciated.

REFERENCES

Aescht E., Foissner W. (1998) Divisional morphogenesis in *Blepharisma americanum*, *B. undulans*, and *B. hyalinum* (Ciliophora: Heterotrichida). *Acta Protozool.* **37:** 71-92

AL-Rasheid K. A. S., Foissner W. (0000) Apical feeding in *Sultanophrys arabica* (Ciliophora, Karyorelictea). *J. Euk. Microbiol.* (in press)

Bardele C. F. (1989) From ciliate ontogeny to ciliate phylogeny: a program. *Boll. Zool.* **56:** 235-244

Bardele C. F., Klindworth T. (1996) Stomatogenesis in the karyorelictean ciliate *Loxodes striatus*: a light and scanning microscopical study. *Acta Protozool.* **35:** 29-40

Corliss J. O. (1974) Remarks on the composition of the large ciliate class Kinetofragmophora de Puytorac *et al.*, 1974, and recognition of several new taxa therein, with emphasis on the primitive order Primociliatida n. ord. *J. Protozool.* **21:** 207-220

Corliss J. O. (1979) The Ciliated Protozoa. Characterization, Classification and Guide to the Literature. 2nd ed. Pergamon Press, Oxford, New York, Toronto, Sydney, Paris, Frankfurt.

Dragesco J., Dragesco-Kernéis A. (1986) Ciliés libres de l'Afrique intertropicale. *Faune tropicale* **26:** 1-559

Eisler K. (1992) Somatic kineties or paroral membrane: which came first in ciliate evolution? *BioSystems* **26:** 239-254

Foissner W. (1991) Basic light and scanning electron microscopic methods for taxonomic studies of ciliated protozoa. *Europ. J. Protistol.* **27:** 313-330

Foissner W. (1995a) A redescription of *Remanella multinucleata* (Kahl, 1933) nov. gen., nov. comb. (Ciliophora, Karyorelictea), emphasizing the infraciliature and extrusomes. *Europ. J. Protistol.* **32:** 234-250

Foissner W. (1995b) The infraciliature of *Cryptopharynx setigerus* Kahl, 1928 and *Apocryptopharynx hippocampoides* nov. gen., nov. spec. (Ciliophora, Karyorelictea), with an account on evolution in loxodid ciliates. *Arch. Protistenk.* **146:** 309-327

Foissner W. (1995c) *Kentrophoros* (Ciliophora, Karyorelictea) has oral vestiges: a reinvestigation of *K. fistulosus* (Fauré-Fremiet, 1950) using protargol impregnation. *Arch. Protistenk.* **146:** 165-179

Foissner W. (1996a) Updating the trachelocercids (Ciliophora, Karyorelictea). II. *Prototrachelocerca* nov. gen. (Prototrachelocercidae nov. fam.), with a redescription of *P. fasciolata* (Sauerbrey, 1928) nov. comb. and *P. caudata* (Dragesco & Raikov, 1966) nov. comb. *Europ. J. Protistol.* **32:** 336-355

Foissner W. (1996b) Ontogenesis in ciliated protozoa, with emphasis on stomatogenesis. In: Ciliates. Cells as Organisms, (Eds. K. Hausmann and P. C. Bradbury). Fischer Verlag, Stuttgart, Jena, New York **46:** 174-193

Foissner W. (1998) The karyorelictids (Protozoa: Ciliophora), a unique and enigmatic assemblage of marine, interstitial ciliates: a review emphasizing ciliary patterns and evolution. In: Evolutionary Relationships among Protozoa, (Eds. G. H. Coombs, K. Vickermann, M. A. Sleigh and A. Warren). Kluwer Academic Publishers, Dordrecht, Boston, London, 305-325

Foissner W., Agatha S. (1999) Morphology and morphogenesis of *Metopus hasei* Sondheim, 1929 and *M. inversus* (Jankowski, 1964) nov. comb. (Ciliophora, Metopida). *J. Euk. Microbiol.*

Foissner W., AL-Rasheid K. A. S. (1999) Updating the trachelocercids (Ciliophora, Karyorelictea). VI. A detailed description of *Sultanophrys arabica* nov. gen., nov. spec. (Sultanophryidae nov. fam.). *Europ. J. Protistol.* **35:** 146-160

Foissner W., Dragesco J. (1996a) Updating the trachelocercids (Ciliophora, Karyorelictea). I. A detailed description of the infraciliature of *Trachelolophos gigas* n. g., n. sp. and *T. filum* (Dragesco & Dragesco-Kernéis, 1986) n. comb. *J. Euk. Microbiol.* **43:** 12-25

Foissner W., Dragesco J. (1996b) Updating the trachelocercids (Ciliophora, Karyorelictea). III. Redefinition of the genera *Trachelocerca* Ehrenberg and *Trachelorаphis* Dragesco, and evolution in trachelocercid ciliates. *Arch. Protistenk.* **147:** 43-91

Gerassimova Z. P., Seravin L. N. (1976) Ectoplasmic fibrillar system of infusoria and its role for the understanding of their phylogeny. *Zool. Zh.* **55:** 645-656 (in Russian with English summary)

Hiller S. A. (1992) *Bursellopsis spaniopogon* (Ciliophora: Prostomatida) II. Stomatogenesis as revealed by light microscopy and scanning electron microscopy and some phylogenetic implications concerning prostome ciliates. *Europ. J. Protistol.* **28:** 102-119

Hirt R. P., Wilkinson M., Embley M. T. (1998) Molecular and cellular evolution of ciliates: a phylogenetic perspective. In: Evolutionary Relationships among Protozoa, (Eds. G. H. Coombs, K. Vickermann, M. A. Sleigh and A. Warren). Kluwer Academic Publishers, Dordrecht, Boston, London, 327-340

Klindworth T., Bardele C. F. (1996) The ultrastructure of the somatic and oral cortex of the karyorelictean ciliate *Loxodes striatus*. *Acta Protozool.* **35:** 13-28

Lynn D. H. (1981) The organization and evolution of microtubular organelles in ciliated protozoa. *Biol. Rev.* **56:** 243-292

Lynn D. H. (1996) My journey in ciliate systematics. *J. Euk. Microbiol.* **43:** 253-260

Lynn D. H., Small E. B. (1997) A revised classification of the phylum Ciliophora Doflein, 1901. *Revta Soc. mex. Hist. nat.* **47:** 65-78

Orias E. (1976) Derivation of ciliate architecture from a simple flagellate: an evolutionary model. *Trans. Am. microsc. Soc.* **95:** 415-429

Orias E. (1991) On the evolution of the karyorelict ciliate life cycle: heterophasic ciliates and the origin of the ciliate binary fission. *BioSystems* **25:** 67-73

Raikov I. B. (1958) Der Formwechsel des Kernapparates einiger niederer Ciliaten. I. Die Gattung *Trachelocerca*. *Arch. Protistenk.* **103:** 129-192

Raikov I. B. (1982) The protozoan nucleus. Morphology and evolution. *Cell Biol. Monogr.* **9:** XII + 474 pp

Raikov I. B., Gerassimova-Matvejeva Z. P., Puytorac P. de (1975) Cytoplasmic fine structure of the marine psammobiotic ciliate *Trachelorаphis dogieli* Raikov. I. Somatic infraciliature and cortical organelles. *Acta Protozool.* **14:** 17-42

Schlegel M., Eisler K. (1996) Evolution of ciliates. In: Ciliates. Cells as Organisms, (Eds. K. Hausmann and P. C. Bradbury). Fischer Verlag, Stuttgart, Jena, New York, 73-94

Small E. B. (1984) An essay on the evolution of ciliophoran oral cytoarchitecture based on descent from within a karyorelictean ancestry. *Origins of Life* **13:** 217-228

Tuffrau M. (1961) Les structures infraciliaires et la stomatogenèse chez les *Loxodes*. Proc. 1st Internat. Congr. Protozool., Prague: 278-280

Received on 29th December, 1998; accepted on 6th May, 1999

Acta Protozool. (1999) 38: 291 - 298

ACTA
PROTOZOOLOGICA

Biochemical and Spectroscopic Characterization of the Cyanobacterium *Lyngbya* sp. Inhabiting Mango (*Mangifera indica*) Trees: Presence of an Ultraviolet-Absorbing Pigment, Scytonemin

Rajeshwar P. SINHA[1,2], Manfred KLISCH[1], Akhouri VAISHAMPAYAN[2] and Donat-P. HÄDER[1]

[1]Institut für Botanik und Pharmazeutische Biologie, Friedrich-Alexander-Universität, Erlangen, Germany; [2]Photobiological Nitrogen Fixation Research Laboratory, Department of Genetics and Plant Breeding, Institute of Agricultural Sciences, Banaras Hindu University, Varanasi, India

Summary. Dried, yellow-brown, leathery mats of a cyanobacterium were collected from the bark of mango (*Mangifera indica*) trees and characterized by biochemical and spectroscopic methods. Based on morphological characteristics, the strain was identified as *Lyngbya* sp., a filamentous and non-heterocystous cyanobacterium belonging to the order Oscillatoriales. The sheath of *Lyngbya* sp. was typically colored by a yellow-brown, UV-absorbing pigment, scytonemin. The phycobiliproteins from *Lyngbya* sp. were separated into six vividly colored fractions by sucrose density gradient ultracentrifugation. SDS-PAGE analyses of the fractions revealed the presence of α and β subunits of phycocyanin (around 20 kDa) and phycoerythrin (around 22 kDa). In addition, the mostly non-pigmented rod and rod-core (molecular masses between 24 and 45 kDa) and core-membrane (molecular masses around 66 kDa) linker polypeptides were also detected on SDS-PAGE. Spectroscopic analyses of the fractions also confirmed the presence of phycobiliproteins viz., phycoerythrin (560 nm), phycocyanin (620 nm) and allophycocyanin (650 nm). HPLC analysis of the samples revealed the existence of UV-absorbing/screening pigment, scytonemin, with an absorption maximum at 386 nm in the UV-A (315 - 400 nm) range. In addition, the purified scytonemin also absorbed significantly in the UV-B (280 - 315 nm) and UV-C (100 - 280 nm) regions with peaks at 300, 278, 252 and 212 nm. The presence of mycosporines could not be detected.

Key words: HPLC analysis, *Lyngbya*, *Mangifera indica*, phycobiliproteins, scytonemin, SDS-PAGE, spectroscopy.

Abbreviations: EDTA - ethylenediamine tetraacetic acid, HPLC - high performance liquid chromatography, PMSF - phenylmethylsulfonylfluoride, SDS-PAGE - sodium dodecyl sulfate-polyacrylamide gel electrophoresis, UV - ultraviolet.

INTRODUCTION

The members of cyanobacteria are unique in their cosmopolitan distribution ranging from hot springs to arctic regions, and they are therefore expected to encounter different types of stresses in their natural environment (Tandeau de Marsac and Houmard 1993). The colonization of diverse habitats by cyanobacteria demands a high variability in adaptation to various environmental stimuli (Sinha and Häder 1996).

The phycobiliproteins of cyanobacteria serve as accessory light harvesting pigments organized in macromolecu-

Address for correspondence: Donat-P. Häder, Institut für Botanik und Pharmazeutische Biologie, Friedrich-Alexander-Universität, Staudtstr. 5, D-91058 Erlangen, Germany; Tel.: +49 9131 8528216; Fax: +49 9131 8528215; E-mail: dphaeder@biologie.uni-erlangen.de

lar complexes called phycobilisomes (Glazer 1989, Grossman *et al.* 1993). Each phycobiliprotein is made up of two different subunits, α and β, which usually occur in equal amount but differ in their molecular weight, chromophore content and amino acid sequence. In addition, phycobilisomes also contain about 15 % of proteins, most of which lack a chromophore, referred to as linker polypeptides, mainly divided into rod, rod-core and core-membrane linker polypeptides. The electrostatic interactions between linker polypeptides and biliproteins significantly stabilize the phycobilisome assembly and promote the unidirectional highly efficient energy flow both within as well as from the phycobilisomes to the chlorophylls of the thylakoid membrane (Grossman *et al.* 1993, Sinha *et al.* 1995b).

Depletion of the stratospheric ozone layer has resulted in an increase in solar UV-B (280 - 315 nm) radiation reaching the Earth's surface (Crutzen 1992, Kerr and McElroy 1993, Lubin and Jensen 1995). Because of its high energy, UV-B easily destroys proteins, DNA and other biologically relevant molecules (Vincent and Roy 1993, Häder *et al.* 1995, Sinha and Häder 1996). Since cyanobacteria are simultaneously exposed to visible and UV radiation in their natural habitats, they tend to develop mechanisms counteracting the damaging effects of UV. Besides repair of UV-induced damage of DNA by photoreactivation and excision repair (Britt 1995, Kim and Sancar 1995), some cyanobacteria synthesize UV-absorbing compounds such as mycosporine-like amino acids and scytonemin that appear to act as sunscreens and enable them to inhabit environments that are exposed to intense solar radiation (Garcia-Pichel and Castenholz 1991, Garcia-Pichel *et al.* 1992, Brenowitz and Castenholz 1997, Ehling-Schulz *et al.* 1997).

Scytonemin, which has an *in vivo* absorption maximum at 370 nm and is located in the extracellular polysaccharide sheath of some cyanobacteria, has been proposed to serve as a UV-A sunscreen (Garcia-Pichel *et al.* 1992). The occurrence of scytonemin is restricted to cyanobacteria, but it is widespread among the diverse group. It is a yellow-brown, lipid soluble dimeric pigment with a molecular mass of 544 Da and a structure based on indolic and phenolic subunits. Purified scytonemin has an absorption maximum at 386 nm, but also absorbs significantly at 252, 278, and 300 nm (Proteau *et al.* 1993).

In the present investigation we have characterized a cyanobacterium, *Lyngbya* sp., that contains scytonemin and is resistant to high light irradiances coupled with high temperature and desiccation.

MATERIALS AND METHODS

Cyanobacterial strain

Dried mats of a cyanobacterium were collected in the months of May - June 1997 from the bark of mango (*Mangifera indica*) trees, growing on the campus of the Institute of Agricultural Sciences, Banaras Hindu University, Varanasi, India. Based on morphological characteristics described in standard taxonomic keys and monographs (Geitler 1932, Desikachary 1959), the cyanobacterial strain was identified as *Lyngbya* sp., a filamentous and non-heterocystous cyanobacterium belonging to the order Oscillatoriales, with sheaths typically colored by a yellow-brown pigment, scytonemin (Fig. 1 B).

Isolation of phycobiliproteins

Phycobiliproteins were isolated by a method described earlier (Sinha *et al.* 1995a) with a few modifications. Dried cyanobacterial (algal) mats (1.0 g) were washed twice with 0.75 M phosphate buffer (pH 7.0) and resuspended in the same buffer. To this, 1 mM PMSF and 2 mM EDTA were added and the cells were disrupted twice in a French press (Aminco Urbana IL, USA) at 70 bar using a flow rate of 1 - 2 drops per second. The resulting suspension was incubated for 2 h at room temperature in the presence of 1 % Triton X-100 and 5 % (w/v) sucrose. To remove cell debris, the suspension was centrifuged at 40 000 x g at 15 °C for 10 min (75 Ti rotor, Beckman, Palo Alto, USA). The supernatant contained most of the free phycobiliproteins.

Separation of phycobiliproteins

Phycobiliproteins were further separated by sucrose density gradient (5 - 40 %; w/v in 0.75 M phosphate buffer at pH 7.0) ultracentrifugation. Aliquots of 1 mL were deposited on top of the 11 mL volume of the sucrose gradient and centrifuged for 18 h (15 °C) at 150 000 x g in a swinging bucket rotor (SW 40, Beckman). The resulting fractions were retrieved with a syringe. The protein concentration was determined by the method of Bradford (Bradford 1976). Bovine serum albumin was used as a standard.

Extraction of scytonemin

Dried cyanobacterial mats (0.5 g) were homogenized in acetone (100 %) with a mortar and pestle and kept overnight in a refrigerator at 4 °C. The resulting suspension was centrifuged (10 000 x g for 10 min) and the supernatant was filtered through 0.2 µm pore-sized micro centrifuge filters (Mikro-Spin Zentrifugenfilter, Roth, Karlsruhe, Germany) in order to obtain partially purified scytonemin. Further analysis/purification of the pigment was done by HPLC.

Extraction and purification of mycosporine-like amino acids

Cells were harvested by centrifugation (J2-21M/E, Beckman Instruments, Palo Alto, CA, USA using a JA 20 rotor) at 1500 x g for 10 min at room temperature. Samples were extracted in 5 ml of 20 % (v/v) aqueous methanol (HPLC grade) by incubating at 45 °C for 2.5 h. After centrifugation (5000 x g; GP centrifuge, Beckman) the supernatant was lyophilized (Lyovac GT 2, Leybold, Köln, Germany) and redissolved in 2 ml 100 % methanol, vortexed for 2 - 3 min (L46, GLW, Würzburg,

Germany) and centrifuged at 10 000 x g for 10 min (Sigma2-MK, Sigma Laborzentrifugen GmbH, Osterode, Germany). Thereafter a 1.5 ml aliquot of the supernatant was evaporated to dryness at 45 °C and the extract redissolved in 1.5 ml of 0.2 % acetic acid. The samples were filtered through 0.2 µm pore-sized microcentrifuge filters (Mikro-Spin Zentrifugenfilter, Roth, Karlsruhe, Germany) to partially purify the mycosporine like amino acid (MAA). This partially purified MAA was subjected to HPLC analysis.

HPLC analysis

Analysis of scytonemin and MAAs was performed with a HPLC (Merck Hitachi; Interface D-7000, UV-Detector L-7400, Pump L-7100, Darmstadt, Germany) equipped with a Purospher RP 18 column and guard (5 µm packing; 125 ´4 mm I.D.). The sample was injected with a Hamilton syringe into the HPLC column through a Rheodyne injection valve equipped with a 20 µl sample loop. For scytonemin the wavelength for detection was 320 nm with a flow rate of 1.5 mL min^{-1}. A mobile phase of solvent A (double distilled water) and solvent B (acetonitrile/methanol/tetrahydrofuran, 75/15/10, v/v/v) was used with a 0 - 3 min linear increase from 30 % solvent B to 3 - 23 min at 100 % solvent B. For MAAs the wavelength for detection was 330 nm at a flow rate of 1.0 ml min^{-1} and a mobile phase of 0.2 % acetic acid. Scytonemin was identified by comparing the characteristic absorption maxima with those published earlier (Garcia-Pichel and Castenholz 1991, Proteau *et al.* 1993).

Absorption spectroscopy

Samples were transferred into a quartz cuvette (optical path length of 10 mm, 2 mm thickness, Hellma, Müllheim, Germany), and the absorption spectra were measured in a single beam spectrophotometer (DU 70, Beckman, Palo Alto, USA). The raw spectra were transferred to a microcomputer and treated mathematically and statistically using the software provided by the manufacturer (Beckman). Further evaluation was performed on a microcomputer using the RF-PC software developed by Shimadzu.

SDS-PAGE

SDS-PAGE of the samples was carried out in a vertical system (2001, Pharmacia, LKB, Uppsala, Sweden) with gels of 155 x 130 mm, 1.5 mm thick, using the method described by Laemmli (1970), with a gradient (5 - 20 % T) in the resolving gel. The electrophoresis was run initially at 300 V and 30 mA for about 1 h. The power was increased to 500 V and 60 mA as soon as the samples had moved in the resolving gel. Gels were stained with Coomassie brilliant blue R 250 and dried in a gel dryer (Bio-Rad, Richmond, CA, USA). Samples were run along with standard SDS molecular weight markers (SDS-7; approx. mol. wt. ranging from 14.2 to 66 kDa, as described in Sigma Technical Bulletein No. MWS-877L). All experiments were repeated at least three times.

RESULTS

Yellow-brown, leathery mats of a cyanobacterium were collected from the bark of mango trees (Fig. 1 A). Based on morphological characteristics, the strain was identified as *Lyngbya* sp.; a filamentous and non-heterocystous cyanobacterium with sheaths typically colored by a yellow-brown pigment, scytonemin (Fig. 1 B). The phycobiliproteins of *Lyngbya* sp. were separated into six vividly colored fractions (Fig. 1 C). SDS-PAGE analyses of the phycobiliprotein fracions of *Lyngbya* sp. are presented in Fig. 1 D. Fraction 2 contained bands with molecular masses between 14 and 66 kDa. Fractions 3 and 4 had a whole range of polypeptides between 14 and 66 kDa. Polypeptides at around 20 kDa denote the presence of α and β subunits of the phycocyanin. A prominent band at around 22 kDa in both fractions 3 and 4 indicates the presence of another accessory light harvesting pigment, phycoerythrin. Bands between 24 and 45 kDa in fractions 3 and 4 are indicative of the presence of rod and rod-core linker polypeptides of the phycobilisomes. The presence of some core-membrane linker polypeptides was also observed at around 66 kDa in fraction 4. Fraction 5 contained mainly low molecular mass proteins at around 20 kDa showing the presence of α and β monomers of phycocyanin. Data for fractions 1 and 6 are not presented since they had similar protein pattern as that of fraction 2 and 5, respectively.

The absorption spectra of the phycobiliprotein fractions (1-6) of *Lyngbya* sp. are illustrated in Fig. 2, showing photosynthetic light harvesting pigments such as chlorophylls (663 and 436 nm) and carotenoids (480 nm), and accessory light harvesting pigments such as phycoerythrin (560 nm), phycocyanin (620 nm), and allophycocyanin (650 nm).

HPLC analysis of the yellow brown pigment of *Lyngbya* sp. revealed only one prominent peak of scytonemin with a retention time of 4.4 min (Fig. 3) and an absorption maximum at 386 nm in the UV-A (315-400 nm) region (Fig. 4). In addition, the purified scytonemin also had significant absorbance in the UV-B (280-315 nm) and UV-C (100-280 nm) regions at 300, 278, 252, and 212 nm (Fig. 4). No trace of MAAs could be found in the samples.

DISCUSSION

The studied cyanobacterium *Lyngbya* sp. has certain properties that may enable it to survive and grow in the tropical environment, particularly during hot summer seasons when temperature rises above 45°C, coupled with excessive irradiances and extreme dryness. These properties include the presence of (a) photosynthetic light harvesting pigments (chlorophylls and carotenoids),

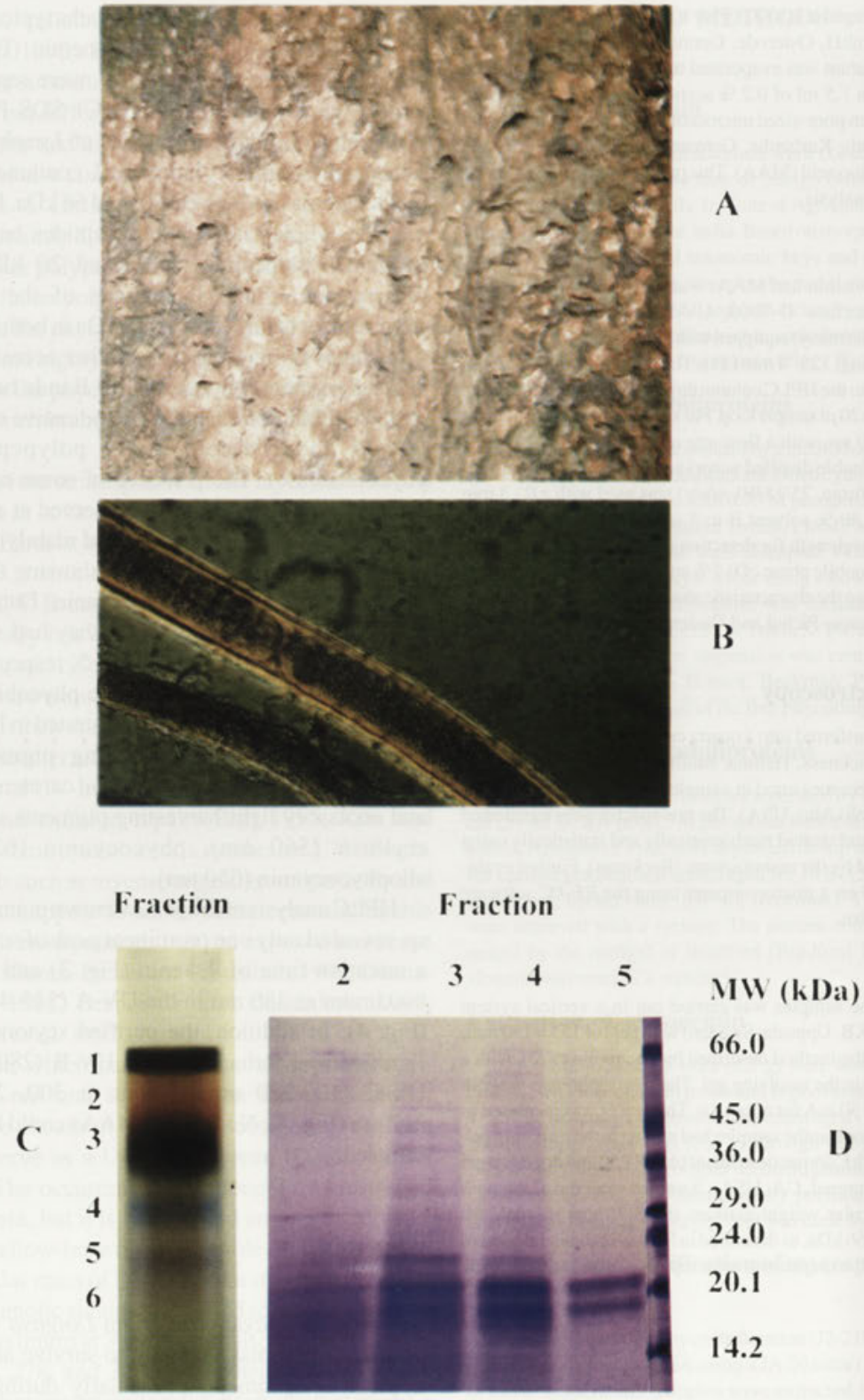

Fig. 1. (A) Photograph showing a yellow-brown leathery mat of *Lyngbya* sp. inhabiting the bark of a mango (*Mangifera indica*) tree. (B) Filaments of *Lyngbya* sp. with sheaths typically colored by the yellow-brown pigment scytonemin. Microphotographs were made with a x 40 objective. (C) Sucrose density gradient (5 - 40 %, w/v sucrose in 0.75 M phosphate buffer, pH 7.0) pattern of phycobiliproteins from *Lyngbya* sp. (D) Vertical SDS-PAGE (gradient 5 - 20 % T) analyses of various fraction as indicated in Fig. 1 C. Protein bands at extreme right represent molecular weight markers

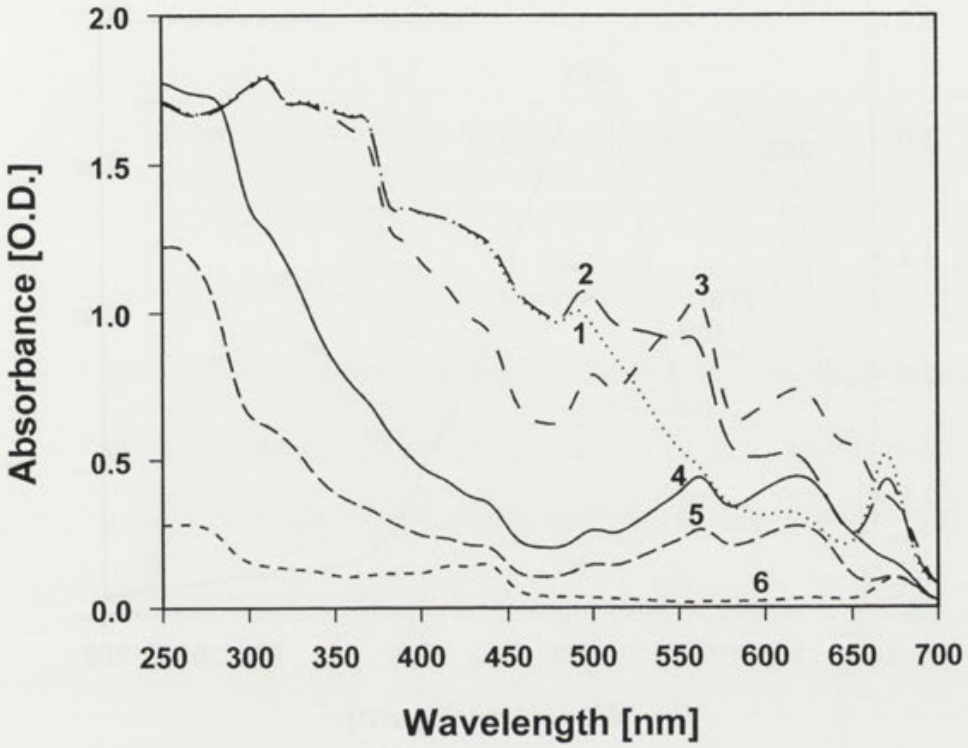

Fig. 2. Absorption spectra of the fractions 1-6 separated from *Lyngbya* sp. following sucrose density gradient ultracentrifugation. For details see text

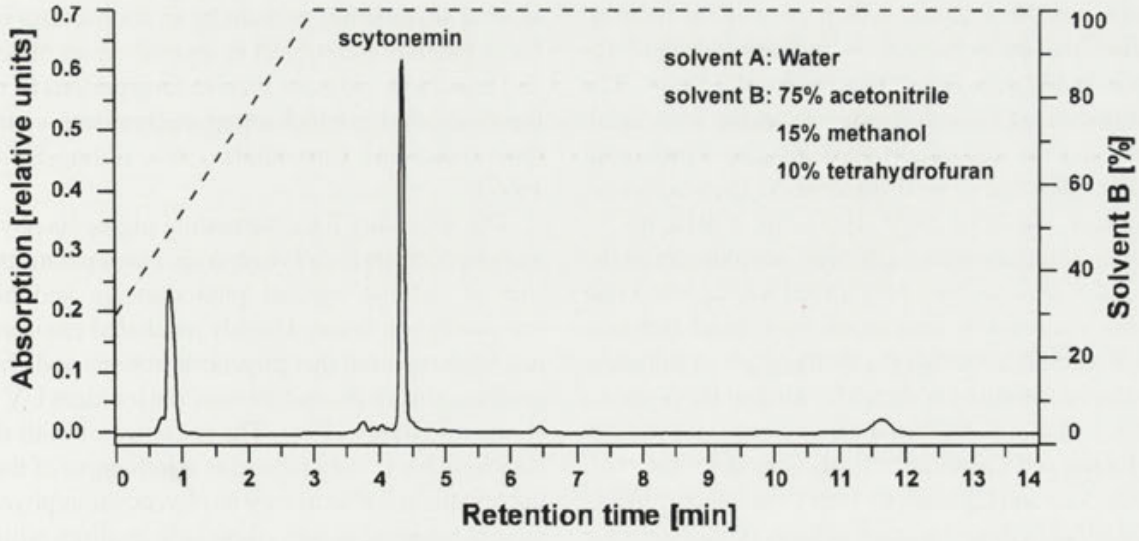

Fig. 3. High performance liquid chromatographic separation of the scytonemin from *Lyngbya* sp. Purospher RP 18 column and guard; flow rate 1.5 ml min^{-1}; detection by absorbance at 320 nm. For further details see text

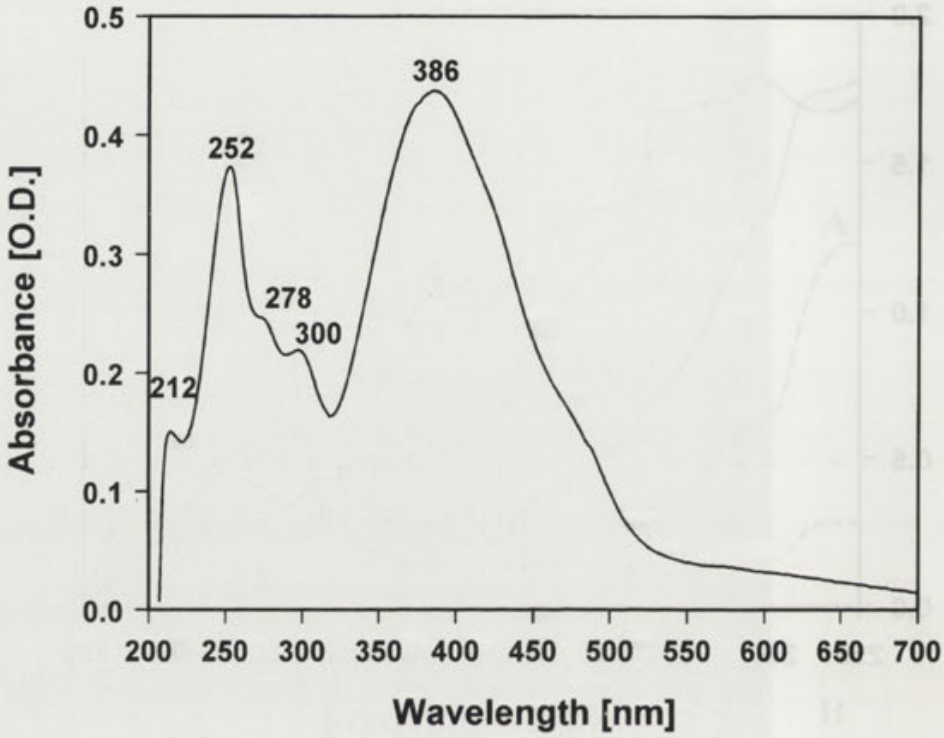

Fig. 4. Absorption spectra of the purified scytonemin of *Lyngbya* sp. as separated by HPLC

(b) UV-absorbing/screening compound (scytonemin), and (c) accessory light harvesting pigments (phycocyanin and phycoerythrin). Of particular interest is the viability of this cyanobacterium under the conditions of extreme temperature and desiccation which prevail for months. Presumably the cyanobacterium remains dormant for these periods but recovers after the onset of rain. The stringent feature of cyanobacteria to survive such harsh conditions and the role of certain water stress protein in desiccation tolerance is well understood (Scherer *et al.* 1984, Scherer and Potts 1989, Hill *et al.* 1994a, b).

The ultraviolet-absorbing pigment, scytonemin in the sheaths of *Lyngbya* sp. may play a vital role as a first line of defense against UV irradiation in natural habitats. Previous studies indicate that the incident UV-A radiation entering the cells may be reduced by around 90 % due to the presence of scytonemin in the cyanobacterial sheaths (Garcia-Pichel and Castenholz 1991, Garcia-Pichel *et al.* 1992, Brenowitz and Castenholz 1997). Field experiments have shown that high scytonemin content is necessary for uninhibited photosynthesis under high UV flux (Brenowitz and Castenholz 1997). Once synthesized, scytonemin remains highly stable and carries out its screening activity without further metabolic investment from the cell. Rapid photodegradation of scytonemin does not occur which is evidenced by its long persistence in terrestrial cyanobacterial crusts or dried mats (Garcia-Pichel *et al.* 1992, Brenowitz and Castenholz 1997). This strategy may be invaluable to several scytonemin containing cyanobacteria inhabiting harsh habitats and subject to regular cycles of desiccation and rewetting and must survive long periods of metabolic inactivity, during which repair mechanisms are ineffective (Brenowitz and Castenholz 1997, Ehling-Schulz *et al.* 1997).

The accessory light harvesting pigments phycocyanin and phycoerythrin in *Lyngbya* sp. may operate as a second line of defense against photodamage and help them survive in hot, dry and highly irradiated environments. It has been reported that phycobiliproteins and chlorophyll proteins absorb around 99 % of the incident UV radiation (Lao and Glazer 1996). The presence of both the accessory light harvesting pigments is indicative of the fact that the organism is able to vary its phycocyanin/phycoerythrin ratio in response to prevailing light qualities which allows regulation of the balance of wavelengths of light absorbed by the organism, a phenomenon known as chromatic adaptation (Tandeau de Marsac 1977). Phycobilisomes are designed to funnel radiant energy specifically

to photosystem II (PS II) at wavelengths where chlorophyll *a* molecules do not absorb, hence optimizing the energy capture and the colonization of environments with different light regimes (Tandeau de Marsac and Houmard 1993). UV induced phycobiliprotein destruction, disassembly of the phycobilisomal complexes and hence impaired energy transfer from phycobiliproteins to PS II has been reported in several cyanobacteria lacking phycoerythrin (Sinha *et al.* 1995 a,b), which has been reported to play an important role in the photoadaptation of cyanobacteria to UV photodamage (Wyman *et al.* 1985, Tyagi *et al.* 1992, Sinha and Häder 1998, Aráoz and Häder 1999). Phycoerythrin is less susceptible to photobleaching in comparison to phycocyanin and allophycocyanin. In addition, it can be excited by a broad range of wavelengths including UV radiation. The absorption of photons generates excited states with the chromophores and the excess energy is released as autofluorescence. Therefore, a significant amount of the energy may not be transferred to the underlying PS II preventing damage to the photosynthetic apparatus and other molecular targets. Furthermore, phycobiliproteins may play a significant role as a nitrogen storage compound during desiccation period.

It seems probable that a particular cyanobacterium having photoprotective mechanisms and a capacity to alter its phycobiliproteins in response to prevailing light qualities may be a potent candidate as a biofertilizer for crop plants, particularly rice in the tropical rice-growing countries.

Acknowledgements. The help from F. Garcia-Pichel (MPI for Marine Microbiology, Bremen, Germany) with the confirmation of scytonemin is greatly acknowledged. This work was financially supported by the C. S. I. R. (9/13(795)/96-EMR-I(RK)213108), New Delhi, India to R. P. Sinha and by European Union (DGXII, Environmental programme, ENV4-CT97-0580) to D.-P. Häder. We thank M. Schuster for excellent technical assistance.

REFERENCES

Aráoz R., Häder D.-P. (1999) Phycoerythrin synthesis is induced by solar UV-B in the cyanobacteriunm *Nostoc*. *Plant Physiol. Biochem.* **37:** 223-229.

Bradford M. M. (1976) A rapid and sensitive method for the quantification of microgram quantities of protein utilizing the principle of protein-dye binding. *Anal. Biochem.* **72:** 248-254

Brenowitz S., Castenholz R. W. (1997) Long-term effects of UV and visible irradiance on natural populations of a scytonemin-containing cyanobacterium (*Calothrix* sp.). *FEMS Microbiol. Ecol.* **24:** 343-352

Britt A. B. (1995) Repair of DNA damage induced by ultraviolet radiation. *Plant Physiol.* **108:** 891-896

Crutzen P. J. (1992) Ultraviolet on the increase. *Nature* **356:** 104-105

Desikachary T. V. (1959) Cyanophyta. Indian Council of Agricultural Research, New Delhi, India, 1-686

Ehling-Schulz M., Bilger W., Scherer S. (1997) UV-B-induced synthesis of photoprotective pigments and extracellular polysaccharides in the terrestrial cyanobacterium *Nostoc commune*. *J. Bacteriol.* **179:** 1940-1945

Garcia-Pichel F., Castenholz R. W. (1991) Characterization and biological implications of scytonemin, a cyanobacterial sheath pigment. *J. Phycol.* **27:** 395-409

Garcia-Pichel F., Sherry N. D., Castenholz R. W. (1992) Evidence for an ultraviolet sunscreen role of the extracellular pigment scytonemin in the terrestrial cyanobacterium *Chlorogloeopsis* sp. *Photochem. Photobiol.* **56:** 17-23

Geitler L. (1932) Cyanophyceae (Blaualgen). In: Kryptogamen-Flora von Deutschland, Österreich und der Schweiz, (Ed. L. Rabenhorst). Akademische Verlagsgesellschaft, Leipzig, **14:** 1-1196

Glazer A. N. (1989) Directional energy transfer in a photosynthetic antenna. *J. Biol. Chem.* **264:** 1-4

Grossman A. R., Schaefer M. R., Chiang G. G., Collier J. L. (1993) The phycobilisome, a light harvesting complex responsive to environmental conditions. *Microbiol. Rev.* **57:** 725-749

Häder D.-P., Worrest R. C., Kumar H. D., Smith R. C. (1995) Effects of increased solar ultraviolet radiation on aquatic ecosystems. *Ambio* **24:** 174-180

Hill D. R., Peat A., Potts M. (1994a) Biochemistry and structure of the glycan secreted by desiccation-tolerant *Nostoc commune* (cyanobacteria). *Protoplasma* **182:** 126-148

Hill D. R., Hladun S. L., Scherer S., Potts M. (1994b) Water stress proteins of *Nostoc commune* (cyanobacteria) are secreted with UV-A/B-absorbing pigments and associate with 1,4-b-D-xylanxylanohydrolase activity. *J. Biol. Chem.* **269:** 7726-7734

Kerr J. B., McElroy C. T. (1993) Evidence for large upward trends of ultraviolet-B radiation linked to ozone depletion. *Science* **262:** 1032-1034

Kim S.-T., Sancar A. (1995) Photorepair of nonadjacent pyrimidine dimers by DNA photolyase. *Photochem. Photobiol.* **61:** 171-174

Lao K., Glazer A. N. (1996) Ultraviolet-B photodestruction of a light-harvesting complex. *Proc. Natl. Acad. Sci.* **93:** 5258-5263

Laemmli U. K. (1970) Cleavage of structural proteins during the assembly of the head of bacteriophage T4. *Nature* **227:** 680-685

Lubin D., Jensen E. H. (1995) Effects of clouds and stratospheric ozone depletion on ultraviolet radiation trends. *Nature* **377:** 710-713.

Proteau P. J., Gerwick W. H., Garcia-Pichel F., Castenholz R. W. (1993) The structure of scytonemin, an ultraviolet sunscreen pigment from the sheaths of cyanobacteria. *Experientia* **49:** 825-829

Scherer S., Potts M. (1989) Novel water stress protein from a desiccation-tolerant cyanobacterium. *J. Biol. Chem.* **264:** 12546-12553

Scherer S., Ernst A., Chen T. W., Boger P. (1984) Rewetting of drought-resistant blue-green algae: time course of water uptake and reappearance of respiration, photosynthesis, and nitrogen fixation. *Oecologia* **62:** 418-423

Sinha R. P., Häder D.-P. (1996) Photobiology and ecophysiology of rice field cyanobacteria. *Photochem. Photobiol.* **64:** 887-896

Sinha R. P., Häder D.-P. (1998) Effects of ultraviolet-B radiation in three rice field cyanobacteria. *J. Plant Physiol.* **153:** 763-769

Sinha R. P., Lebert M., Kumar A., Kumar H. D., Häder D.-P. (1995a) Spectroscopic and biochemical analyses of UV effects on phycobiliproteins of *Anabaena* sp. and *Nostoc carmium*. *Bot. Acta* **108:** 87-92

Sinha R. P., Lebert M., Kumar A., Kumar H. D., Häder D.-P. (1995b) Disintegration of phycobilisomes in a rice field cyanobacterium *Nostoc* sp. following UV irradiation. *Biochem. Mol. Biol. Int.* **37:** 697-706

Tandeau de Marsac N. (1977) Occurrence and nature of chromatic adaptation in cyanobacteria. *J. Bacteriol.* **130:** 82-91

Tandeau de Marsac N., Houmard J. (1993) Adaptation of cyanobacteria to environmental stimuli: new steps towards molecular mechanisms. *FEMS Microbiol. Rev.* **104:** 119-190

Tyagi R., Srinivas G., Vyas D., Kumar A., Kumar H. D. (1992) Differential effect of ultraviolet-B radiation on certain metabolic processes in a chromatically adapting *Nostoc*. *Photochem. Photobiol.* **55:** 401-407.

Vincent W. F., Roy S. (1993) Solar ultraviolet-B radiation and aquatic primary production: damage, protection, and recovery. *Environ. Rev.* **1:** 1-12.

Wyman M., Gregory R. P. F., Carr N. G. (1985) Novel role for phycoerythrin in a marine cyanobacterium, *Synechococcus* strain DC2. *Science* **230:** 818-820

Received on 11th November, 1998; accepted on 16th August, 1999

Acta Protozool. (1999) 38: 299 - 303

ACTA
PROTOZOOLOGICA

Testing for Toxic Effects of Alcohols on *Polytomella papillata* (Chlorophyceae) Aggregation Behavior Using the Spectrophotometer to Measure the Endpoint

Salvatore P. GIMELLI, Stephen M. GITTLESON and Tae J. UM

School of Natural Sciences, Fairleigh Dickinson University, Teaneck, New Jersey, U.S.A.

Summary. The flagellated protozoan *Polytomella papillata* (Chlorophyceae) forms macroscopic aggregates in 24 h axenic cultures. Thorough agitation of the culture, disperses the aggregates which reform normally in about 30 s at 25 °C. We have developed a testing procedure using the Spectronic 20 spectrophotometer to establish a reference point for timing the reappearance of the aggregates under normal conditions and with the addition of chemicals. With two series of related alcohols, the following increasing orders of toxicity were determined: methanol < ethanol < iso-propanol < n-propanol < n-butanol and ethylene glycol < propylene glycol < glycerol. The *Polytomella* aggregation response indicated a typical dose-response relationship for each alcohol and also differentiated the alcohols from one another in relation to the number of carbon atoms and the arrangement of OH groups attached to the carbon chain. This test may provide a rapid, economical, sensitive and easy to perform method for screening the toxicity of chemicals and drugs.

Key words: aggregation, alcohols, n-butanol, ethanol, ethylene glycol, glycerol, methanol, *Polytomella*, iso-propanol, n-propanol, propylene glycol, spectrophotometer, toxicity test.

INTRODUCTION

Aggregation of *Polytomella* spp. (Chlorophyceae) is a characteristic phenomenon in axenic cultures related to population density (minimum about 100,000 cells/ml), depth of medium, and cell locomotion (Gittleson and Jahn 1968). The cells do not become attached to each other but develop aggregates when individual cells actively swim upwards and collect near the medium/air interface. Crowding of the cells impairs normal swimming behavior. The loss of effective cell locomotion in such dense numbers leads to the falling of groups of cells or aggregates. Since the cells are not attached, the falling aggregate is not perfectly isolated and so, a trail of organisms swept behind generates a column. This phenomenon is also referred to as bioconvection (Bees and Hill 1999). A photograph showing these vertical patterns can be seen in Gittleson and Jahn (1968). Upon reaching the bottom of the container, the cells disperse and swim back toward the surface. The vertical columns and aggregates falling along them constitute a series of mac-

Address for correspondence: Stephen M. Gittleson, School of Natural Sciences (H4440), Fairleigh Dickinson University, 1000 River Road, Teaneck, New Jersey, 07666 USA; Fax: (201) 6927349; E-mail: Gittleso@mailbox.fdu.edu

roscopic events that are easily characterized. The falling rate of *Polytomella* aggregates was used to measure the comparative influences of formaldehyde and glutaraldehyde (Gittleson 1975). The use of *Polytomella* aggregation behavior to evaluate physicochemical changes in their environment was further reported (Gittleson and de la Cruz 1994) where reformation time after randomizing the cells was used as the endpoint. The implication is that effects on individual cells are reflected in the gross population dynamics of the aggregation phenomenon. A preliminary discussion of the spectrophotometric technique was described in a platform presentation to the New Jersey Academy of Sciences (Gimelli and Gittleson 1998).

In this paper we describe how the effect of a chemical on *Polytomella* can be easily evaluated using the Spectronic 20 spectrophotometer to determine the intensity of aggregation after the aggregating cells are completely randomized.

MATERIALS AND METHODS

Source of *Polytomella papillata*. This protozoan is available from the University of Texas Algal Collection where it is noted that *Polytomella papillata* is equivalent to *P. caeca*.

Glassware. All glassware was washed with Alconox soap (Alconox Inc. N Y, USA) and rinsed ten times with tap water, then with dilute nitric acid (1%) to remove any soap traces, and subsequently rinsed three times with deionized water. The glassware used for culturing was isolated from the glassware used in preparing chemicals and test materials.

Culture method. *Polytomella papillata* was grown axenically in a medium consisting of 0.1% w/v sodium acetate, 0.1% bacto-tryptone (Difco) and 0.2% yeast extract (Difco) autoclaved for 20 min at 121 °C. Tube stock cultures of *P. papillata* were maintained at 24 °C with sub culturing every 2-3 days. One ml of a 2-3 days stock culture was transferred aseptically to a tube containing 10 ml of sterile culture medium. These transfers were repeatedly carried out to maintain the culture.

For experimental use, 5 ml of a 2-3 days stock culture was transferred aseptically to 100 ml of sterile culture medium in a 250 ml Erlenmeyer flask to prepare a batch of *P. papillata* for toxicity tests. This batch culture was grown at 24 °C for about 24 h and used immediately for toxicity testing.

Experimental procedure. A Spectronic 20 spectrophotometer (Spectronic Instruments, Inc. NY, 14625 USA) was warmed-up 15 min and then calibrated using sterile medium as the blank. After mechanically agitating the batch culture (using a Vortex Genie mechanical vibrator) for 10 s to randomize the distribution of *P. papillata*, a 5 ml aliquot was transferred to one test tube that received the test chemical (solution of chemical prepared in deionized water) and another 5 ml aliquot was transferred to a second test tube that received an equivalent volume of deionized water. The test tubes used for testing were disposable borosilicate glass tubes 13x100 mm. The deionized water was prepared by passing tap water through United States Filter Corporation carbon (ZWDJ02511) and mixed bed (ZWDJ02512) prefilters and then through a Barnstead Nanopure II unit. The tests were run immediately. For example, after loading the tubes with culture, 0.1 ml of 0.1 M ethanol was added to one tube (experimental) and 0.1 ml of deionized water was added to the other tube (control). Separately each tube was agitated for 10 s to insure that the cells were randomly distributed. Tests showed that varying times of agitation from about 10 s up to 1 min did not alter results. Agitation for less than 10 s gave inconsistent results apparently due to lingering aggregation. Immediately upon preparing the control or experimental tube, the tube was placed in the Spectronic 20 sample compartment. At this point the maximum persentage transmission (%Tmax) was recorded. Typically the meter needle declined sharply as the forming aggregate passed through the Spectronic 20 window. The minimum % transmission (%Tmin) was recorded. Experiments were run in a temperature controlled room at 23 ± 1 °C. The test works just as well at other temperatures in the range from 20 to 25 °C. All chemicals used in the tests were USP certified from Fisher Scientific, N J, USA.

Data analysis. Each chemical concentration was tested in three separate setups from the same batch culture of *P. papillata*. The tests on each setup of control and experimental tubes were performed in triplicate. Therefore, averages given in the figures and the range of Standard Error of the Mean (SEM) values given in Table 1 are based on nine values at each concentration. Statistical significance was evaluated with the 1-tailed paired Students t-test. In order to easily compare control and experimental values, a *Polytomella* Aggregation Factor (PAF) was calculated:

$$PAF = 1 - [(\%Tmax - \%Tmin)/\%Tmax]$$

At one extreme where there was no difference between control and experimental tests, the PAF = 1 and at the other where the aggregates fail to appear, the PAF = 0. The transition between 1 and 0 indicates increasing toxicity of the chemical. Any values of PAF exceeding 1 would indicate an excitatory effect of the chemical on aggregation of *P. papillata*.

RESULTS

Alcohols used in this study range from one carbon atom (methanol) to another with a four carbon atom chain (n-butanol). Biological activity related to chemical structure is discussed below. Figures 1 and 2 show that certain concentrations of each of the eight alcohols tested affects the aggregating behavior of *P. papillata*. The *Polytomella* aggregation response indicated as PAF not only illustrates a typical dose-response relationship for each alcohol but also differentiates the alcohols from one another. In Fig. 1 the following increasing order of toxicity is indicated:

methanol < ethanol < iso-propanol < n-propanol < n-butanol based on a comparison at a PAF of 0.5. The PAF values at 0.5 compared to controls are significantly different ($p < .05$). Table 1 gives the concentrations of these alcohols at a PAF of 0.5. Methanol stands out as the least toxic, i.e. more is required to produce an effect. The most toxic is n-butanol. In Fig. 2, the following increasing order of toxicity is indicated: ethylene glycol < propylene glycol < glycerol based on a comparison at a PAF of 0.5 (also see Table 1). Ethylene glycol is the least toxic while glycerol shows the highest degree of toxicity in this group. A PAF value of 0 occurs when aggregation of *P. papillata* ceases to occur. Therefore, concentrations of alcohols that cause lethal effects are detected by the lowest PAF values. Near a PAF of 0 n-butanol at 500 mM has the same toxicity as methanol at about 5000 mM (Fig. 2).

When cells of *P. papillata* were examined microscopically there was a strong correlation observed between abnormal motile behavior and decreasing PAF values associated with all of the alcohols. For example, when no aggregation occurred (at a PAF = 0) all of the cells were observed to be stationary. Typically the cells spin and bounce in place and change from the normal oval shape to a rounded shape in response to increasing concentration of each alcohol.

DISCUSSION

This report describes a toxicity test that is rapid, sensitive, economical and easy to perform. It is based on the highly consistent aggregating behavior of the flagellated cell *Polytomella papillata*. Generally, the literature on standardized toxicity tests lacks representation by protozoa (Toussaint *et al.* 1995). There have been studies which link the locomotor behavior and cell morphology of individual protozoa to carbon dioxide and other gases (Sears and Elveback 1961, Gittleson and Sears 1964, Sears and Gittleson 1964), heparin (Lantos *et al.* 1965), human serums (Nemeth 1972) and detergents (Dryl and Mehr 1976). Noever and Matsos (1991) found a correlation between the appearance of *Tetrahymena pyriformis* bioconvective patterns and cadmium toxicity. In this study we further show that protozoa have potential for toxicity testing. Using the macroscopic aggregating behavior of *Polytomella* to test for the biological activity of chemicals, drugs and environmental situations is quick to setup and to learn. The low cost of analyzing three samples of a chemical solution at approximately US 15 cents is a definite advantage. Importantly, the spectrophotometer provides a measurement that is consistent from operator to operator.

Some insight into how the n-alcohol series (only one hydroxyl group at the end of the chain) may produce the relative effects observed is suggested by the correlation with the dielectric constants of these alcohols. As the number of carbon atoms increase in the n-alcohol series, the dielectric constants decrease: methanol - 32.63, ethanol - 24.30, iso-propanol - 18.3, n-propanol - 20.1, n-butanol - 17.1 (Lide 1998). As the dielectric constant decreases, solubility of the alcohol decreases in water and increases in lipid. The greater toxicity of longer chain alcohols may be associated with their higher lipid solubility. Dryl (1959) and Isquith and Bobrow (1973) found the same increasing toxicity of the n-alcohol series as chain length increases on *Paramecium caudatum*.

Although those alcohols with more than one hydroxyl group also have an effect correlated with carbon chain length (see Table 1) they possess considerably greater dielectric constants: glycerol - 42.5, ethylene glycol - 37, propylene glycol - 32. This suggests that alcohols with two and three OH groups have an effect more dependent on greater solubility in the aqueous components of the cell. The two alcohols, n-butanol having the lowest dielectric constant (highest lipid solubility) and glycerol having the highest dielectric constant (highest aqueous solubility) were the most toxic. They also have the longer carbon chain lengths. Compared to the other alcohols it appears that n-butanol and glycerol are more toxic because they possess two important biologically active properties: longer chain length and extreme opposite degrees of lipid and aqueous solubilities.

Comparison of the relative effects of the n- alcohol series on *Polytomella* with LD50 data for these alcohols when given to rats orally shows a strong positive correlation (Oregon State System of Higher Education 1998, Rusho 1998, Mallinckrodt 1999). For *Polytomella*, the order of increasing effect at a PAF = 0.5 is methanol < ethanol < iso-propanol < n-propanol < n-butanol. For rats, the order of increasing effect according to LD50 data (mg/Kg) is as follows: methanol (9800) < ethanol (7060) < iso-propanol (5840) < n-propanol (1870) < n-butanol (790). This identical relative effect of the n-alcohol series between a protozoan and a mammal supports the effort to use unicellular

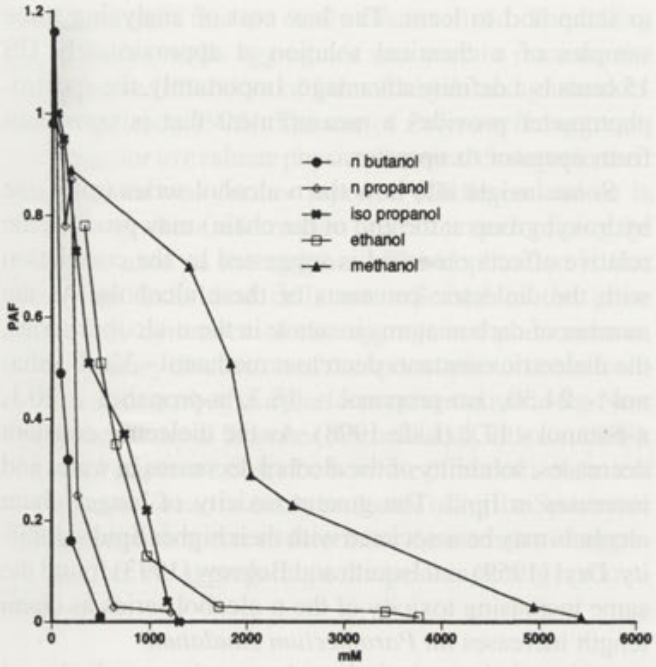

Fig. 1. Effects of n-butanol, n-propanol, iso-propanol, ethanol and methanol expressed as *Polytomella* Aggregation Factor (PAF) where 1.0 indicates no effect and 0 indicates a complete loss of biological activity. Each point is an average of nine experimental values. Variability expressed as standard error of the mean is indicated in Table 1

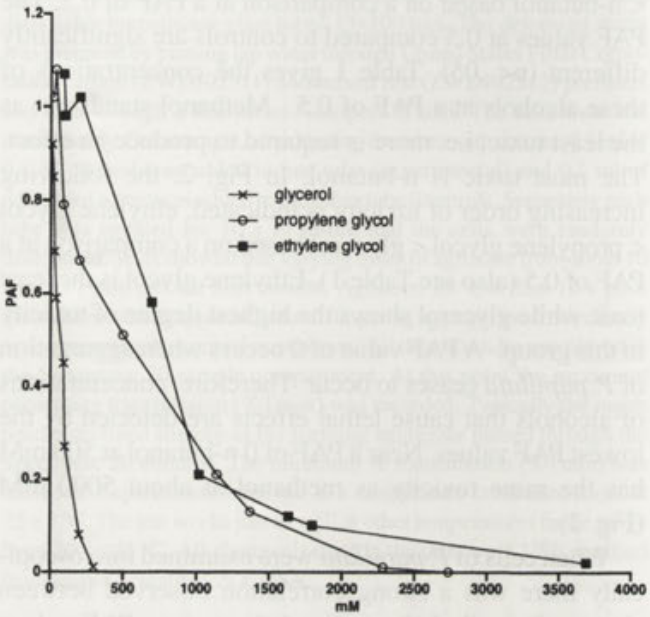

Fig. 2. Effects of glycerol, propylene glycol and ethylene glycol expressed as *Polytomella* Aggregation Factor (PAF) where 1.0 indicates no effect and 0 indicates complete loss of biological activity. Each point is an average of nine experimental values. Variability expressed as standard error of the mean is indicated in Table 1

Table 1. The comparative effect of alcohols on *Polytomella papillata* at a PAF = 0.5 related to the number of carbons in the alcohol chain (column 2) and concentration in mM (column 3). Column 4 shows the range of the standard error of the mean (SEM) for all of the concentrations of the chemical tested

Alcohol	Number of carbons	mM	SEM
n-butanol	4	40	0.01-0.08
glycerol	3	90	0.03-0.25
n-propanol	3	250	0.01-0.06
iso-propanol	3	490	0.02-0.12
propylene glycol	3	580	0.01-0.14
ethanol	2	700	0.01-0.19
ethylene glycol	2	800	0.01-0.17
methanol	1	1880	0.01-0.19

systems such as *Polytomella papillata* as an alternative in toxicity testing.

Acknowledgements. We are grateful to Ms. Evelyn Libertelli our laboratory coordinator in the School of Natural Sciences for her assistance.

REFERENCES

Bees M.A., Hill N.A. (1999) Non-linear bioconvection in a deep suspension of gyrotactic swimming microorganisms. *J. Math. Biol.* **38:** 135-168

Dryl S. (1959) Chemotactic and toxic effects of lower alcohols on *Paramecium caudatum*. *Acta Biol. Exp.* **19:** 95-104

Dryl S., Mehr K. (1976) Physiological and toxic effects of detergents on *Paramecium caudatum*. *Acta Protozool.* **15:** 501-513

Gimelli S. P., Gittleson S. M. (1998) Prototox: A rapid and economical spectrophotometric method for testing chemical toxicity. *Bull. N. J. Acad. Sci.* **43:** 20

Gittleson S.M. (1975) Measurement of aggregate sedimentation rate as a chemical bioassay. *Acta Protozool.* **14:** 217-223

Gittleson S.M., Jahn T. L. (1968) Vertical aggregations of *Polytomella agilis*. *Exp. Cell Res.* **51:** 579-586

Gittleson S.M., de la Cruz V. (1994) A cell aggregation toxicity test. *J. Euk. Microbiol.* **42:** 29A

Isquith I.R., Bobrow A. (1973) The effect of high intensity magnetic field on the entrance of various molecules into *Paramecium caudatum*. *Acta Protozool.* **12:**125-131

Lantos T., Muller M., Csaba G. (1965) Effect of heparin on locomotion and potassium reversal in *Paramecium multimicronucleatum*. *Acta Protozool.* **3:** 291-297

Lide D. (1998) Handbook of Chemistry and Physics. 78 ed. CRC Press. Boca Raton, Florida

Mallinckrodt-JT Baker. Material Safety Data Sheets http://www.jtbaker.com/msds/p6390.htm (15 April 1999)

Nemeth G. (1972) The use of Protozoa as test organisms for studies of toxic effects of human serums from schizophrenic patients. *Acta Protozool.* **9:** 365-372

Noever D. A., Matsos H. C. (1991) Calcium protection from cadmium poisoning: bioconvective indicators in *Tetrahymena*. *J. Enviorn. Sci. Health* A **26:** 1105-1114

Oregon State System of Higher Education. Material Safety Data Sheets http://www.pp.orst.edu/msds.htm 28 November 1998)

Rusho J. Material Safety Data Sheets http://www.chem.utah.edu/msds (28 November 1998)

Toussaint M. W. (1995) A comparison of standard acute toxicity tests with rapid- screening toxicity tests. *Envir. Tox. Chem.* **14:** 907-915

Received on 10th May, 1999; accepted on 14th September, 1999

Acta Protozool. (1999) 38: 305 - 311

ACTA
PROTOZOOLOGICA

Redescription of Trichodinid *Dipartiella simplex* (Raabe, 1959) (Ciliophora: Peritrichida) and Remarks on the Genus *Dipartiella* Stein, 1961

Stanisław L. KAZUBSKI

Museum and Institute of Zoology, Polish Academy of Sciences, Warszawa, Poland

Summary. Trichodinid *Dipartiella simplex* (Ciliophora: Peritrichida) is redescribed on the basis of original preparations from Z. Raabe's collection. The correctness of the original description of *D. simplex* by Raabe (1959) and the validity of the species and the genus *Dipartiella* Stein, 1961 are confirmed. The interpopulational variability of *D. simplex* occurring on the fish *Gobius niger* in Gdańsk Bay (Baltic Sea) is analysed.

Key Words: *Dipartiella simplex*, redescription, Trichodinidae, variability.

INTRODUCTION

The trichodinid species, *Dipartiella simplex* (Ciliata: Peritrichida) was described by Raabe (1959) as the type species of the new genus *Dogielina* Raabe, 1959. The material originated from the gills of black goby (*Gobius niger* L.) caught in Gdańsk Bay and Puck Bay (Baltic Sea) in the summer 1958. Later Stein (1961) noted that the generic name *Dogielina* was preoccupied by genera of Foraminifera and Nematoda, and she proposed the new name *Dipartiella*.

The species has not been found ever since. This fact, as well as a very short, compact description and imprecise drawings probably have led Lom and Dykova (1992) to regard the genus as "spurious" and the species as a "possible mistaken interpretation of the genus *Trichodinella*".

As the preparations made by Professor Z. Raabe come into my hands, I feel a duty to redescribe this species as precisely as possible.

Address for correspondence: Stanisław L. Kazubski, Museum and Institute of Zoology of the Polish Academy of Sciences, 00-950 Warsawa, ul. Wilcza 64, Poland; Fax 629-63-02; E-mail: stankaz@robal.miiz.waw.pl

MATERIALS AND METHODS

In Raabe's collection I found a box containing 9 Klein's silver-impregnated preparations and 7 preparations fixed in Schaudinn's fluid and stained with Heidenhain's iron hematoxylin. I arranged them according to the method of staining and the locality of the origin, providing them with numbers and the letter "a" for silver-impregnated preparations, or the letter "b" for hematoxylin stained ones; original notes for each slide made by Z. Raabe are given in quotation marks.

Silver-impregnated preparations:

slide No a16: "*Gobius niger* Kuźnica Zatoka 30 VII 1958"

slide No a24: "*Gobius niger* Kuźnica 3 VIII 1958"

slide No a35: "*Gobius niger* Kuźnica 3 VIII 1958"
slide No a47: "*Gobius niger* Kuźnica na Helu 18 VII 1959 *Dogielina simplex*"
slide No a59: "*Gobius niger* 3 Swarzewo" (missing date)
slide No a73: "*Gobius niger* 5 Swarzewo" (missing date)
slide No a81: "*Gobius niger* 8 Swarzewo" (missing date)
slide No a98: "*Gobius niger* Rewa 11 VIII 58"
Hematoxylin-stained preparations:
slide No b1: "*Gobius niger* Kuźnica 3 VIII 1958"
slide No b2: "*Gobius niger* Kuźnica 3 VIII 1958"
slide No b3: "*Gobius niger* Kuźnica 3 VIII 1958"
slide No b4: "*Gobius niger* Kuźnica 4 IX 1958"
slide No b5: "*Gobius niger* 5 Swarzewo" (missing date)
slide No b6: "*Gobius niger* 8 Swarzewo" (missing date)
slide No b7: "*Gobius niger* Rewa 11 VIII 1958"

I suppose that preparation a24 and a35 were made from different fish specimens, as Professor Raabe's custom was to make only one preparation from each host specimen; the same concern preparation b1, b2, and b3. It may be also supposed that at least some of the silver-impregnated and hematoxylin-stained preparations were made from the same fish. According to Raabe (1959) these trichodinid occurred on all fish examined, sometimes in mass numbers.

All preparations were re-examined using an Olympus BH-2 microscope with an immersion objective SPlan 100, 1.250 Oil. Measurements were made on a monitor screen in μm. Working pictures were made with a Video Copy Processor, Mitsubishi model P66E. Pictures for publication were registered by the computer program Screen Machine II and elaborated with Corel Photo-Paint 5.0.

All measurements were made according to the procedure of Kazubski (1979a,b), adapted to *Dipartiella* (see Fig. 1). From each population (ciliates from one host specimen) about 50 randomly chosen ciliates were measured. Statistics were calculated and the interpopulational variability was assessed using nested ANOVA.

Examined preparations of *D. simplex* are stored in the Museum and Institute of Zoology of the Polish Academy of Sciences in Warsaw.

RESULTS

On the basis of the preparations listed above, especially those fixed in Schaudinn's fixative and stained with hematoxylin the body shape of *Dipartiella simplex* is seen as a slightly asymmetric dome, whose relative height is equal to 2/3 of the cell diameter (Figs. 2, 3). In 8 cells found in lateral position, the cell height was 10-15 μm (mean 12.9), while the cell diameter was 15.5-21.5 μm (mean 18.7). Cell diameter, seen from the oral or the aboral side, measured on 130 specimens fixed and stained as above, from 3 populations (b5, b6, b7) ranged from 10.6 to 29 μm (mean 20.34).

The adoral ciliary spiral runs slightly above the widest part of the cell, forming an arch of about 270°; it is easily visible in both hematoxylin-stained (Fig. 4) and silver-impregnated preparations (Fig. 5). Its diameter, measured on stained preparations, is only about 2 μm smaller than the cell diameter, attaining 18 μm in a cell of 20 μm diameter and 19 μm in those of 20.5 μm diameter.

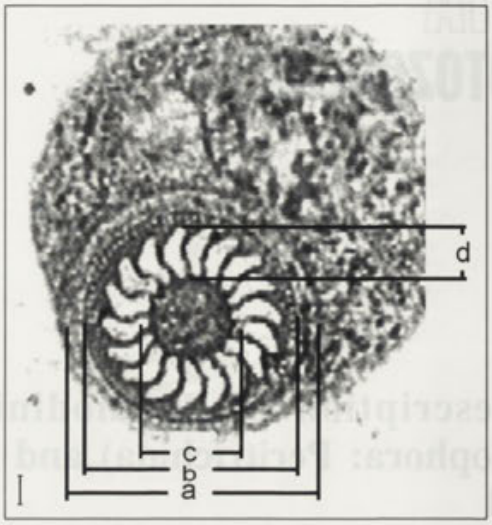

Fig. 1. The method of measuring of *Dipartiella simplex*; a - diameter of the adhesive disc with border membrane, b - diameter of the adhesive disc, c - diameter of the denticulate ring, d - length of the denticle. Scale bar - 2 μm

The aboral surface bearing the adhesive disc is conspicuously concave.

Dimensions of the cell, the adhesive disc and the denticulate ring, measured on silver impregnated preparations, as well as the number of denticles in 9 populations of *Dipartiella simplex*, as well as summary data, are given in Table 1.

The border membrane in silver-impregnated specimens measures up to 2.5 μm (mean 1.5); while in stained specimens it ranges from 0.25 to 1.25 μm (mean 0.70).

Denticles of *D. simplex* are small, their height ranging from 2.2 to 4.0 μm. Beside the median part joining adjacent denticles; they have only outer blades. There are no elements directed to the centre of the adhesive disc. The details of the junctions (central part of denticle) are not clearly seen due to the very small dimensions.

The size, especially the width, of the denticles is very variable. In smaller ciliates, having thus denticulate rings of small diameter, the blades are narrow with sharply tapered outer edges (Figs. 6-8); in larger specimens, with larger diameter of denticulate ring, the blades are wide and their distal ends are rounded (Figs. 9, 10). Sometimes, however, the blades are wide with sharp ends (Fig. 11).

There are 4-5 radial pins of the adhesive disc per denticle. In 6 specimens for which all radial pins were counted, the number radial pins per denticle are 4.3-4.7 (mean 4.48).

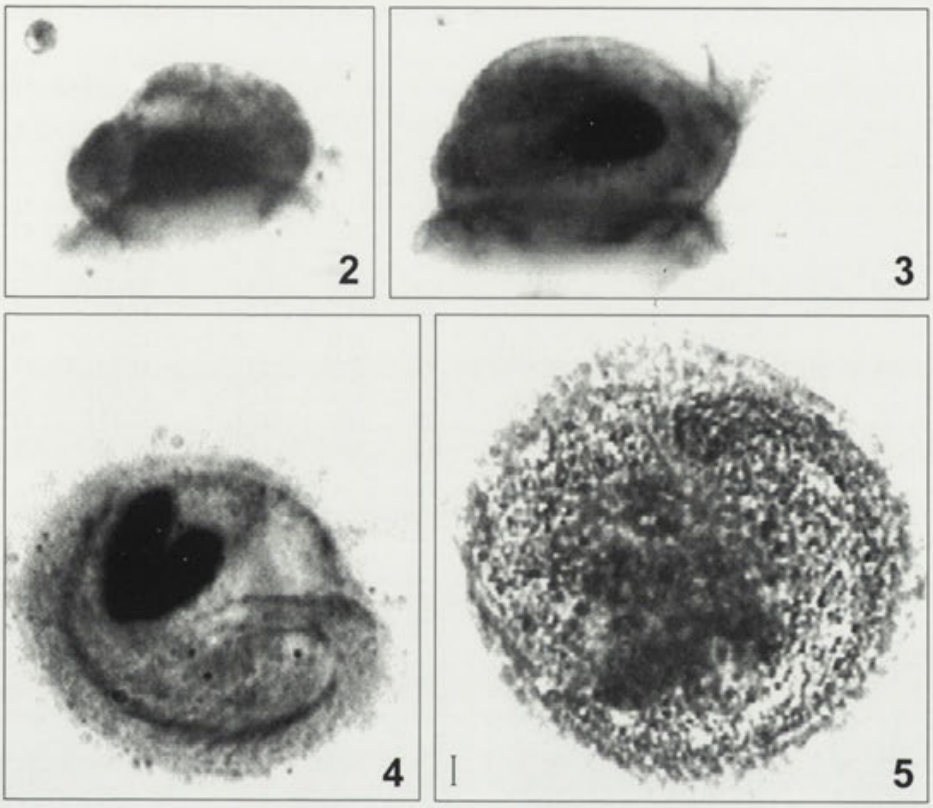

Figs 2-5. *Dipartiella simplex*. 2-4 - hematoxylin-stained specimens; 2 and 3 lateral view, circle of locomotory cilia on both and the adoral cilia around infundibulum on one (Fig. 3) are visible; 4 - adoral view, the adoral ciliary zone and infundibulum are visible; 5 - silver-impregnated specimen, adoral zone of cilia. Scale bar - 2 μm

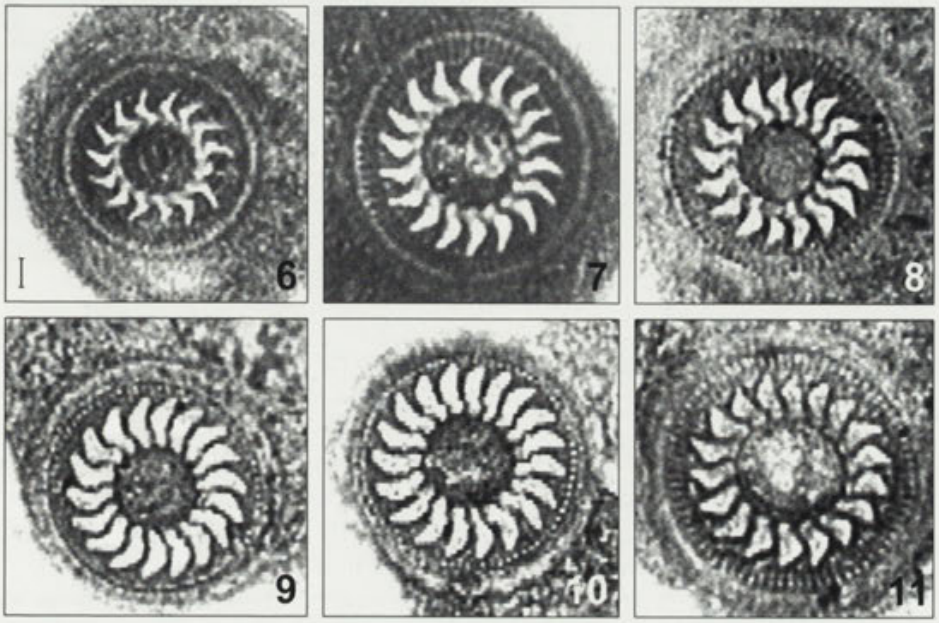

Figs 6-11. *Dipartiella simplex*, adhesive disc. 6-8 - specimens with narrow and 9-11 with wide blade. Scale bar - 2 μm

Table 1. Metric and meristic data (in μm) of main characters of 9 examined populations of *Dipartiella simplex* (Raabe)

	Diameter of the cell				Diameter of the adhesive disc with border membrane				Diameter of the adhesive disc			
	range	n	mean	SD	range	n	mean	SD	range	n	mean	SD
D. simplex a16	21-34.5	51	27.0	2.90	14.5-22	51	17.5	1.53	12-18.5	51	14.6	1.50
D. simplex a24	17-27.5	52	23.1	2.57	14-20.5	52	17.1	1.63	11-18	52	14.1	1.68
D. simplex a35	15-30	57	21.9	3.10	11.5-20	56	16.3	1.88	10-56	56	13.5	1.69
D. simplex a47	17.5-30.5	56	24.8	3.31	13-21	55	16.4	1.81	9.5-17.5	57	13.8	1.57
D. simplex a59	21.5-38	50	28.6	3.82	13-20	50	17.4	1.72	11-17	51	14.2	1.50
D. simplex a62	20-30	50	23.8	2.17	14.5-19.5	49	17.0	1.14	12-15.5	50	13.9	1.09
D. simplex a73	18.5-29	54	23.8	2.39	14-19	53	17.0	1.51	11.5-16.5	54	13.9	1.28
D. simplex a81	20-29.5	51	24.2	2.24	14-19	55	17.4	1.35	11.5-16.5	55	14.3	1.31
D. simplex a98	18-30	47	22.6	2.60	13.5-19.5	52	16.4	1.43	11-17.5	52	13.2	1.37
Total	15-38	468	24.4	3.47	11.5-22	473	16.9	1.63	9.5-18.5	478	13.9	1.51
Raabe 1959									15.5-22.0		18.0	

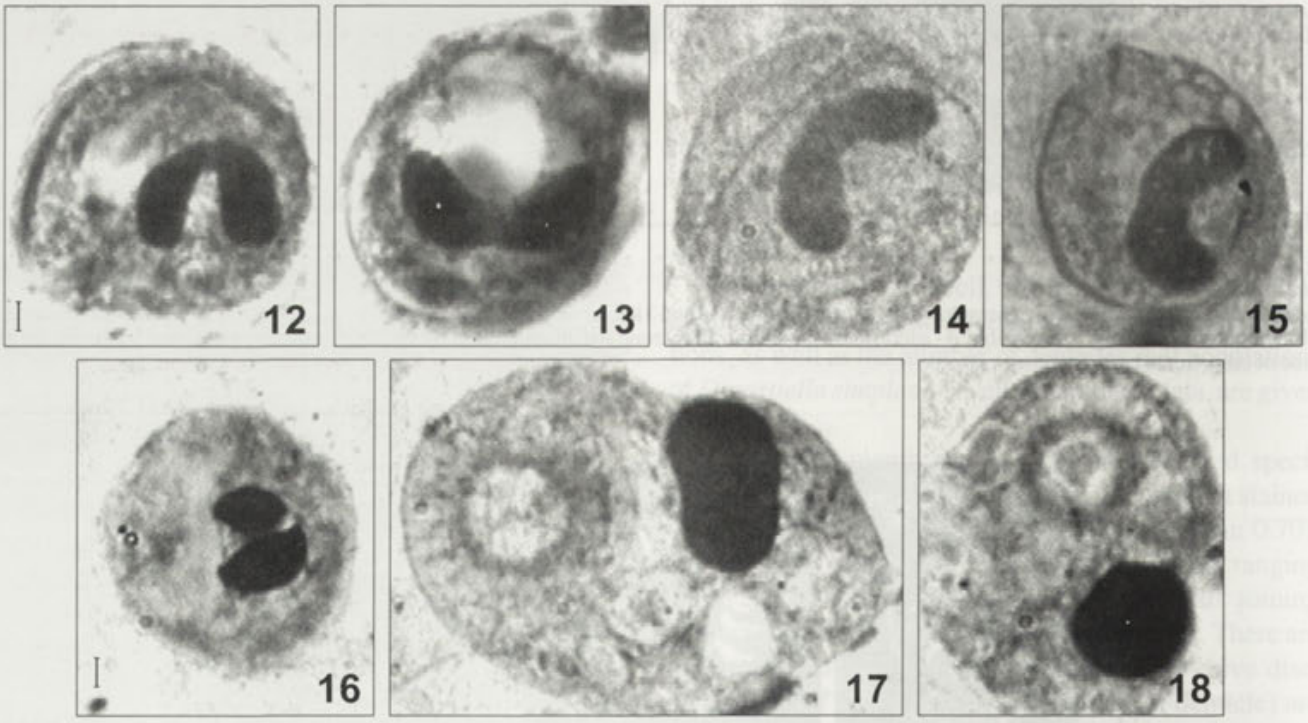

Figs 12-18. *Dipartiella simplex*, nuclear apparatus. 12-15 - different aspects of typical macronucleus; 16 - macronucleus with two parts connected by narrow commissure; 17 - bean-like and 18 - oval-shaped macronuclei. Scale bar - 2 μm

Two different "pictures" of the denticulate ring were recognised in the material examined. The first group of ciliates posses loosely arranged denticles, which appear to be, unlinked (Figs. 9, 10). One such specimen is shown in the Fig. 9a by Raabe (1959). The second type has denticles whose central parts are much more tightly linked (Figs. 6, 7). Generally, in individual populations (slides) one type dominates but mixed populations also occur. Sometimes, even individual specimens have their denticles loosely arranged in part of the ring and densely arranged in other places (Figs. 8, 11).

The macronucleus is usually horse-shoe shaped with characteristic dilation at both ends and a narrowing of the most convex part, giving the appearance of being com-

Table 1. (contd)

Diameter of the denticulate ring				Number of the denticles				Length of the denticles				Locality
range	n	mean	SD	range	n	mean	SD	range	n	mean	SD	
5.3-8.7	51	6.7	0.79	14-20	51	17.7	1.16	2.7-3.8	51	3.3	0.26	Kuźnica
4.7-8.3	52	6.1	0.79	15-21	52	17.3	1.07	2.3-3.6	52	3.1	0.29	Kuźnica
4.4-7.9	56	6.1	0.89	15-20	56	17.2	1.12	2.2-3.5	56	3.0	0.31	Kuźnica
5-8.8	57	6.8	0.80	15-20	56	17.6	1.09	2.3-3.5	57	2.9	0.26	Kuźnica
5-8	51	6.7	0.93	16-18	51	17.3	0.68	2.7-3.6	51	3.1	0.25	Kuźnica
4.5-8.3	50	6.1	0.62	16-21	50	18.1	0.89	2.7-3.7	50	3.3	0.25	Swarzewo
4.5-7	54	5.8	0.60	15-19	54	17.1	0.84	2.6-3.9	54	3.3	0.26	Swarzewo
4.5-7.5	55	6.2	0.72	14-18	55	16.9	0.84	3-4	55	3.4	0.25	Swarzewo
4.5-7.5	52	6.0	0.72	16-20	52	18.1	1.00	2.5-3.8	52	3.2	0.29	Rewa
4.4-8.8	478	6.3	0.84	14-21	477	17.5	1.06	2.2-4	478	3.2	0.32	
6.5-9.5		8.0		17-20		18						

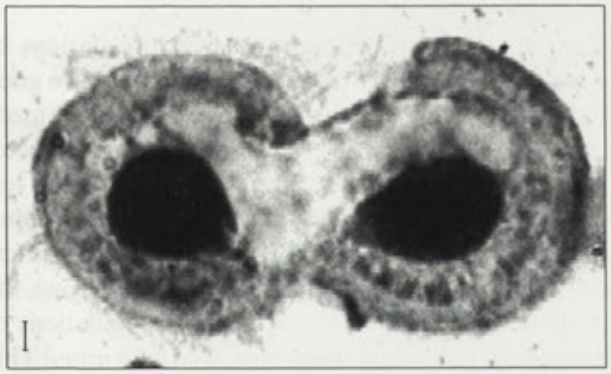

Fig. 19. *Dipartiella simplex*, dividing specimen, note the shape of the macronucleus. Scale bar - 2 μm

posed of two more or less unequal parts (Figs. 12-15). The dimensions of these parts are as follows: 5.5-11 x 2.3-5.5 and 5-10 x 1.8-5.5 μm (mean 8.06 x 3.78 and 7.21-3.6), the narrowing are 1-4.5 μm (mean 2.06) thick (n=61).

The angle between the lobes of the macronucleus is variable, so that the outer diameter reaches 8-18 μm (mean 12.69). Sometimes the macronucleus appears as two elongate lobes joined by a narrow connecting piece (Fig. 16). In the sagittal plane, the macronucleus is subcircular in outline, being slightly vertically flattened.

In some cells, the macronucleus has an oval or bean-like shape (Figs. 17, 18) and measures 5.5-14 μm (mean 8.99) in length and 1.8-9 μm (mean 5.35) in width (n=17). The micronucleus was not observed.

The large amount of material available, comprising samples of several dozen specimens from 9 populations provided the possibility to examine the interpopulational variation in *Dipartiella simplex*. Results of a two-level nested ANOVA for three main characters (diameter of the adhesive disc, diameter of the denticulate ring and number of denticles) are presented in Table 2. The analysis shows no significant differences between groups of populations originating from various parts of Puck Bay and Gdańsk Bay, while there are highly significant differences between populations from individual host specimens of *Gobius niger*.

DISCUSSION

I had examined Raabe's original material of *Dipartiella simplex* from the gills of *Gobius niger* from Gdańsk Bay and its innermost part, Puck Bay. At least a part of this material, collected by Z. Raabe in 1958 at Kuźnica and Rewa, and Swarzewo, compose a typical series of ciliates on which the description of the new species and genus were based.

This redescription completes the original description by Raabe (1959), providing a more precise characterisation due to better technical equipment (microscope) and more precise methods of measurement and photomicrography. Also, measuring many specimens and the statistical analysis of the data give a more comprehensive description of the species.

The cell dimensions (diameter and height), as well as the body shape observed in preparations stained with hematoxylin in both, the original descriptions by Raabe (1959) and in the present study are very similar, although the dimensions given in the present paper are slightly larger. The shape of the adoral spiral is described identically, as well as the shape of the macronucleus. In both descriptions, dilation of the arms of the "horse-shoe" and

Table 2. Two-level nested ANOVA table for three main characters of 9 polulations of *Dipartiella simplex*

Source of variation	Degree of freedom	Diameter of		Number of denticles	Critical value		
		adhesive disc	denticulate ring		df	$F_{.01}$	$F_{.05}$
Among local groups of populations	3-1=2	2.226 ns	2.181 ns	1.176 ns	(2,6)	10.925	5.143
Among populations	9-3=6	3.328 s	8.899 s	9.017 s	(6,450)	2.8426	2.119
Within populations	n-9	n=469	n=469	n=468			

the narrowing between them are noted. This macronucleus shape should be recognised as a specific and generic character, as well. In some specimens, this narrowing was extremely thin, forming only a fine strand joining the arms. As previously noted some specimens had oval or bean-shaped macronuclei. May be, these ciliates were preparing to division, or those being in the process of reconstruction of the nuclear apparatus just after division. Such specimens were fairly frequent in the material examined, especially in silver-impregnated preparations (Fig. 19).

The present paper for the first time gives the dimensions of the macronucleus of *D. simplex*. In order to eliminate inconsistency in measuring, only specimens with the macronucleus situated in a transverse plane were chosen for measurement. In spite of this, great variation in the diameter of this organelle is observed, due to the variable angle between both arms. Generally, pictures of the macronucleus of *D. simplex* are highly variable. No micronucleus was observed, probably owing to its very small size or low intensity of staining.

Cell dimensions of silver-impregnated specimens of *D. simplex* according to Raabe (1959) and the present study are given in Table 1. New dimensions are slightly smaller, probably due to the fact that they were taken from many specimens chosen at random, while in former studies usually the "nicest" and the largest specimens were measured. Differences observed in the denticle shape may be related to cell growth, but this question will be discussed elsewhere, based on more suitable material.

In the present investigation, attention has been drawn to the occurrence of specimens with loosely arranged denticles and to those with much more densely arranged denticles. Sometimes the differences were so great that there appeared to be two different forms. However, the occurrence of specimens with mixed arrangement of denticles contradicted such supposition. It seems rather that these differences are the result of deformation of denticulate ring during desiccation of preparations before impregnation with silver.

The large material obtained from 9 populations of *D. simplex* originating from 3 localities provides a good basis for statistical comparison. Analysis of variance made on 3 characters, diameter of the adhesive disc, diameter of the denticulate ring and the number of denticles, has shown no significant differences between groups of populations from particular localities and high significant differences between individual populations. This shows the important role played by the isolation of populations of *D. simplex* on individual specimens of *Gobius niger*. This result agrees with the behaviour of fish hosts that live in pairs occupying their own territory, never in shoals (Wiktor 1962). Thus, *D. simplex* shows similar type of interpopulational variation as other species of trichodinid from "closed" populations, e.g. *T. vesicularum* Faure-Fremiet, *T. ranae* da Cunha or *T. urinaria* Dogiel (Kazubski 1982).

Finally, there is the question of the validity of this species and genus raised by Lom and Dyková (1992) may be resolved. In light of the data presented in this paper, the species *D. simplex* should be regarded as valid. It was properly described by Raabe (1959) and the type material is preserved. Of course, it would be useful to find once more this species[1] and re-examine it with more advanced methods, especially to determine more exactly the structure of the adoral spiral and oral ciliature in order to adjust the description to the standard postulated by J. Lom. It seems however, that the structure of the denticles, as well

[1]Collection of the new material of *D. simplex* is rather difficult because their fish host *Gobius niger* in Gdańsk Bay has been rarely observed in last years (Horackiewicz and Skóra 1996).

as that of the nuclear apparatus distinguish *D. simplex* from all other trichodinid and are sufficient to maintain as valid the genus *Dipartiella* Stein.

REFERENCES

Horackiewicz J., Skóra K. E. (1996) Występowanie babkowatych (Gobiidae, Pisces) w polskiej strefie przybrzeżnej Morza Bałtyckiego. *Zool. Pol.*, **41 (Suppl.):** 179-188

Kazubski S. L. (1979a) *Trichodina vesicularum* Faure-Fremiet, 1943 and *T. faure-fremieti* nom. nov. (Ciliata, Peritrichida) - parasites of newts of the genus *Triturus*. *Acta Protozool.* **18:** 371-383

Kazubski S. L. (1979b) Morphological variability of *Trichodina vesicularum* Faure-Fremiet and *T. faure-fremieti* Kazubski, parasites of newts from Poland and France. *Acta Protozool.* **18:** 385-400

Kazubski S. L. (1982) Studies on the interpopulational variability of trichodinas (Ciliata). *Acta Protozool.* **21:** 135-148

Lom J., Dyková I. (1992) Protozoan Parasites of Fishes. Elsevier, Amsterdam

Raabe Z. (1959) Urceolariidae of gills of Gobiidae and Cottidae from Baltic Sea. *Acta Parasit. Pol.* **7:** 441-452

Stein G. A. (1961) On the systematics of Urceolariidae (Infusoria, Peritricha). *Zool. Zh.* **60:**1137-1142 (In Russian, with English summary)

Wiktor J. (1962) Gobiidae. In: Klucze do Oznaczania Kręgowców Polski, część I, Kręgłouste - Cyclostomi, Ryby - Pisces, (Ed. M. Gąsowska), Państwowe Wydawnictwo Naukowe, Warszawa, Kraków

Received on 21st December, 1998; accepted on 25th May, 1999

Acta Protozool. (1999) 38: 313 - 316

ACTA
PROTOZOOLOGICA

Eimeria kuhliensis sp.n. (Apicomplexa: Eimeriidae) from Pipistrelle Bat, *Pipistrellus kuhlii*

Mohamed S. ALYOUSIF

Department of Zoology, College of Science, King Saud University, Riyadh, Saudi Arabia

Summary. Oocysts of *Eimeria kuhliensis* sp. n. are described from the intestinal contents of the pipistrelle bat, *Pipistrellus kuhlii* in Saudi Arabia. Sporulated oocysts of E. *kuhliensis* are subspherical 27.6 x 25.9 µm (25.4-31.5 x 23.3-29.6). A small, spherical polar granule present but a micropyle is absent. An oocyst residuum present, consisting of several globules that is irregular in shape and size. Sporocysts are elongate-ovoid, 12.6 x 8.5 µm (12.1-13.6 x 8.1-9.3), with Stieda and substiedal bodies. A sporocyst residuum is present. Sporozoites are elongate, each with two refractile globules.

Key words: description, *Eimeria kuhliensis* sp.n., pipistrelle bat, *Pipistrellus kuhlii*.

INTRODUCTION

The family Vespertilionidae is represented in Arabia by 7 species of vespertilionid bats. These are *Pipistrellus pipistrelus* (Schreber, 1774), *P. rueppelli* (Fischer, 1829), *P. savii* (Bonaparte 1837), *P. bodenheimeri* (Harrison 1960), *P. ariel* (Thomas, 1904), *P. arabicus* (Harrison, 1979), and *P. kuhlii* Natterer, 1819 (Harrison and Bates 1991). The latter species occurs in some parts of the central region of Saudi Arabia, and the diet of these bats consists of small insects caught in flight (Nowak 1994). To date, only two studies have been performed on the coccidian parasites that infect this species of bat from Saudi Arabia (Alyousif 1999, Alyousif *et al.* 1999). Here, I summarize my findings on a detailed description of a new species of *Eimeria* from *P. kuhlii*.

This study is the sixth in a series dealing with mammalian coccidia in Saudi Arabia (Kasim *et al.* 1991; Alyousif *et al.* 1992, 1999; Alyousif and Al-Shawa 1998; Alyousif 1999).

MATERIALS AND METHODS

Fifteen adult *Pipistrellus kuhlii* were collected by hand from roof crevices of old farm houses in the city of Riyadh during August 1998. All bats were anaesthetized in the laboratory. The abdominal cavity was opened, the intestinal tract removed, and the caecum, rectum, and colon

Addres for corespondence: Mohamed S. Alyousif, Department of Zoology, College of Science, King Saud University, P.O. Box 26213, Riyadh 11486, Saudi Arabia; Fax: 4760657

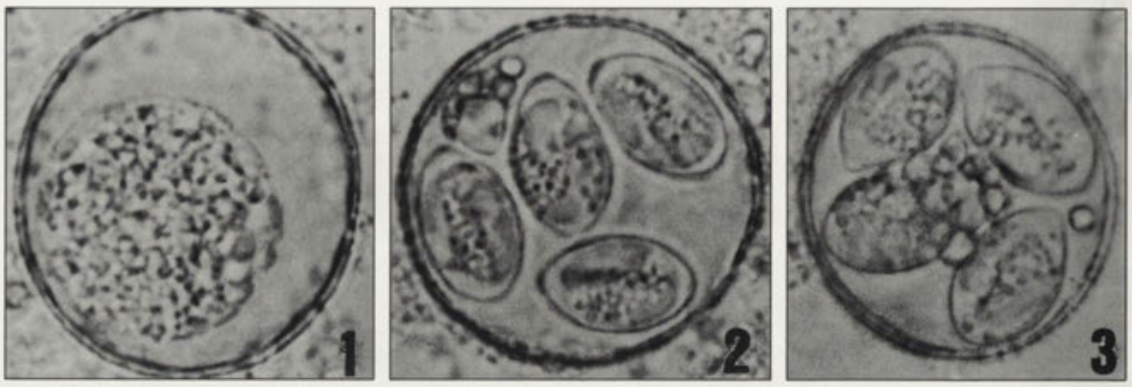

Figs. 1-3. Photomicrographs of *Eimeria kuhliensis* sp.n. from naturally infected *Pipistrellus kuhlii* x 1000. 1 - unsporulated oocyst showing early sporoplast; 2 - sporulated oocyst showing Stieda body, sporocyst residuum, and refractile globule; 3 - sporulated oocyst showing polar body and large, irregularly shaped oocyst residuum.

were slit lengthwise and their contents were collected separately and mixed with 2.5% aqueous (w/v) potassium dichromate solution to inhibit bacterial growth. Feces were initially examined for coccidia using brightfield microscopy. Positive samples were then concentrated for oocysts by coverslip flotation with Sheather's sugar solution technique (Duszyński *et al.* 1982), incubated at 26 ± 2°C and examined periodically to determine the sporulation time. Thirty sporulated oocysts and sporocysts were examined and measured with a microscope fitted with a x 100 apochromatic oil immersion objective and x 10 ocular micrometer. The number of layers of the oocyst wall, its thickness and detailed structure of oocysts, sporocysts and sporozoites were examined. All measurements are in micrometers (μm), with size ranges in parentheses following the means.

RESULTS

Eimeria kuhliensis sp.n. (Figs. 1-4)

Description

Sporulated oocysts are subspherical and measure 27.6 x 25.9 (25-32 x 23-30) (n=30), shape index (length/width ratio) is 1.1 (1-1.2), with slightly striated, light greenish-yellow, apparently single-layered wall 0.8 (0.6-1.0) thick. A small, spherical polar body is present, but a micropyle is absent. Oocyst residuum is irregular in size and shape, consisting of several globules (0.8-5.0). Sporocysts (n=30) are elongate ovoid 12.6 x 8.5 (12-14 x 8-9), with shape index of 1.5 (1.4-1.6). Stieda body is present at slightly tapered portion of sporocyst wall; substiedal body present as a clear space below the pointed end of sporocysts; sporocyst residuum present composed of many small dispersed granules sometimes obscuring sporozoites. Sporozoites are elongated, laying lengthwise in sporocysts, each with a large, posterior refractile body at the broad end and a small refractile body at the tapered end.

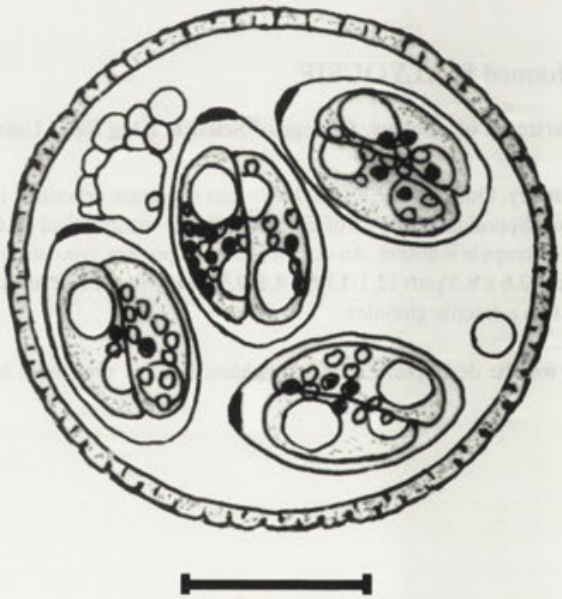

Fig. 4. Camera lucida drawing of sporulated oocyst of *E. kuhliensis* sp.n. Scale bar - 10 μm

Taxonomic summary

Type host: *Pipistrellus kuhlii* (Natterer, 1819).

Type locality: Riyadh, central region, Saudi Arabia.

Prevalence: found in 4 of 15 (27%) bats.

Site of infection: unknown. Oocysts found in intestinal contents.

Sporulation time: 7 days at 26 ± 2°C.

Etymology: the specific name *kuhliensis* is derived from the species name of the host.

Table 1. Comparative data of *Eimeria* species from pipistrelle bats. Size in µm

Original structure	*E. macyi*	*E. redukeri*	*E. pipistrellus*	*E. chiropteri*	*E. kuhliensis* sp.n.
Oocyst					
shape	subspherical to broadly ellipsoid	subspherical	subspherical	broadly ellipsoid	subspherical
size	16-21 x 15-19 (19 x 17.6)	16-25 x 14-21 (20.3 x 18.1)	23.3-27 x 20-25.4 (24.8 x 23.2)	18.8-25.9 x 16.5-25.2 22.5 x 20.3	25.4-31.5 x 23.3-29.6 (27.6 x 25.9)
wall	single rough	bilayered (mammiliated)	smooth	bilayered (mammiliated)	single (striated)
micropyle	absent	absent	absent	absent	absent
residuum	absent	single (2.0 x 3.8)	one to three (4.5-5.6)	spheroid (4.3-5.6)	several globules
polar granule	ellipsoid	ellipsoid	spheroid	spheroid	spheroid
Sporocyst					
shape	ovoid	ovoid	ovoid	ovoid	ovoid
size	10-12 x 6-8 (11 x 7)	8-12 x 5-8 (10.6 x 6.6)	10.5-12.9 x 7.5-9.4 (11.6 x 8.3)	10.1-11.7 x 6.8-8.1 (10.7 x 7.5)	12.1-13.6 x 8.1-9.3 (12.6 x 8.5)
residuum	several granules	1-3 globules	several granules	several granules	several granules
Host	*Pipistrellus subflavus*	*Pipistrellus javanicus*	*Pipistrellus kuhlii*	*Pipistrellus kuhlii*	*Pipistrellus kuhlii*
Locality	U.S.A.	Japan	Saudi Arabia	Saudi Arabia	Saudi Arabia
Citation	Wheat (1975)	Duszyński (1997)	Alyousif *et al.* (1999)	Alyousif (1999)	Present study

Type specimens: oocysts in 10% formalin and a phototype are deposited in the parasitological collection, Zoology Department, College of Science, King Saud University, Riyadh, Saudi Arabia both as (KSUC. 106), 25 September, 1998 from *Pipistrellus kuhlii*, collected in the Riyadh city in the central region of Saudi Arabia.

Holotype specimen: copy of the line drawing is deposited in the parasitological collection, Zoology Department, College of Science, King Saud University, Riyadh, Saudi Arabia as (KSUC. 108).

DISCUSSION

Only four species of *Eimeria* have been described from members of the genus *Pipistrellus*. *Eimeria chiropteri* from *Pipistrellus kuhlii* from Saudi Arabia (Alyousif 1999), *E. pipistrellus* from *Pipistrellus kuhlii* from Saudi Arabia (Alyousif *et al.* 1999), *E. macyi* from *Pipistrellus subflavus* from Alabama U.S.A. (Wheat, 1975) and *E. redukeri* from *Pipisterellus javanicus* from Japan (Duszyński, 1997). However, oocysts of *E. kuhliensis* sp.n. differ considerably from all of these eimerian species. *E. kuhliensis* sp.n. differs from *E. macyi* in having much larger oocysts and sporocysts, in the presence of oocyst residuum, and also in having spheroid polar granule. It also differs from previously described *E. redukeri* in having much larger oocysts and sporocysts, a single striated oocyst wall, an oocyst residuum as several globules, and in having spheroid polar granule and sporocyst residuum of many small granules. *E. kuhliensis* sp.n. differs from both *E. chiropteri* and *E. pipistrellus* in having larger oocysts and sporocysts, a single striated oocyst wall and also in having an oocyst residuum as several globules. These differences in structural features, host species and geographical distributions strongly suggest that *E. kuhliensis* sp.n. is a distinct and hitherto undescribed species.

Finally, it is clear that oocyst wall texture is not an appropriate structural feature for examining phylogenetic origins, thus supporting the finding of Scott and Duszyński (1997).

Acknowledgement: The author wishes to thank Mr. Jamal Tolbah for his assistance in collecting bats.

REFERENCES

Alyousif M.S. (1999) *Eimeria chiropteri* n.sp. (Apicomplexa: Eimeridae) from Saudi Arabian bat *Pipistrellus kuhlii* (Chiroptera: Vespertilionidae). *J. Egypt Soc. Parasitol.* **29:** 275-280

Alyousif M.S., Al-Shawa Y.R. (1998) *Eimeria gnui* sp.n. (Apicomplexa: Eimeriidae) from white-tailed gnu, *Connochactes gnu*. *Acta Protozool.* **37:** 53-55

Alyousif M.S., Kasim A.A., Al-Shawa Y.R. (1992) Coccidia of the domestic goat (*Capra hirucus*) in Saudi Arabia. *Int. J. Parasitol.* **22:** 807-811

Alyousif M.S., Al-Dakhil M., Al-Shawa Y. (1999) *Eimeria pipistrellus* n.sp. from *Pipistrellus kuhlii* (Chiroptera: Vespertilionidae) in Saudi Arabia. *Korean J. Parasitol.* **37:** 1-4

Duszyński D.W. (1997) Coccidia from bats (Chiroptera) of the world: A new *Eimeria* species in *Pipistrellus javanicus* from Japan. *J. Parasitol.* **83:** 280-282

Duszyński D.W., Eastham G., Yates T. L. (1982) *Eimeria* from Jumping mice (*Zapus spp*): A new species and genetic and geographical features of *Z. hudsonicus luteus*. *J. Parasitol.* **68:** 1146-1148

Harrison D.L., Bates P.J. (1991) The Mammals of Arabia Sevenoaks, Kent: Harrison Zoological Museum

Kasim A.A., Alyousif M.S., Al-Shawa Y.R. (1991) Redescription of *Eimeria gazella* Musaev, 1970 (Apicomplexa: Eimeriidae) from the Arabian gazelle, *Gazella gazella, arabica* (Artiodactyla: Bovidae) in Saudi Arabia. *Parassitologia* **33:** 107-109

Nowak R.M. (1994) Walker's Bats of the World. The Johns Hopkins Press. Ltd., London, U.K., 287

Scott D.T., Duszyński D.W. (1997) Eimeria from bats of the world: Two new species from *Myotis* spp. (Chiroptera: Vespertilionidae). *J. Parasitol.* **83:** 495-501

Wheat B.E. (1975) *Eimeria macyi* sp.n. (Protozoa: Eimeriidae) from the eastern *Pipistrellus subflaves* from Alabama. *J. Parasitol.* **61:** 920-922

Received on 2nd November, 1998; accepted on 2nd June, 1999

Acta Protozool. (1999) 38: 317 - 321

ACTA
PROTOZOOLOGICA

Light and Electron Microscopic Observations on *Kudoa boopsi* sp. n. (Myxosporea: Kudoidae), a Gill Parasite of *Boops boops* (Pisces: Teleostei: Sparidae) from Coasts of Senegal (West Africa)

Takouda Kossi KPATCHA, Cheikhna DIEBAKATE, Ngor FAYE and Bhen Sikina TOGUEBAYE

Laboratory of Parasitology, Department of Animal Biology, Faculty of Sciences and Technologies, University C. A. DIOP of Dakar, Dakar, Senegal

Summary. *Kudoa boopsi* sp. n. is described from the gill filaments of *Boops boops* from coasts of Senegal (West Africa). Out of 141 fish examined, nine were found to be parasitized. The cysts (plasmodia) formed were located at the base of gill filaments in the epithelial tissue. They were ellipsoidal and measured 0.5 to 1.5 mm. The dimensions of spores were width - 8.87 ± 0.18 (8-10) µm, thickness - 7.61 ± 0.11 (7-8) µm, length - 5.73 ± 0.13 (4-6) µm. The polar capsules were equal in size and measured 2.98 ± 0.09 (2-4) x 1.73 ± 0.07 (1-2) µm. Ultrastructural observations have shown that sporogenesis was initiated by bicellular stages, one of cells enveloping the other. Valvogenic cells cytoplasm presented electron-dense bodies. Capsulogenic cells were similar to that of other myxosporidia. The polar filament of polar capsules had 2 to 3 coils. The sporoplasm was constituted of two morphologically distinct cells, one of which surrounding the other.

Key words: *Boops boops*, *Kudoa boopsi* sp. n., Myxosporea, sparid fish, Senegal, ultrastructure, West Africa.

INTRODUCTION

Several myxosporidian species belonging to the genus *Kudoa* Meglitsch, 1947 have been described in fishes. Some of them, as *Kudoa paniformis* Kabata and Whitaker, 1981; *Kudoa ciliatae* Lom, Rohde and Dykova, 1992; *Kudoa thyrsites* (Gilchrist, 1924) and *Kudoa lunata* Lom, Dykova and Lhotakova, 1983 were examined in the electron microscope (Stehr 1986, Stehr and Whitaker 1986, Lom and Dykova 1988, Lom *et al.* 1992). The majority of *Kudoa* species were found in the skeletal muscle of their hosts (Lom and Dykova 1992). The only species which infects the gills of its host is *Kudoa branchiata* Joy, 1972. The present study is a second report of a *Kudoa* species from the world that found in the fish gill.

Address for correspondence: Bhen S. Toguebaye, Department of Animal Biology, Faculty of Sciences and Technologies, University C. A. DIOP of Dakar, Dakar, Senegal; Fax: (221) 825 25 29 or 824 63 18; E. mail: parasito@ucad.refer.sn

MATERIALS AND METHODS

141 specimens of *Boops boops* (Sparid fish) caught from coasts of Senegal (West Africa) were examined for the presence of myxosporean parasites. Fresh smears of cysts (plasmodia) located at the base of gill filaments were used for measuring living spores by means of light microscopy.

For ultrastructural studies, fresh cysts were fixed at 4°C with 2.5% glutaraldehyde in 0.1 M sodium cacodylate buffer (pH 7.2) for 24h, then post-fixed at 4°C with 1% osmium tetroxide in the same buffer for 1 h. After dehydration through a gradual ethanol series and propylene oxide, the cysts were embedded in Spurr resin. Ultrathin sections were stained with uranyl acetate and lead citrate, and examined under a Jeol 100CXII electron microscope. Semithin sections were stained with Toluidine blue and examined under a light microscope.

For scanning electron microscopy, spores were smeared on circular cover glasses, lightly air-dried and fixed in 2.5% glutaraldehyde in 0.1 M sodium cacodylate buffer (pH 7.2) at 4°C for 12h. After washing in the buffer and critical point drying, the smears were covered with metallic gold and palladium and observed with a Jeol 35 CF scanning electron microscope.

RESULTS

Light microscope observations

Nine of 141 *Boops boops* examined were found to be parasitized. The myxosporidium infected only the gill filaments. It formed whitish and ellipsoidal cysts (plasmodia) at the base of gill filaments (Fig. 1). Semithin sections shown that the cysts were localized in the epithelial tissue of gill filaments and were filled of development stages of the myxosporidium (Fig. 2). They measured 0.5 to1.5 mm long. In apical view, the spores (Fig. 3) were rounded quadrate. In lateral view, they were ellipsoidal (Fig. 4). The sutural lines were well visible (Fig. 3). The spores dimensions were: width - 8.87± 0.18 (8-10) µm, thickness - 7.61 ± 0.11 (7-8) µm, length - 5.73 ± 0.13 (4-6) µm. Four polar capsules were equal in size - 2.98 ± 0.09 (2-4) x 1.73 ± 0.07 (1-2) µm.

Ultrastructure

Under the electron microscope, the inner of cysts did not show many sporogonic plasmodia and the stages of the myxosporidium were mixed (Fig.6).

The earliest stages of sporogenesis observed were bicellular forms with a cell enveloping the other (Figs. 6, 7). The enveloping cell was spherical (Fig. 6) or elongated (Fig. 7) and bound by a simple membrane. Their cytoplasm contained one nucleus, mitochondria, electron lucent vesicles and cisternae of endoplasmic reticulum and numerous ribosomes. The enveloped cell were rounded and bound by a double plasma membrane. Their cytoplasm contained numerous ribosomes, a large nucleus, mitochondria and endoplasmic reticulum.

Spores had a smooth surface (Fig. 5). A section through these spores showed the sporoplasm, the valvogenic cells and the capsulogenic cells. The sporoplasm (Figs. 8, 9) was constituted of a smaller cell with a more electron-dense cytoplasm surrounded by a larger cell with a cytoplasm containing sometimes dense striated rod-like organelle (Fig. 8). Valvogenic cells were located at the periphery of the spores. Their cytoplasm presented dense bodies (Figs. 8, 9). Capsulogenic cells were grouped at apical pole of spores. Each of them presented one polar capsule in which, the polar filament had 2 to 3 coils.

DISCUSSION

Taxonomy

The species described in this work produces spores which form and dimensions are the same that those of spores of *Kudoa nova* Najdenova, 1975, found in muscles of the numerous species of fish (among them two species of Sparid fish, *Pagellus acarnae* and *Dentex macrophtalmus*) of Atlantic Ocean, Mediterranean and Black Sea. Indeed, according to Kovaleva *et al.* (1979), *K. nova* produces spores which dimensions are following - width 8.5-9.8 µm, thickness - 7.5-8 µm, length - 5.3 - 6.5 µm. The polar capsules measure - 2.7-3.2 x 2 µm. However, the present species differs from *K. nova* by its host and its site of infection.

The only species of *Kudoa* which infected gill filaments is *Kudoa branchiata* Joy, 1972 described from *Leiostomus xanthurus* in Clear Lake Texas. It forms elongate cysts (trophozoites) and its spores are rounded, appically tuberculated, with 4µm length and 4.5 µm width (Joy 1972). It differs from the present species by the shape and size of its spores and by its host.

We conclude that the *Kudoa* species of *Boops boops* is a new species and we propose the name *Kudoa boopsi* sp. n. after the name of its host.

Ultrastructure

Our observations show that during sporogenesis in *K. nova*, it forms bicellular stages, one of cells enveloping

Figs. 1-6. *Kudoa boopsi* sp. n. 1 - cyst on a gill filament; 2 - semithin section; 3 - fresh spores in apical view; 4 - fresh spores seen from the side (arrows) and apical (curved arrow) views; 5 - spore observed in scanning electron microscopy; 6 - spherical bicellular stage inside the cyst (plasmodium). C - cyst, ED - enveloped cell, EDN - enveloped cell nucleus, EG - enveloping cell, EGN - enveloping cell nucleus, HET - host epithelial tissue, M - mitochondria, S - spore, VN - vegetative nucleus. Scale bars: 1 - 1 mm; 2 - 80 µm; 3, 4 - 6 µm; 5 - 1.5 µm; 6 - 1µm

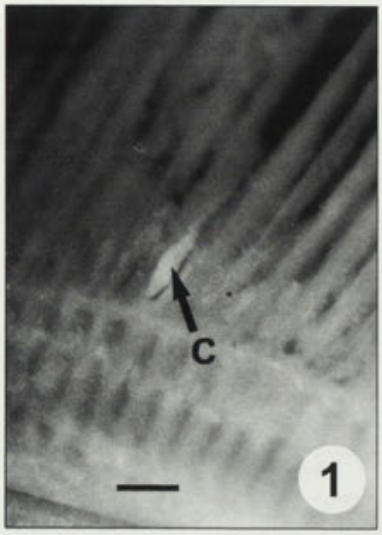

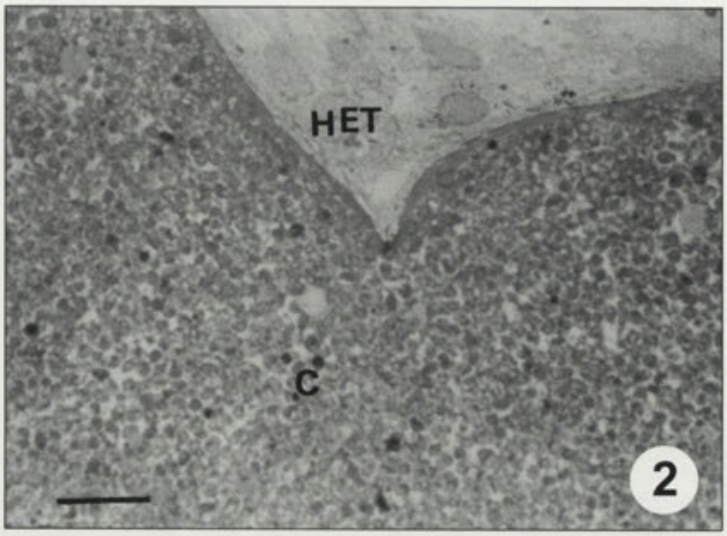

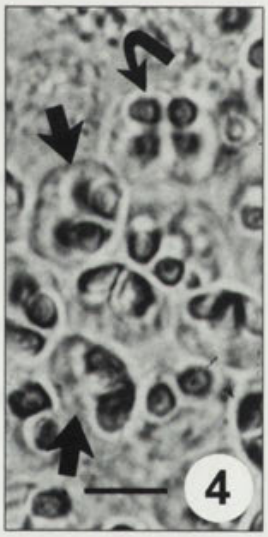

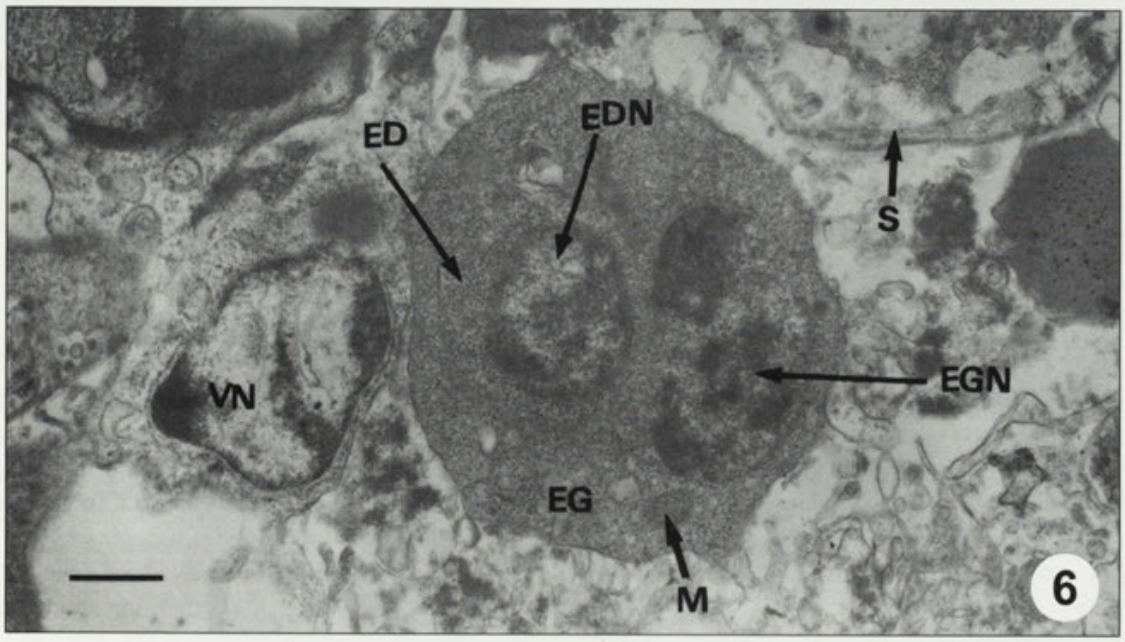

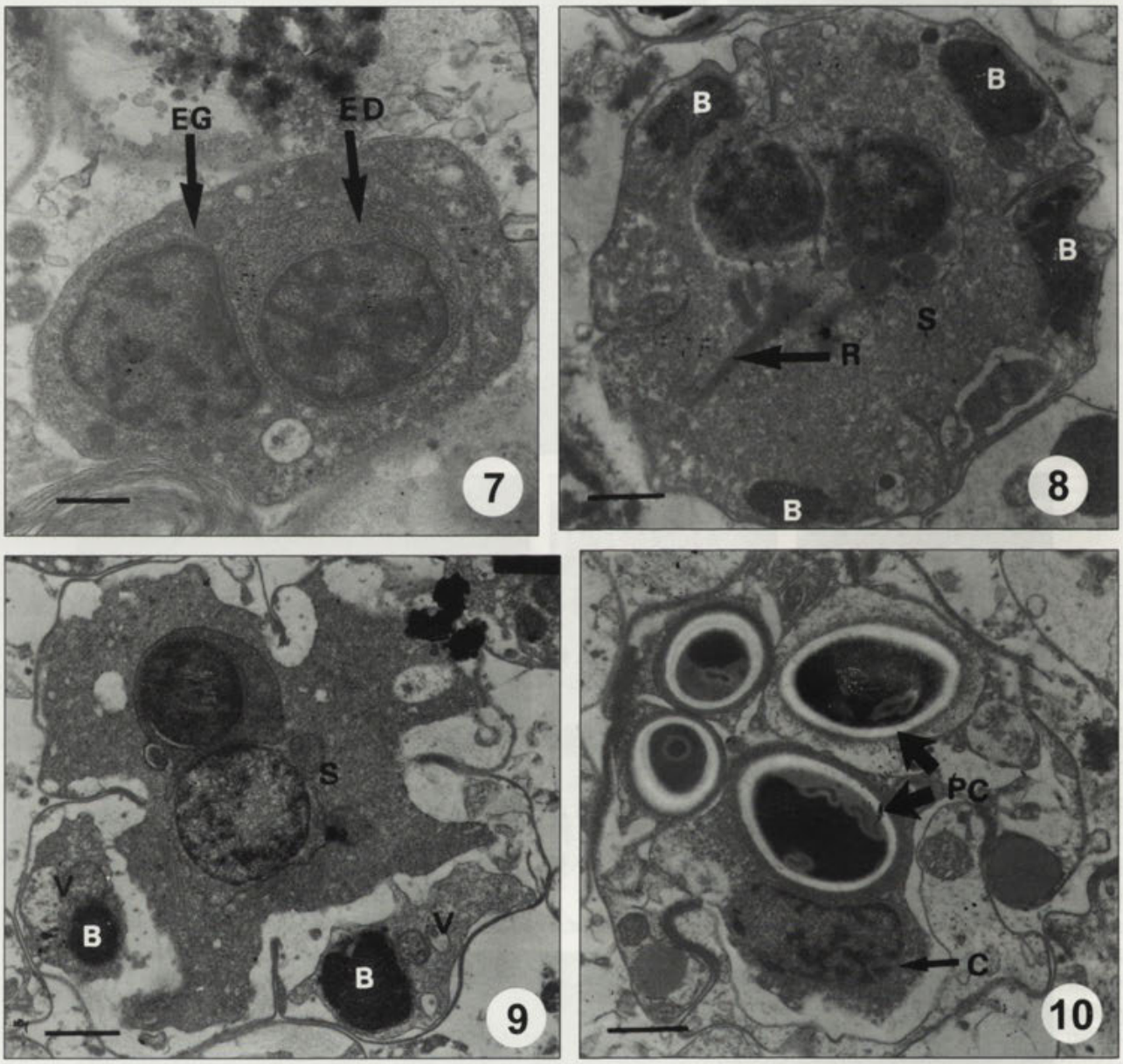

Figs. 7-10. *Kudoa boopsi* sp. n. spore. 7 - elongate bicellular stage; 8 - section showing dense striated rod-like organelle (R) within the sporoplasm (S) and dense bodies (B) within the valvogenic cells; 9 - section showing the sporoplasm (S); 10 - mature spore showing capsulogenic cells (C) and polar capsules (PC). B - dense body, ED - enveloped cell, EG - enveloping cell, V - valvogenic cell. Scale bars: 7-10 - 1 μm

the other. It is for the first time that these stages were observed in *Kudoa* species. These stages have been observed in many others genera of myxosporidia. It is the case in *Myxidium* spp., *Henneguya* spp., *Myxobolus* spp., *Hoferellus* spp., *Sphaerospora* spp., *Ceratomyxa* spp. and *Thelohanellus* spp. (Siau 1978, Desportes and Théodorides 1982, Desser *et al.* 1983, Lom and Dykova 1985, Lom *et al.* 1985, Lom 1987, El-Matbouli and Hoffman 1996, Kpatcha *et al.* 1997). Stehr (1986) and Lom and Dykova (1988) had not observed these bicellular stages in *Kudoa paniformis* and *Kudoa lunata*.

The origin and nature of these bicellular stages differ according to genera of myxosporidia. In genera having a pansporoblast, the sporogenesis begins by the union of two generative cells, one of which, the pericyte or pansporoblast, envelops the other, the sporogenic cell. It

is for example the case in *Myxobolus exiguus* (Siau 1978) and *Henneguya adiposa* (Current 1979). In genera devoid of a pansporoblast, the sporogenesis begins by the endogenous division of generative cells to give bicellular stages, one of which, the pseudoplasmodium cell, envelops the other, the sporogonic cell. It is for example the case in *Sphaerospora coregoni* (El-Matbouli and Hoffman 1996) and *Ceratomyxa shasta* (Yamamoto and Sanders 1979). According to some authors (Stehr 1986; Lom and Dykova 1988, 1992), *Kudoa* species produce spores without pansporoblast. In *Kudoa boopsi* we have not been able to prove how the bicellular stages are produced. We do not know therefore if these stages arise by fusion of two generative cells or by endogenous cleavage of a generative cell.

The sporoplasm of *Kudoa nova* presents sometimes striated rod-like organelles. It is for the first time that this organelle is observed in the sporoplasm of *Kudoa* spp. We ignore its origin and its functions. Dense bodies observed in valvogenic cells have been equally observed by Stehr (1986) in valvogenic cells of *Kudoa paniformis*. According to Stehr (1986), these dense bodies would be precursor materials for valve wall formation. The polar capsule of *K. boopsi* presents no particularity, it is similar to that described in many other myxosporidia.

REFERENCES

Current W. L. (1979) *Henneguya adiposa* Minchew (Myxsporidia) in the channel catfish: ultrastructure of the plasmodium wall and sporogenesis. *J. Protozool.* **26:** 209-217

Desportes L., Théodoridès J. (1982) Données ultrastructurales sur la sporogenèse de deux Myxosporidies rapportées aux genres *Leptotheca* et *Ceratomyxa* parasites de *Merluccius merluccius* (L.) (Téléostéen, Merluciidae). *Protistologica* **18:** 533-557

Desser S. S., Molnar K., Weller I. (1983) Ultrastructure of sporogenesis of *Thelohanellus nikolski* Akhmerov, 1955 (Myxozoa: Myxosporea) from the common carp, *Cyprinus carpio*. *J. Parasitol.* **69:** 504-518

El-Matbouli M., Hoffman R. W. (1996) Light and electron microscopic descriptions of *Sphaerospora coregoni* El-Matbouli, Hoffman and Kern, 1995 (Myxosporea: Sphearosporidae) from the kidney of Whitefish (*Coregonus lavaretus*). *Europ. J. Protistol.* **32:** 389-398

Joy J. J. (1972) A new species of *Kudoa* (Myxosporidea: Chloromyxidae) from the spot, *Leiostomus xanthurus* Lacépede, in Clear Lake Texas. *J. Protozool.* **19:** 264-265

Kovaleva A. A., Shulman S. S., Yakovlev V. N. (1979) Myxosporidia of the genus *Kudoa* (Myxosporidia, Multivalvulea) from the Atlantic Ocean. In: Systematics and Ecology of Sporozoans and Cnidosporidia (Ed. M.V. Krylov), Akad. Nauk SSSR, Leningrad, 42-64 (In Russian)

Kpatcha T. K., Faye N., Diébakate C., Fall M., Toguebaye B. S. (1997) Nouvelles espèces d'*Henneguya* Thélohan, 1895 (Myxozoa, Myxosporea) parasites des poissons marins du Sénégal: étude en microscopie photonique et électronique. *Ann. Sci. nat., Zoologie, Paris* **18:** 81-91

Lom J. (1987) Myxosporea: a new look at long-known parasites of fish. *Parasitology Today* **3:** 327-332

Lom J., Dykova I. (1985) *Hoferellus cyprini* Doflein, 1898 from carp kidney: a well established myxosporean species or a sequence in the developmental cycle of *Sphaerospora renicola* Dykova and Lom, 1982. *Protistologica* **21:** 195-206

Lom J., Dykova I. (1988) Sporogenesis and spore structure in *Kudoa lunata* (Myxosporea, Multivalvulida). *Parasitol. Res.* **74:** 521-530

Lom J., Dykova I. (1992) Protozoan Parasites of Fishes. Development in Aquaculture and Fisheries Science. Elsevier, Amsterdam, **26**

Lom J., Körting W., Dykova I. (1985) Light and electron microscope redescription of *Sphaerospora tincae* Plehn, 1925 and *S. galinae* Evlanov, 1981 (Myxosporea) from the tench, *Tinca tinca* L. *Protistologica* **21:** 487-497

Lom J., Rohde K., Dykova I. (1992) Studies on protozoan parasites of Australian fishes. I. New species of the genera *Coccomyxa* Léger et Hesse, 1907, *Ortholinea* Shulman, 1962 and *Kudoa* Meglitsch, 1947 (Myxozoa, Myxosporea). *Folia Parasit.* **39:** 289-306

Siau Y. (1978) Contribution à la connaisance des Myxosporidies: Etude de *Myxobolus exiguus* Thélohan, 1895 (Cytologie, cycle, actions sur l'hôte, épidémiologie). Thèse de Doctorat d'Etat, Académie de Montpellier, Université des Sciences et Techniques du Languedoc, Montpellier

Stehr C. (1986) Sporogenesis of the myxosporean *Kudoa paniformis* Kabata & Whitaker, 1981 infecting the muscle of the pacific whiting, *Merluccius productus* (Ayres). *J. Fish Dis.* **9:** 493-504

Stehr C., Whitaker D. J. (1986) Host-parasite interaction of the myxosporean *Kudoa paniformis* Kabata & Whitaker, 1981 and *Kudoa thyrsites* (Gilchrist, 1924) in the muscle of Pacific whiting, Merluccius productus (Ayres): an ultrastructural study. *J. Fish Dis.* **9:** 505-517

Yamamoto T., Sanders J.E. (1979) Light and electron microscopic observations of sporogenesis in the myxosporidan, *Ceratomyxa shasta* (Noble, 1950). *J. Fish Dis.* **2:** 411-428

Received on 27th October, 1998; accepted on 8th July, 1999

Acta Protozool. (1999) 38: 323 - 326

ACTA
PROTOZOOLOGICA

Three New Myxosporidian (Myxozoa: Myxosporea) Parasites of Freshwater Fishes from Chad (Central Africa)

Boguyana KOSTOÏNGUÉ, Malick FALL, Ngor FAYE and Bhen Sikina TOGUEBAYE

Laboratory of Parasitology, Department of Animal Biology, Faculty of Sciences and Technologies, University C.A. DIOP of Dakar, Dakar, Senegal

Summary. Examination of freshwater fishes from Chad (Central Africa) revealed the presence of three new species of Myxosporea. They are: *Henneguya fusiformis* sp. n. in *Clarias anguillaris* Linné, 1758 (Clariidae) characterized by a fusiform sporal body (32.0 ± 0.83 x 6.16 ± 0.68 µm) and pyriform polar capsules (5.73 ± 0.43 x 3.5 ± 0.5 µm); *Thelohanellus citharini* sp. n. found in *Citharinus citharus* Geoffroy St-Hilaire, 1809 (Citharinidae) had pyriform spores (11.07 ± 0.62 x 6.15 ± 0.36 µm) and elongated polar capsules (6.57 ± 0.49 x 3.23 ± 0.42 µm); *Thelohanellus ndjamenaensis* sp. n. described from *Labeo parvus* Boulenger, 1902 (Cyprinidae) had ovoid spores (10.28 ± 0.43 x 7.32 ± 0.46 µm) and pyriform polar capsules (4.21 ± 0.4 x 3.21 ± 0.43 µm).

Key words: Central Africa, Chad, freshwater fishes, *Henneguya fusiformis* sp.n., Myxosporidea, *Thelohanellus citharini* sp.n., *T. ndjamenaensis* sp.n.

INTRODUCTION

Myxosporea are essentially fish parasites. The number of papers dealing with myxosporean parasites of African freshwater fishes is limited. The species described belong to nine genera: *Thelohanellus* Kudo, 1933; *Myxidium* Bütschli, 1882; *Sphaerospora* Thélohan, 1892; *Myxobilatus* Davis, 1944; *Myxobolus* Bütschli, 1882; *Unicauda* Davis, 1944; *Henneguya* Thélohan, 1892, *Kudoa* Meglitsch, 1947 and *Chloromyxum* Mingazzini, 1890 (Kudo 1919; Siau 1971; Fomena and Bouix 1986, 1987, 1994, 1997; Obiekezie and Okaeme 1987, 1990; Fomena *et al.* 1993). From freshwater fishes of Chad, 16 species of myxosporea had been described but until now, no species of the genera *Henneguya* Thélohan, 1892 and *Thelohanellus* Kudo, 1933 were discovered (Kostoïngué and Toguebaye 1994, Kostoïngué *et al.* 1999). This note is a first description of these myxosporeans in fishes from Chad.

MATERIALS AND METHODS

The fishes (*Citharinus citharus* Geoffroy St-Hilaire, 1809; *Labeo parvus* Boulenger, 1902; *Clarias anguillaris* Linné, 1758) were collected from Chari River at Ndjamena and Mailao. Spore measure-

Address for correspondence: Bhen S. Toguebaye, Department of Animal Biology, Faculty of Sciences and Technologies, University C. A. DIOP of Dakar, Dakar, Senegal; Fax: (221) 825 25 29 or 824 63 18; E-mail: parasito@ucad.refer.sn

ments, in µm, were made with an eyepiece micrometer at x1000 on live specimens. Standard deviations are given. Line drawings were free hand, made with the aid of an eyepiece graticule. Semi-thin sections were stained with Toluidne blue. For scanning electron microscopy, spores were fixed with glutaraldehyde, dehydrated in ethanol, critical point dried and examined with a JEOL 35CF scanning electron microscope.

RESULTS AND DISCUSSION

Henneguya fusiformis sp. n.

Type host: *Clarias anguillaris* Linné, 1758 (Clariidae).

Site of infection: gills.

Type locality: Chari (Ndjamena).

Prevalence: 9 % (2/44).

Type specimens: one slide deposited in the Parasitological Collection (Coll. N° MYXO-078), Department of Animal Biology, Faculty of Sciences and Technologies, University C. A. DIOP of Dakar, Dakar, Senegal.

Etymology: the specific name relates to the shape of the sporal body

Description: cysts ovoid, whitish and measuring 0.5-2.5 mm. Spore (Figs. 1, 5) fusiform, 32.0 ± 0.8 (29-33) x 6.2 ± 0.7 (5-7) µm. Total length of spores 60.3 ± 0.8 (59-61) µm. Polar capsules pyriform, one located behind the other, of equal size, with 5 to 6 filament coils and measuring 5.7 ± 0.4 (5-6) x 3.5 ± 0.5 (3-4) µm. Large quantity of sporoplasm occupying the half of the spore cavity. Caudal processes equal, divergent curved and measuring 30.0 ± 0.8 (28-31) µm.

Discussion: among the *Henneguya* described in freshwater fishes from Africa (Fomena and Bouix 1997), only spores of *Henneguya laterocapsulata* Landsberg, 1987 described by Landsberg (1987) in *Clarias lazera* from Israel resembles those of this species by their shape. However, the present species differs from *H. laterocapsulata* by the dimensions of its spores and its site of infection. The sporal body of *H. laterocapsulata* is 14.7 x 4.3 µm, the length of caudal processes was 18 µm, the polar capsule measured 4.8 x 2.6 µm and the site of infection is the pectoral and pelvic fins. For all these seasons, we consider the species found in *Clarias anguilaris* as a new species to which the name *Henneguya fusiformis* is given to designate the shape of its spore.

Thelohanellus ndjamenaensis sp. n.

Type host: *Labeo parvus* Boulenger, 1902 (Cyprinidae).

Site of infection: gills.

Type locality: Chari (Ndjamena and Mailao).

Prevalence: 12.5 % (6/48).

Type specimens: one slide deposited in the Parasitological Collection (Coll. N° MYXO-080), Department of

Table 1. *Thelohanus* species of freshwater fishes in Africa

Species	Hosts	Dimensions of spores (in µm)	Sites of infection	Geographic locations
T. niloticus (Gurley, 1893) Fomena & Bouix, 1997	*Labeo niloticus*	Spores: 5 x 3.5	Skin	Egypt
T. valeti Fomena & Bouix, 1987	*Barbus aspilus* *B. jae*	Spores type1: 12.02 x 4.78; Polar capsule: 6.24 x 2.34 Spores type 2: 15.58 x 5.48; Polar capsule: 7.79 x 2.7	Operculum Stomach wall	Cameroon
T. sanagaensis Fomena, Marques, Bouix & Njine, 1994	*Labeo* sp.	Spores: 11.6 x 9.0; Polar capsule: 5.8 x 3.7	Gill Fins	Cameroon
T. assambai Fomena, Marques, Bouix & Njine, 1994	*Labeo* sp.	Spores: 10.8 x 5.5; Polar capsule: 6.3 x 3.4	Gill Fins	Cameroon
Thelohanellus sp. Paperna, 1973	*Labeo* sp. *L. senegalensis* *Barbus altianalis*	No data	Gill	Uganda Ghana

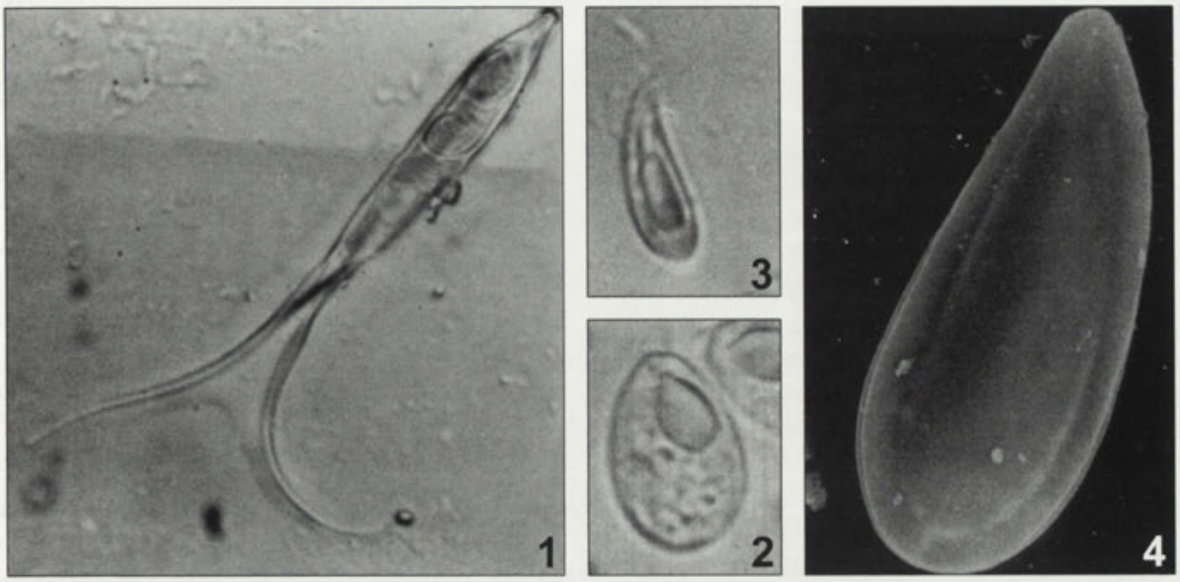

Figs. 1-4. Fresh spores: 1 - *Henneguya fusiformis* sp. n. (x1800), 2 - *Thelohanellus ndjamenaensis* sp. n. (x1800), 3 - *Thelohanellus citharini* sp. n. (x1800). 4 - Mature spore of *Thelohanellus citharini* in scanning electron microscope (x8000)

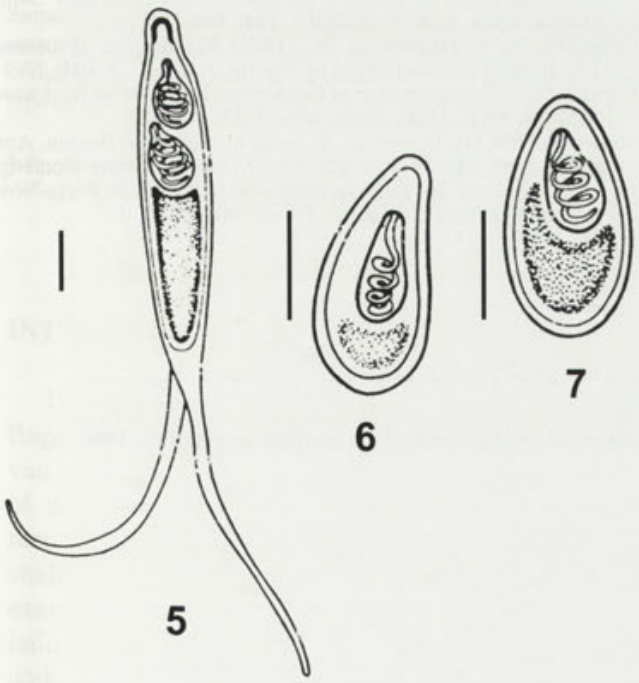

Figs. 5-7. Line drawing of mature spores: 5 - *Henneguya fusiformis* sp. n., 6 - *Thelohanellus citharini* sp. n., 7 - *Thelohanellus ndjamenaensis* sp. n. Scale bars - 5 µm

Animal Biology, Faculty of Sciences and Technologies, University C. A. DIOP of Dakar, Dakar, Senegal.

Etymology: the specific name relates to the country of its origin.

Description: cysts variable in form (ovoid, spherical or elongated) up to 2.5 mm in length. Spores (Figs. 2, 7) ovoid with posterior end usually wider than anterior. Spore size: 10.3 ± 0.4 (10-11) x 7.3 ± 0.5 (7-8) µm. Pyriform polar capsules at anterior end of spore with 4 to 5 filament coils and having 4.21 ± 0.4 (4-5) µm long and 3.2 ± 0.4 (3-5) µm wide. Sporoplasm with a granular mass at the posterior region of the spore cavity.

Discussion: comparing the species described in *Labeo parvus* with others *Thelohanellus* described previously in freshwater fishes in Africa, only spores of *T. sanagaensis* and *T. assambai* described by Fomena *et al.* (1994) in *Labeo* sp. from Cameroon resemble those of this present species by the shape and the length of their spores (Table 1). It appeared that these two species are distinct from the species of *Labeo parvus* by the width of their spores and by the length of their polar capsule. Therefore, we consider the species of *Labeo parvus* as a new species and named *Thelohanellus ndjamenaensis* to remember the locality where it was first found.

***Thelohanellus citharini* sp. n.**

Type host: *Citharinus citharus* Geoffroy St- Hilaire, 1809 (Citharinidae).

Site of infection: heart.

Type locality: Chari (Maïlao).

Prevalence: 3.2 % (2/60).

Type specimens: one slide deposited in the Parasitological Collection (Coll. N° MYXO-079), Department of

Animal Biology, Faculty of Sciences and Technologies, University C. A. DIOP of Dakar, Dakar, Senegal.

Etymology: the specific name of this species relates to the generic name of its type host.

Description: cysts ovoid, whitish and size up to 1.5 mm. Spore (Figs. 3, 4, 6) elongated and slightly curved. Anterior generally blunted (Fig. 4) posterior broad and round. Size: 11.1 ± 10.6 (10-12) µm long and 6.15 ± 0.4.0 (6-7) µm wide. Sutural edge did not bear markings and the surface of valves was smooth (Fig. 4). Polar capsule elongated localized in the middle region of the spore cavity 6.6 ± 0.4 (8-7) x 3.2 ± 0.4 (3-4) µm, four to five filament coils. Sporoplasm small and occupies the posterior region of the spore.

Discussion: five species of *Thelohanellus* was previously known in freshwater fishes from Africa (Table 1). Among these species, only *T. valeti* resembles the species described here by the shape of its spores. According to Fomena and Bouix (1987) *T. valeti*, which parasitizes *Barbus aspilus* and *B. jae* from Cameroon, produced two types of spores. The species found in *Citharinus citharus* from Chad differs by the dimensions of its spores and its polar capsule. Therefore, we propose to establish this species as a new species and the name *Thelohanellus citharini* is given after the name of its host.

REFERENCES

Fomena A., Bouix G. (1986) Contribution à l'étude des Myxosporidies des poissons d'eau douce du Cameroun. I. Espèces nouvelles des genres *Myxidium* Bütschli, 1882. *Acta Tropica* **43:** 319-333

Fomena A., Bouix G. (1987) Contribution à l'étude des Myxosporidies des poissons d'eau douce du Cameroun. II. Espèces nouvelles du genre *Henneguya* Thélohan, 1892 et *Thelohanellus* Kudo, 1933. *Rev. Zool. Afr.* **101:** 43-53

Fomena A., Bouix G. (1994) New Myxosporidea species (Myxozoa) from freshwater teleosts in Southern Cameroon (Central Africa). *J. Afr. Zool.* **108:** 481-491

Fomena A., Bouix G. (1997) Myxosporea (Protozoa: Myxozoa) of freshwater fishes in Africa: keys to genera and species. *Syst. Parasitol.* **37:** 161-178

Fomena A., Marques A., Bouix G. (1993) Myxosporidea (Myxozoa) of *Oreochromis niloticus* (Linnaeus, 1757) (Teleost, Cichlidae) in fish-farming pools at Melen (Yaoundé, Cameroun, Central Africa). *J. Afr. Zool.* **107:** 45-56

Fomena A., Marques A., Bouix G., Njine T. (1994) *Myxobolus bilongi* n. sp., *Thelohanellus assambai* n. sp., *T. sanagaensis* n. sp., Myxosporidies parasites de *Labeo* sp. (Téléostéen, Cyprinidae) du bassin de la Sanaga au Cameroun (Afrique Centrale). *Ann Fac. Sci. H. S. Chim. Sci. Nat.* **3:** 131-142

Kostoïngué B., Toguebaye B. S. (1994) Le genre *Myxobolus* (Myxozoa, Myxosporea) chez les poissons d'eau douce du Tchad avec la description de trois nouvelles espèces. *Bull. Inst. fond. Afr. noire Cheikh Anta Diop, Dakar, Sér. A* **47:** 63-71

Kostoïngué B., Faye N., Toguebaye B.S. (1999) Nouvelles espèces de Myxosporidies des genres *Myxidium* Bütschli, 1882 et *Myxobolus* Bütschli, 1882 (Myxozoa, Myxosporea) chez des poissons d'eau douce du Tchad (Afrique Centrale). *Afr. J. Zool.* (in press)

Kudo R.R. (1919) Studies on Myxosporidia. A synopsis of genera and species of Myxosporidia. III. *Biol. Monogr.* **5:** 1-256

Landsberg J.H. (1987) Myxosporean parasites of the catfish, *Clarias lazera* (Valenciennes 1840). *Syst. Parasitol.* **9:** 73-81

Obiekezie A. I., Okaeme A. N. (1987) *Myxobilatus accessobranchialis* n. sp. (Protozoa: Myxozoa) from the accessory breathing organ of cultured *Heterobranchus bidorsalis* Saint-Hilaire, 1809. *Arch. Protistenkd.* **134:** 409-414

Obiekezie A. I., Okaeme A. N. (1990) Myxosporea (Protozoa) infections of cultured tilapis in Nigeria. *J. Afr. Zool.* **104:** 77-91

Paperna I. (1973) Occurrence of Cnidospora infections in freshwater fishes in Africa. *Bull. IFAN, série A* **33:** 509-527

Siau Y. (1971). Myxosporidies de *Synodontis ansorgii* Boulen. Ann. Et Mag. N. H., 1911 et *Eleotris (Kribia) kribensis* Bouleng., 1964, poissons des eaux saumâtres de la lagune de Porto-Novo (Dahomey). *Bull. Soc. Zool. France* **96:** 563-570

Received on 16th April, 1999; accepted on 10th July, 1999

Acta Protozool. (1999) 38: 327 - 329

ACTA
PROTOZOOLOGICA

Short Communication

On the Development of Multivesicular Bodies in the Cryptophycean Flagellate *Cryptomonas ovata*

Klaus HAUSMANN

Division of Protozoology, Institute of Biology/Zoology, Free University of Berlin, Germany

Summary. Multiinvaginated bodies in the cryptophycean flagellate *Cryptomonas ovata* are demonstrated to be vacuoles in close association with the Golgi complex of these cells. They are distinguished by having an infolded membrane which penetrates into the vacuole. The membrane of these multiinvaginated bodies bears coats on both surfaces. These structures are thought to be the initial step of the development of a certain type of multivesicular bodies.

Key words: *Cryptomonas ovata*, flagellates, multivesicular bodies.

INTRODUCTION

The general ultrastructural features of cryptophycean flagellates (Dodge 1973, 1979; Kugrens and Lee 1991; van den Hoek *et al.*1995), the organization and function of the ejectisomes (Hausmann 1978) as well as the formation of the mitotic spindle (Oakley 1978) are studied in detail. During former electron microscopical examinations of cryptomonadines several different populations of vesicles were detected in these cells. Smooth and coated vesicles were found to cooperate in the function of the contractile vacuole complex in these flagellates (Hausmann and Patterson 1981, Patterson and Hausmann 1981) and other types of coated vesicles at other sites in the cell were depicted (Patterson and Hausmann 1982). The following communication describes the development of multivesicular bodies in these unicellular organisms.

MATERIALS AND METHODS

The source of the flagellates investigated and the methods of preparation for electron microscopy have been described elsewhere (Patterson and Hausmann 1981).

RESULTS AND DISCUSSION

The zone of the Golgi-apparatus of a *Cryptomonas ovata*-cell, shown on Fig. 1, displays two dictyosomes when seen in cross section. The dictyosomes have the usual appearance of these structures except for very peculiar vacuoles in the vicinity of the secretory face of

Address for correspondence: Klaus Hausmann, Division of Protozoology, Institute of Biology/Zoology, Free University of Berlin, D-14195 Berlin, Germany; FAX: +4930-838 6477; E-mail: hausmann@zedat.fu-berlin.de

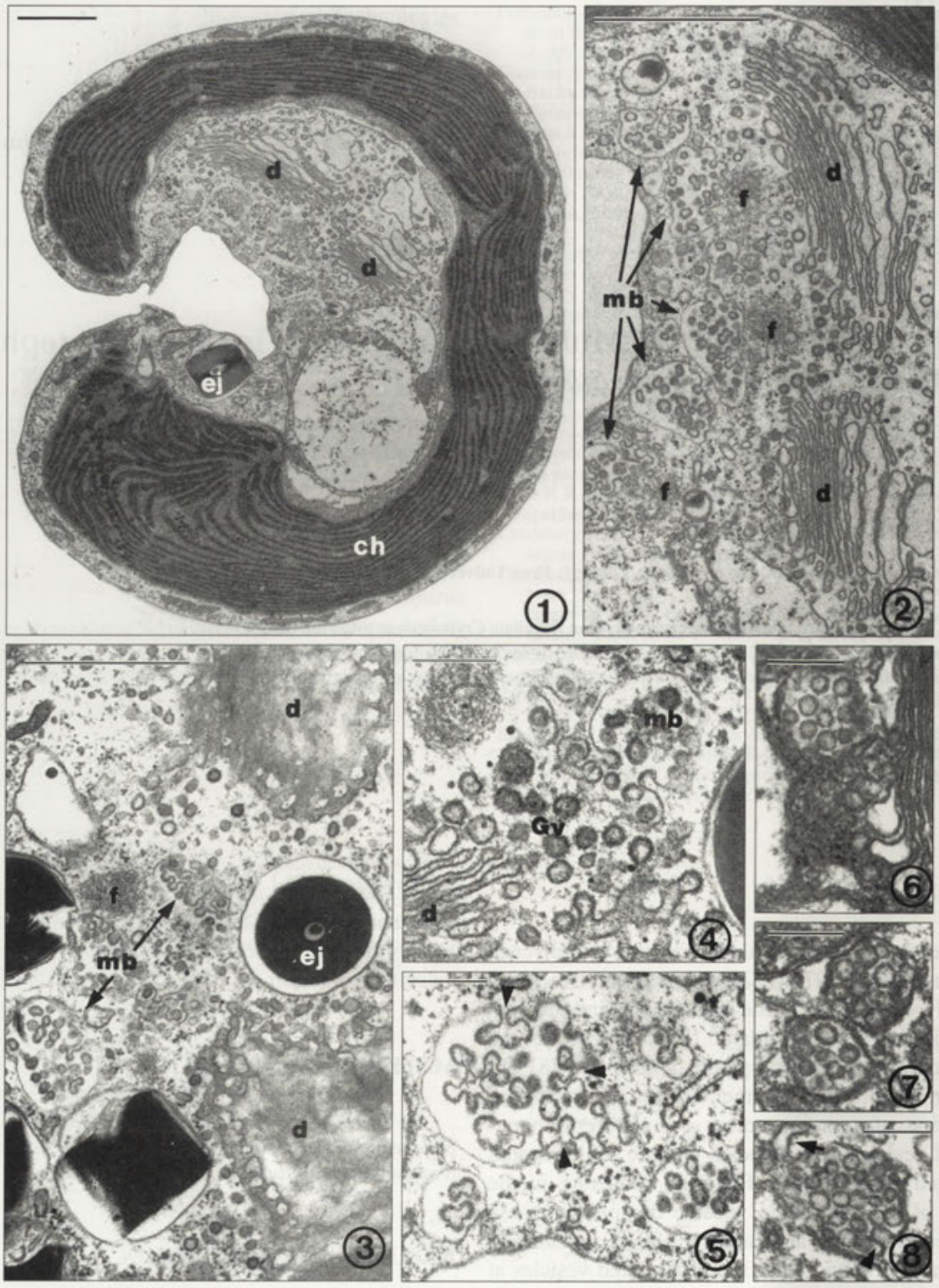

Figs. 1-8. Transmission electron micrographs of *Cryptomonas ovata*. 1 - cross section showing the chloroplast (ch), dictyosomes (d), ejectisome (ej); 2 - dictyosomes (d) with multiinavaginated bodies (mb) in the vicinity of their secretory face, f - bundles of filaments; 3 - grazing sections of dictyosomes (d) showing the typical marginal fenestrations as well as multiinvaginated bodies (mb), ej - ejectisome, f - filament bundle; 4 - high magnification demonstrating the close vicinity of a dictyosome (d), Golgi vesicles (Gv) and a multiinvaginated body (mb); 5 - multiinvaginated body with branching infoldings (arrow heads); 6-8 - multivesicular bodies showing numerous vesicles inside a vesicle (6, 7) as well as an invagination (8, arrow head) and an extension (arrow). Scale bars - 1 µm (1-3) and 0,2 µm (4-8)

these organelles (Figs. 2, 3). These vacuoles have a rather irregular outline and appear to be filled with numerous small vesicles. However, higher magnifications and serial sections of these vacuoles show that the internal vesicles are mainly invaginations of the limiting membrane of the vacuole (Figs. 4, 5). The invaginations which can be branched terminate in round swellings the membranes of which are noticeably thickened. This thickening is due to a coat on both sides of the membranes (Figs. 4, 5). Like the dictyosomes these vacuoles have a very ill defined membrane, and the trilamellar structure is only occasionally detectable.

These multiinvaginated vacuoles are exclusively found in the vicinity of the Golgi-apparatus. Sometimes the close relationship between these two structures suggests a more or less direct transition from dictyosomes to multiinvaginated vesicles (Fig. 4). Several bundles of microfilaments may be seen in the secretory region of the dictyosomes when multiinvaginated vacuoles are present (Fig. 2).

Not only these vacuoles, but also multivesicular bodies, i. e., vacuoles filled with small vesicles are found in the vicinity of dictyosomes (Figs. 6, 7). As in the multiinvaginated vacuoles also in this case the membrane is ill defined. Multivesicular bodies filled with vesicles and showing few invaginations represent transition stages between multiinvaginated vacuoles and multivesicular bodies (Fig. 8).

The multiinvaginated vacuoles as well as the multivesicular bodies were not found in all cryptophycean cells investigated. Possibly they appear only at certain stages of the life cycle of the cells or under special culture conditions. It is not yet possible to indicate those circumstances which would be necessary for the appearance of these structures.

Multivesicular bodies are reported to originate from secondary lysosomes by inward budding of its limiting membrane (Holtzman 1989). There is strong evidence that the multivesicular bodies in the cryptophycean flagellates originate more or less directly from the dictyosmes. The multiinvaginated vacuoles represent a transient, developmental stage of multivesicular bodies. Multivesicular bodies which are described for the cryptophycean species *Cryptomonas reticulata* (Lucas 1970) show the structural organization which is basically the same as in the flagellate species investigated in this study. Lucas (1970) demonstrated the lysosomal nature of the multivesicular bodies in *C. reticulata* by staining for acid phosphatase. This author believes that the multivesicular bodies are related to the 'corps de Maupas' which are - in all likelihood - autophagosomes (for reviews see, Santore 1987, Novarino and Lucas 1993).

REFERENCES

Dodge J. D. (1973) The Fine Structure of Algal Cells. Academic Press, London

Dodge J. D. (1979) The Phytoflagellates: Fine structure and Phylogeny. In: Biochemistry and Physiology of Protozoa, 2 ed., (Eds. M. Levandowsky and S. H. Hutner). Academic Press, New York, **1:** 7-57

Hausmann K. (1978) Extrusive organelles in protists. *Int. Rev. Cytol.* **52:** 197-176

Hausmann K., Patterson D. J. (1981) Involvement of smooth and coated vesicles in the function of the contractile vacuole complex in some cryptophycean flagellates. *Exp. Cell Res.* **135:** 449-453

Holtzman E. (1989) Lysosomes. In: Cellular Organelles, (Ed. P. Siekevitz). Plenum Press, New York, **3**

Kugrens P., Lee R. E. (1991) Organization of Cryptomonads. In: The Biology of Free-living Flagellates (Eds. D. J. Patterson and J. Larsen). Claredon Press, Oxford, 219-233

Lucas I. A. N. (1970) Observations on the fine structure of the Cryptophyceae. I. The genus *Cryptomonas*. *J. Phycol.* **6:** 30-38

Novarino G., Lucas I. A. N. (1993) A comparison of some morphological characters in *Chroomonas ligulata* sp. nov. and *C. placoidea* sp. nov. (Cryptophyceae). *Nord. J. Botany* **13:** 583-591

Oakley B. R. (1978) Mitotic spindle formation in *Cryptomonas* and *Chroomonas* (Cryptophyceae). *Protoplasma* **95:** 333-346

Patterson D. J., Hausmann K. (1981) The behaviour of contractile vacuole complexes of cryptophycean flagellates. *Br. phycol. J.* **16:** 429-439

Patterson D. J., Hausmann K. (1982) Coated vesicle heterogeneity in some cryptophycean flagellates. *Cell Biol. Int. Rep.* **6:** 513-521

Santore U. J. (1987) A cytological survey of the genus *Chroomonas*-with comments on the taxonomy of this natural group of the Cryptophyceae. *Arch. Protistenkd.* **134:** 83-114

van den Hoek C., Mann D. G., Jahns H. M. (1995) Algae - An Introduction to Phycology. Cambridge University Press, Cambridge

Received on 7th October, 1999

Acknowledgement

The editors wish to acknowledge the help of the following colleagues who have served as reviewers for one or more manuscripts submitted to publication in our journal in 1999.

André Adoutte
Mohamed S. Alyousif
Richard J. Arthur
Christian F. Bardele
Greg J. Barrit
Linda Basson
Luis Beyens
Richard Bräucker
Dan Charman
John C. Clamp
Bryan H. Clubb
John O. Corliss
Jean Dragesco
J. P. Dubey
Donald W. Duszynski
Iva Dyková
M. El-Matbouli
Tom Fenchel
Wilhelm Foissner
Ferran Garcia-Pichel
Vasil Golemansky
John A. Gooday
Klaus Hausmann
Wieger Homan
Norbert Hülsmann
Jan-Ove Joseffson
Stanisław L. Kazubski
Paweł Kałużny
Hansuki U. Keller
Michael Kent
John J. Lee
Jiří Lom
Denis H. Lynn
Kálmán Molnar
Gianfranco Novarino
David J. Patterson
James Pratt
Frank F. Pindak
Helmut Plattner
Philip J. Proteau
Siegfried Scherer
Martin Schlegel
Serguey Skarlato
Michael Sleigh
Humphrey G. Smith
Milena Svobodova
Helge A. Thomsen
Steve J. Upton
Jiři Vavra
Barry G. Warner
Norbert Wilbert
Krzysztof Wiąckowski

Author Index: Acta Protozoologica 38 (1-4) 1999

Subject Index: Acta Protozoologica 38 (1-4) 1999

Polish Academy of Sciences
Nencki Institute of Experimental Biology
and
Polish Society of Cell Biology

ACTA PROTOZOOLOGICA

International Journal on Protistology

ACTA PROTOZOOLOGICA appears quarterly.

The price (including Air Mail postage) of subscription to ACTA PROTOZOOLOGICA at 2000 is: US $ 180.- by institutions and US $ 120.- by individual subscribers. Limited numbers of back volumes at reduced rate are available. TERMS OF PAYMENT: check, money oder or payment to be made to the Nencki Institute of Experimental Biology account: 11101053-3522-2700-1-34 at Państwowy Bank Kredytowy XIII Oddz. Warszawa, Poland. For matters regarding ACTA PROTOZOOLOGICA, contact Editor, Nencki Institute of Experimental Biology, ul. Pasteura 3, 02-093 Warszawa, Poland; Fax: (4822) 822 53 42; E-mail: jurek@ameba.nencki.gov.pl For more information see Web page **http://www.nencki.gov.pl/public.htm**).

Front cover: *Trichomonas aotus* sp. n. In: F. F. Pindak and M. Mora de Pindak (1998) Diagnostic characteristics of owl monkey *(Aotus trivignatus)* intestinal trichomonads. *Acta Protozool.* **37:** 159-172

This publication is supported by the State Committee for Scientific Research

Desktop processing: Justyna Osmulska, Data Processing Laboratory of the Nencki Institute
Printed at the MARBIS, ul. Kombatantów 60, 05-070 Sulejówek, Poland

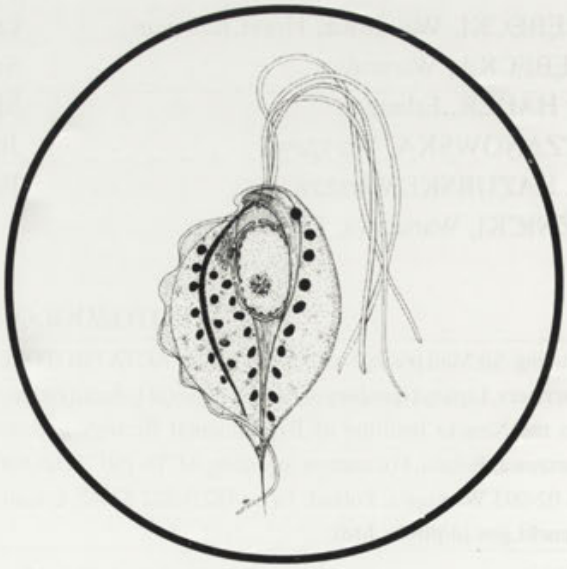

NENCKI INSTITUTE OF EXPERIMENTAL BIOLOGY
WARSAW, POLAND

1999

VOLUME 38
ISSN 0065-1583

Contents of Volume 38 (1-4) 1999

Number 1

Number 2

Number 3

Number 4

INSTRUCTIONS FOR AUTHORS

ACTA PROTOZOOLOGICA publishes original papers on experimental or theoretical research in all fields of protistology with the exception of faunistic notices of local character and purely clinical reports. Short communications, as well as longer review articles may also be submitted. Contributions should be written in English. Submission of a manuscript to ACTA PROTOZOOLOGICA implies that the contents are original and have not been published previously, and are not under consideration or accepted for publication elsewhere. There are no page charges except colour illustration. Names and addresses of suggested reviewers will be appreciated. In case of any question please do not hesitate to contact Editor. Authors should submit papers to:

Miss Małgorzata Woronowicz
Managing Editor of ACTA PROTOZOOLOGICA
Nencki Institute of Experimental Biology,
ul. Pasteura 3
02-093 Warszawa, Poland
Fax: (4822) 822 53 42
E-mail: jurek@ameba.nencki.gov.pl

Extensive information on ACTA PROTOZOOLOGICA is now available *via* internet. The address is: **http://www.nencki.gov.pl/public.htm**

Organization of Manuscripts

Submissions

Please enclose three copies of the text, one set of original of line drawings (without lettering!) and three sets of copies with lettering, four sets of photographs (one without lettering). In case of photographs arranged in the form of plate, please submit one set of original photographs unmounted and without lettering, and three sets of plates with lettering.

The ACTA PROTOZOOLOGICA prefers to use the author's word-processor disks (3.5" and 5.25" format IBM or IBM compatible, and MacIntosh 6 or 7 system on 3.5" 1.44 MB disk only) of the manuscripts instead of rekeying articles. If available, please send a copy of the disk with your manuscript. Preferable programs are Word or WordPerfect for Windows and DOS WordPerfect 5.1. Disks will be returned with galley proof of accepted article at the same time. Please observe the following instructions:

1. Label the disk with your name: the word processor/computer used, e.g. IBM; the printer used, e.g. Laserwriter; the name of the program, e.g. Word for Windows or WordPerfect 5.1.
2. Send the manuscript as a single file; do not split it into smaller files.
3. Give the file a name which is no longer than 8 characters.
4. If necessary, use only italic, bold, underline, subscript and superscript. Multiple font, style or ruler changes, or graphics inserted the text, reduce the usefulness of the disc.
5. Do not right-justify and use of hyphen at the end of line.
6. Avoid the use of footnotes.
7. Distinguish the numerals 0 and 1 from the letters O and l.

Text (three copies)

The text must be typewritten, double-spaced, with numbered pages. The manuscript should be organized into Summary, Key words, Abbreviations used, Introduction, Materials and Methods, Results, Discussion, Acknowledgements, References, Tables and Figure Legends. The Title Page should include the full title of the article, first name(s) in full and surname(s) of author(s), the address(es) where the work was carried out, page heading of up to 40 characters. The present address for correspondence, Fax, and E-mail should also be given.

Each table must be on a separate page. Figure legends must be in a single series at the end of the manuscript. References must be listed alphabetically, abbreviated according to the World List of Scientific Periodicals, 4th ed. (1963). Nomenclature of genera and species names must agree with the International Code of Zoological Nomenclature, third edition, London (1985) or International Code of Botanical Nomenclature, adopted by XIV International Botanical Congress, Berlin, 1987. SI units are preferred.

Examples for bibliographic arrangement of references:

Journals:

Häder D-P., Reinecke E. (1991) Phototactic and polarotactic responses of the photosynthetic flagellate, *Euglena gracilis*. *Acta Protozool.* **30:** 13-18

Books:

Wichterman R. (1986) The Biology of *Paramecium*. 2 ed. Plenum Press, New York

Articles from books:

Allen R. D. (1988) Cytology. In: *Paramecium*, (Ed. H.-D. Görtz). Springer-Verlag, Berlin, Heidelberg, 4-40

Zeuthen E., Rasmussen L. (1972) Synchronized cell division in protozoa. In: Research in Protozoology, (Ed. T. T. Chen). Pergamon Press, Oxford, **4:** 9-145

Illustrations

All line drawings and photographs should be labelled, with the first author's name written on the back. The figures should be numbered in the text as Arabic numerals (e.g. Fig. 1). Illustrations must fit within either one column (86 x 231 mm) or the full width and length of the page (177 x 231 mm). Figures and legends should fit on the same page. Lettering will be inserted by the printers and should be indicated on a tracing-paper overlay or a duplicate copy.

Line drawings (three copies + one copy without lettering)

Line drawings should preferably be drawn about twice in size, suitable for reproduction in the form of well-defined line drawings and should have a white background. Avoid fine stippling or shading. Computer printouts of laser printer quality may be accepted, however *.TIF, *.PCX, *.BMP graphic formats on disk are preferred.

Photographs (three copies + one copy without lettering)

Photographs at final size should be sharp, with a glossy finish, bromide prints. Photographs grouped as plates (in size not exceeding 177 x 231 including legend) must be trimmed at right angles accurately mounted and with edges touching and mounted on firm board. The engraver will then cut a fine line of separation between figures. Magnification should be indicated. Colour illustration on transparent positive media (slides 60 x 45 mm, 60 x 60 mm or transparency) are preferred.

Proof sheets and offprints

Authors will receive one set of page proofs for correction and are asked to return these to the Editor within 48-hours. Fifty reprints will be furnished free of charge. Orders for additional reprints have to be submitted with the proofs.

Indexed in Chemical Abstracts Service, Current Contents (Agriculture, Biology and Environmental Sciences), Elsevier BIOBASE/Current Awareness in Biological Sciences, LIBREX-AGEN, Protozoological Abstracts. POLISH SCIENTIFIC JOURNALS CONTENTS - AGRIC. & BIOL. SCI. data base is available in INTERNET under URL (UNIFORM RESOURCE LOCATOR) address: http://ciuw.warman.net.pl/alf/psjc/ any WWW browser; in graphical operating systems: MS Windows, Mac OS, X Windows - mosaic and Netscape programs and OS/2 - Web Explorer program; in text operating systems: DOS, UNIX, VM - Lynx and WWW programs.

ACTA
PROTOZOOLOGICA

ORIGINAL ARTICLES

SHORT COMMUNICATION

1999 NOVEMBER
VOLUME 38 NUMBER 4